Hip, Pelvis and Sacro-Iliac Joints

V. V. Mascarenhas, M. O. Castro,
and P. Diana Afonso

Contents

V. V. Mascarenhas (✉) · P. D. Afonso
Imaging Center, MSK Imaging Unit (UIME),
Hospital da Luz Lisboa, Luz Saúde, Lisbon, Portugal
e-mail: mascarenhas.vasco@gmail.com;
p.diana.a@gmail.com

M. O. Castro
Radiology Department, Centro Hospitalar
Universitário do Algarve, Portimão, Portugal
e-mail: migkastro@yahoo.com

Abstract

Hip and groin pain in athletes is common and clinical presentation is often non-specific. Causal pathology represents a complex scenario in athletes, with improper diagnosis serving as a cause of delayed return to sports.

Radiologists play an essential role in guiding the work-up of athletes with hip pain. This chapter provides an overview on hip and pelvis anatomy and biomechanics and discusses strategies for imaging assessment. Magnetic resonance imaging (MRI) is often the modality of choice for evaluating many of the injuries observed, although preliminary evaluation with conventional radiography and use of other imaging modalities such as ultrasonography (US), computed tomography (CT) and bone scintigraphy may be supplementary or important in some situations.

With the main focus on MRI, the authors present abnormalities of the pelvis and hip joint and the surrounding soft tissues that can occur in athletes: intra- and extra-articular hip impingement syndromes, labral and cartilage disease, microinstability of the hip, bone and myotendinous injuries of the pelvis and sacroiliac dysfunction.

Muscle injuries, stress fractures, thigh splints and apophyseal injuries are particularly important to consider in young athletes and may be acute or related to chronic repetitive microtrauma. The authors highlight current concepts of femoroacetabular impinge-

Med Radiol Diagn Imaging (2020)
https://doi.org/10.1007/174_2020_256, © Springer Nature Switzerland AG
Published Online: 01 January 2021

ment (FAI), labral tears and cartilage abnormalities. Tear of the *ligamentum teres* is now recognized as a potential cause of hip pain and instability, best evaluated with MR arthrography (MRA).

Greater trochanteric pain syndrome encompasses a group of conditions leading to lateral hip pain, with US playing an increasingly important role for both evaluation and image-guided treatment. Snapping hip syndrome and sacroiliac joint pathology are also important considerations.

Innovation has been the catalyst for the transformation of hip imaging, as the arrival of new modalities and the widespread introduction of MRI resulted in a paradigm shift from bone morphology analysis to integrated soft tissue, joint and cartilage assessment. Understanding the pathophysiology through the visualization of osseous structures and detailed depiction of soft tissues has become part of routine imaging and has had a major impact on therapeutic decision-making.

1 Introduction

Imaging of the hip, pelvis and sacroiliac joints (SIJ) is presently in the spotlight, boosted by both new technical developments and novel clinical conditions discovered in the past decade, such as the recognition of femoroacetabular impingement syndrome (FAIS) as a cause of early-onset osteoarthritis (Ganz et al. 2003; Lynch et al. 2016).

Clinically, hip and groin pain lists in the top 6 most common athletic injuries (up to 23% of athletes during a 1-year period) (Jónasson et al. 2011), mainly affecting activities that involve accelerations/decelerations, rapid direction changes and kicking (Table 1). The most common hip/groin injuries in soccer players are adductor injuries (63%; not counting hamstring injuries), followed by hip flexor/iliopsoas injury (8%) (Werner et al. 2019). In professional soccer players, overuse hip injuries are up to three times more common compared with acute injuries (73% vs. 27%) (Agten et al. 2016). Intra-articular hip injuries in athletes are less frequent (6.2% in soccer and 5% in American football) (Makovicka et al. 2019; Werner et al. 2019; Cruz et al. 2019).

Hip and groin injuries constitute a considerable proportion of all time-loss injuries in men's professional football. Interestingly, athletes with hip pain typically consult a large number of different medical specialists, with time to return to sport (RTS) often being the main question asked by every stakeholder (Cruz and Mascarenhas 2018). Mean number of days lost before RTS in hip/groin injuries largely varies by injury type (Table 2). Although there was a promising slight

Table 1 Frequencies and most common sports-related hip/groin injuries in professional athletes by type of sport (as a percentage of all injuries)

Sports	Frequency of injuries affecting the hip/groin	Most common injury type in the hip/groin
Soccer (Ekstrand et al. 2011; Werner et al. 2019)	11–17%	Adductor (63%)/ hamstring injuries
American football(Makovicka et al. 2019)	3.1%	Adductor (38%)/ Hip flexor injury (28%)
Basketball (Zuckerman et al. 2018)	2.1–7.8%	Hamstring injury
Ice hockey (McKay et al. 2014)	4–13.1%	Muscle-tendon injury

Table 2 Days lost before return to sports per hip/groin injury (Werner et al. 2019)

Injury type	Mean no. of days lost
Adductor injury	14 (20)
Hip flexor/iliopsoas injury	11 (10)
Symphysitis/pelvic stress fracture	40 (34)
Chondral lesion	46 (53)
Labral tear	56 (61)
FAI	64 (60)
Fracture	99

Note: Numbers are mean days lost before full return to sports for soccer (Union of European Football Associations), with SD in parentheses
FAI femoroacetabular impingement

decreasing trend in the rates of hip and groin injury (as a category) and adductor-related injury (as a specific diagnosis), the injury burden at a consistent level over the last 15 years (Werner et al. 2019). Accordingly, imaging has a pivotal role in the athlete's clinical management.

Sports-related injuries mainly depend on (1) sex, (2) age, (3) type of sport and (4) activity level.

1. **Sex**: Men have a higher risk of hip/groin injury than women when playing the same sport (Orchard 2015). Additionally it has been reported that hip pathology is more common in white males with a family history of hip surgery (Cruz et al. 2019).
2. **Age**: Sports injuries in children differ by age diagnosis, type and body area. In children and adolescents, up to 24% of injuries affect the hip as opposed to only 5–6% in adults (Stracciolini et al. 2013). Older children sustain a greater proportion of overuse injuries.
3. **Type of sport:** An increased incidence of hip injuries in specific sports is reported, including soccer, basketball, martial arts and ice hockey. By category these most frequently occur in impingement sports, followed by contact sports, and cutting sports (Cruz et al. 2019) (Table 3).
4. **Activity level:** When compared with recreational athletes undergoing arthroscopic treatment for FAI, high-level athletes are more likely to be younger, male, and to undergo bilateral surgery. When high-level athletes are grouped by the mechanical demands placed on the hip by their sport, athletes participating in cutting sports are more likely to be younger than those in the other groups (Nawabi et al. 2014).

2 Aetiology, Diagnosis and Prognosis of Hip and Groin Pain

Aetiology*:* Hip pain is a common but non-specific symptom that has many aetiologies. These include multiple pathologies, most of which have been extensively studied (Blankenbaker and al 2006). Interestingly, with the development of newer imaging modalities several additional causes of hip pain have become apparent, namely FAIS, labral tears and snapping hip (Mascarenhas et al. 2016) (Table 4).

Table 3 Sports Categories for Athletes according to Nawabi et al. (Nawabi et al. 2014) and rates of hip/groin injury (per 100,000 Athletic Exposures)

Sport category	Impingement	Contact	Cutting	Flexibility	Asymmetric overhead	Endurance
Examples	• Ice hockey • Baseball • Crew/ rowing • Equestrian polo, water polo	• American football • Rugby • Wrestling	• Soccer • Basketball • Lacrosse • Field hockey	• Dance • Gymnastics • Yoga • Figure skating • Martial arts	• Tennis • Golf • Volleyball • Baseball • Softball • Field events: javelin, discus, hammer throw	• Track, cross-country, other running • Cycling • Swimming (not breaststroke)
Rate of injury per 100,000 AE	96.90	60.33	57.92	37.51	31.26	27.93

Data from National Collegiate Athletic Association (NCAA) athletes across 25 collegiate sports during the 2009/10 to 2013/14 academic years (Cruz et al. 2019)
AE Athletic exposure

Table 4 Differential diagnosis of hip and groin-related pain: an overview of possible causes of intra-articular and extra-articular causes

Intra-articular	Peri-articular	Mimickers
FAI **Instability** **Microinstability**	**Muscle and Tendon-related pathology** – Iliopsoas-related pathology – Iliotibial band pathology – *Rectus femoris* pathology – Gluteal pathology – Hamstring pathology	**Axial skeletal pathology** – Lumbar spine pathology – Sacroiliac joints pathology
Osteoarthritis	**Stress fracture** – Femoral neck or acetabulum – Pubic ramus	**Pubic-related pathology**
Non-FAI related – Chondrolabral injuries – Loose bodies – *Ligamentum teres* pathology – Capsular laxity	**Greater trochanteric pain syndrome** – Gluteus medius or minimus pathology – Trochanteric bursitis	**Neurological** disorders and nerve entrapment – Obturator – Ilioinguinal – Genitofemoral – Iliohypogastric
Developmental disorders – Acetabular dysplasia – Slipped capital femoral epiphysis – Perthes disease	**Apophysitis or avulsion fracture** – Anterior superior iliac spine – Anterior inferior iliac spine – Iliac crest – Ischial tuberosity – Lesser trochanter	**Hernia** – Femoral or inguinal – Posthernioplasty
Avascular necrosis and **Acute bone marrow oedema syndrome**	**Extra-articular impingement** – External/internal snapping hip – Trochanteric-pelvic impingement – Pectineo-foveal impingement – Ischiofemoral impingement – Subspine impingement	**Intra-abdominal/pelvic abnormality** – Gynaecological conditions – Prostatitis/urinary tract infections/kidney stone – Appendicitis/diverticulitis
Arthritis (autoimmune, reactive or infectious) and **synovial disorders** (PVNS, chondromatosis)	**Deep gluteal syndrome**	**Tumours** and pseudo tumours of the hip and pelvis

PVNS pigmented villonodular synovitis. *FAI* femoroacetabular impingement

A recent practical classification system (Weir et al. 2015) described three major subheadings of hip/groin pain in athletes: (1) Defined clinical entities for ***groin pain***: Adductor-related, iliopsoas-related, inguinal-related and pubic-related groin pain; (2) ***Hip-related*** groin pain and (3) ***other causes*** of groin pain in athletes.

Diagnosis: The complex anatomy of the hip/pelvis region and the high prevalence of "pathologic" findings in asymptomatic athletes are likely the main reasons why making a clear diagnosis is often challenging. Accordingly, a myriad of intra- and extra-articular lesions can contribute to symptoms. After a thorough clinical examination and close communication between radiologists/referring colleagues, the **imaging work-up** should: (1) begin with a **dedicated radiographic series**, including an anteroposterior (AP) view of the pelvis and views tailored to the region of interest (if appropriate); (2) **Comprehensive imaging** is often crucial to assess intra- and extra-articular disease (Mascarenhas et al. 2018a) as well as for treatment planning. Considering that several conditions can mimic and/or frequently coexist when assessing an athlete, if other potential causes are not considered, patients may fail to improve after conservative treatment or surgery (Tibor and Sekiya 2008; Krishnamoorthy et al. 2019a, b) (further discussed under Imaging Techniques).

Treatment: Although beyond the scope of this chapter, treatment strategies for hip and groin pain include conservative care/rehabilitation, surgery and post-surgery care. Each of these may

have a role in different injuries, type and level of activity, but there is little evidence to compare their effectiveness, namely for FAI (Griffin et al. 2018). This is best done in a shared decision-making process, supporting the individual athlete to make an informed decision on the best treatment option (Alonso-Coello et al. 2016).

Prognosis: Accurately predicting an individual's RTS using current strategies is challenging because of the complexity/heterogeneity of lesions. In many ways, sports physicians and radiologists still cannot satisfy these high expectations from an evidence-based point of view (Cruz and Mascarenhas 2018). In the setting of FAI and hip preservation surgery (HPS), there is emerging evidence on the prognostic value of age and hip intra-articular lesions detected on MRI, namely (1) femoral and acetabular subchondral cysts are associated with increased rates of clinical failure at short and long term (Krych et al. 2016; Hartigan et al. 2017), (2) cartilage damage exceeding 2 o'clock/60° on the acetabular clockface and (3) central acetabular osteophytes are poor prognostic factors and are associated with higher rates of clinical failure 10 years after HPS (Hanke et al. 2016).

3 Anatomy

3.1 Hip and Pelvis Morphology

Presently there is no detailed knowledge about the combined function of the pelvic/abdominal muscle girdle and the mobility of the hip, but there is a clear relationship between these two anatomical regions (Rivière et al. 2017a). The pelvic ring is formed by the 2 innominate bones and the sacrum, united by the SI joints posteriorly and the pubic symphysis anteriorly. Stability of this ring is provided mainly by the strong SI ligaments, sacrospinous and sacrotuberous ligaments. Classically, the hip has been described as one morphologically simple loading joint, although the recent description of some anatomical features has enriched this simplicity. The functional interpretation of anatomical structures by "layers", with specific and complementary function levels, more closely parallels clinical significance (Ranawat and Kelly 2005; Rivière et al. 2017a, b; Grammatopoulos et al. 2018).

The basic anatomy around the hip consists of the superficial surface anatomy (and palpable bony prominences) and deep bony, muscular and neurovascular anatomy. The anterior landmarks consist of the prominent anterior superior iliac spine (ASIS) and anterior inferior iliac spine (AIIS), which serve as insertion points for the *sartorius* and direct head of the *rectus femoris*, respectively. The greater trochanter (GT) and posterior superior iliac spine (PSIS) are also easily identifiable. They are important landmarks for clinical/imaging diagnosis and incision planning.

3.1.1 Structural Layer

This layer consists of the proximal femur, the acetabulum, the hyaline cartilage and the acetabular labrum. The hip is a diarthrodial joint and is defined by the constrained bony articulation of the proximal femur and acetabulum. Labrum and cartilage will be discussed in the appropriate sections.

Femur: The femoral head (FH) has a spherical shape in continuity with the femoral neck, which usually has a cylindrical shape flattened from front to back. Although this is the normal anatomy classically described, we now know that in up to 7–100% of humans there are variants of this morphology, with the presence of a non-spherical sector at the FHN junction (Anwander et al. 2018). Usually, the articular cartilage covers about 2/3 of the FH and presents a variable thickness (higher in its central region and in the loading zone). The *fovea capitis* is a small area devoid of cartilage, located slightly posterior and inferior to the centre of the FH cartilage (Fig. 1).

Acetabulum: The acetabular cavity has a concave hemispherical shape (Seldes et al. 2001) that results from the contributions of the 3 pelvic bones, the ilium, ischium and pubis. It is orientated approximately 45° caudally (abduction) and 15° anteriorly (anteversion) (Philippon et al. 2014). Its hemispherical shape covers 170° of the FH (Seldes et al. 2001; Philippon et al. 2014). The acetabular fossa (non-articular surface of the acetabulum, covered by synovia) is located in the inferior region of the acetabulum and is sur-

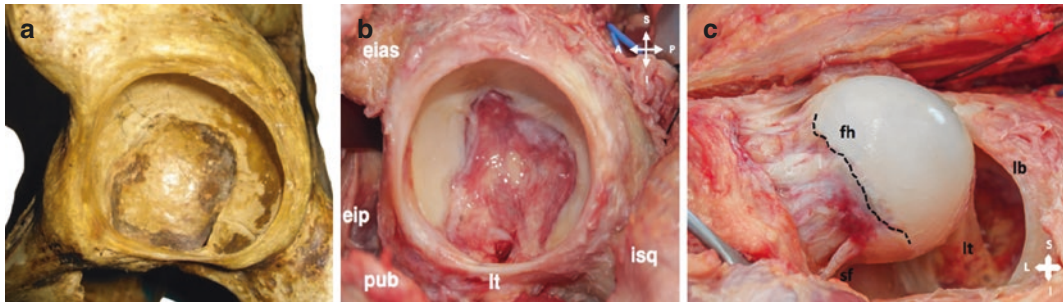

Fig. 1 (**a–c**) (**a**) Bony pelvis cadaveric specimen, representing the acetabulum anatomy. (**b**) Soft tissue cadaveric specimen of the acetabulum. *(eias)* anterosuperior iliac spine, *(eip)* eminence iliopectineus, *(pub)* pubis, *lt* transverse ligament, *isq* ischion. *S* superior, *I* inferior, *A* anterior, *P* posterior. Dissection photography of the hip. (**c**) Femoral head with the typical spherical shape of a *coxa rotunda* and the hyaline articular cartilage lining slightly lateral to the equatorial region and with an irregular border (dashed line). *fh* femoral head, *lb* labrum, *lt ligamentum teres*, *sf* synovial fold, *S* superior, *I* inferior, *M* medial, *L* lateral

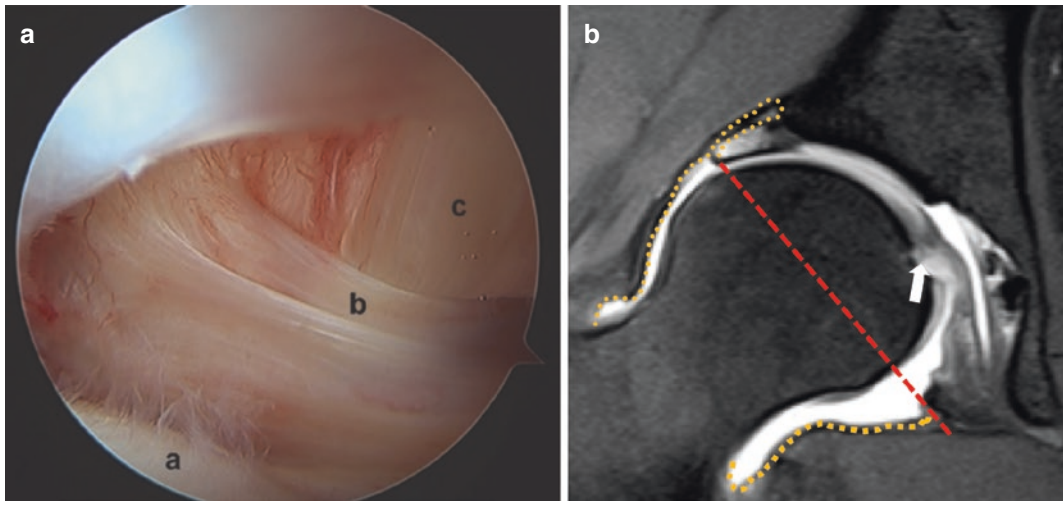

Fig. 2 (**a–b**) (**a**) Arthroscopic image of the peripheral compartment of a right hip with an articular communication with the iliopsoas tendon. The femoral head (**a**), the anterior capsule (**b**) and the iliopsoas tendon (**c**). (**b**) Arthrography magnetic resonance image of the hip, coronal proton-density with fat-sat. *Fovea capitis* with *ligamentum teres* insertions are shown (arrow). Dashed red line represents virtual separation between the peripheral and central compartments. Dashed orange curved line represents capsular contour

rounded by the horseshoe-shaped lunate articular surface. The transverse ligament limits the inferior margin of the fossa (Dienst 2005).

3.1.2 Capsulo-ligamentous Layer (Fig. 2)

The anatomical structure that most influences the peripheral space is the joint capsule. It is a thick and tense fibrous sleeve extending from the outer neck to the acetabular rim. The spiral orientation of the capsular ligaments provides a "screw" effect in full extension. Some portions of the capsule have an increased thickness or are reinforced. Namely, (1) the superolateral part is reinforced by the reflected **tendon of the *rectus femoris***, (2) the anterolateral part by the **iliofemoral ligament** (y-shaped ligament of Bigelow), (3) the anteromedial part by the **pubofemoral ligament**, (4) the posterior capsule by the **ischio-femoral ligament** (Ranawat and Kelly 2005) and (5) circumferentially by the ***zona orbicularis* (ZO)** or femoral arcuate ligament form-

ing a ring around the femoral head-neck (FHN) (a major hip stabilizer). The *iliopsoas bursa* is located beneath the myotendinous portion of the iliopsoas muscle, anterior to the hip joint capsule. It may directly communicate with the peripheral compartment in 15–20% of cases (clinical relevance: can increase the risk of fluid extravasation during hip arthroscopy) (Dienst 2005). *Ligamentum teres* (LT) will be discussed in the appropriate section.

3.1.3 Muscular Layer

The muscular attachments surrounding the hip and pelvis are extensive, with a total of 27 muscles crossing the hip joint. A detailed understanding of the muscular attachments and innervations is critical (Aprato et al. 2016). They can be broadly broken down by their main function (Ranawat and Kelly 2005; Dienst 2005):

1. **Primary flexors**: iliac, psoas, *iliocapsularis*, *pectineus*, *rectus femoris* (direct and indirect heads) and *sartorius*.
2. **Extensors**: *gluteus maximus*, *semimembranosus*, *semitendinosus*, *biceps femoris* (long and short heads) and *adductor magnus* (ischiocondyle part).
3. **Abductors**: *gluteus medius*, *gluteus minimus*, *tensor fascia lata* and iliotibial band.
4. **Adductors**: *adductor brevis*, *adductor longus*, *gracilis* and the anterior part of the *adductor magnus*.
5. **External rotators**: *piriformis*, *quadratus femoris*, *inferior gemellus*, *superior gemellus*, *obturator externus* and *obturator internus*.

3.1.4 Neuromechanical Layer

This is a theoretical concept that integrates multiple interlinked anatomical structures, physiological events and kinematic changes that depend on the proprioception and pain sensitivity of the periarticular structures. This layer is formed by the neurovascular structures, mechanoreceptors and nociceptors present in LT, capsule, labrum and tendons. On a broader view, this level refers to the principle of "reciprocal interaction" which explains the difficulty to set threshold values for morphologic parameters predisposing to impingement, with only extreme values being strongly predictive for the development of impingement or instability (Rivière et al. 2017a).

3.1.5 Vascular Anatomy of the Hip

Detailed knowledge of the vascularization of the proximal femur and iliac allowed the development of HPS techniques (Ganz et al. 2001). The primary vascular pathways are extensions from the internal and external iliac vessels. From the internal iliac system, the superior and inferior gluteal arteries and obturator artery supply most of the surrounding hip musculature (laterally and medially respectively) and periacetabular region (Kalhor et al. 2010). From the external iliac system, the medial and lateral femoral circumflex arteries anastomose around the proximal femur. The main blood supply to the femoral head arises from the medial circumflex femoral artery (Rego et al. 2017). The femoral, obturator and superior gluteal nerves all supply innervation to the hip (Fig. 3).

4 Imaging Techniques

Radiographs (CR) remain the standard imaging modality to assess the hip and pelvis despite US and modern three-dimensional CT, or MRI being increasingly used. For most clinical scenarios US, MRI and MRA remain the decisive imaging tools in sports and prearthritic patients, although their application mainly depends on the specific clinical indication. In this setting, MRI protocols combining hip dedicated sequences as well as sequences covering the pelvis offer the best chance of identifying all potential sources of symptoms. In MRA, the anaesthetic arthrogram combined with the increased diagnostic accuracy provided by the intra-articular contrast can both be extremely useful diagnostic features (Agten et al. 2016). Although very promising, quantitative MRI cartilage imaging still needs to be further validated. Whenever appropriate diagnostic injections may prove useful to confirm the source of symptoms (namely for deep gluteal pain syndrome, ischiofemoral impingement and in certain FAI cases) (Khan et al. 2015).

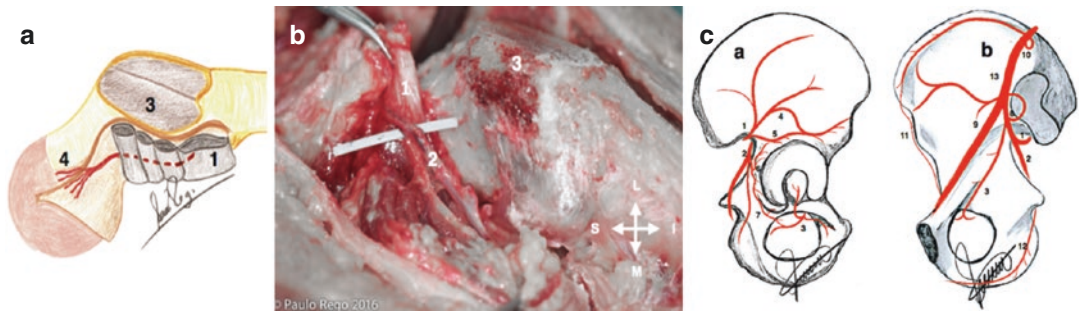

Fig. 3 (**a–c**) (**a**) Schematic drawing of the external rotators' flap containing the deep branch of the posterior circumflex artery (posterior view), the most important branch for femoral vascularization. (**b**) Representative cadaveric photograph of the same anatomy. (1) External rotators; (2) deep branch of the posterior circumflex artery; (3) great trochanter; *S* superior; *I* inferior; *L* lateral; *M* medial. (**c**) Illustration of the lateral (**a**) and medial (**b**) facets of the iliac with the respective arterial anastomotic network of the peri-acetabular region. (1) Upper gluteal artery; (2) gluteal inferior artery; (3) obturator a.; (4) supra-acetabular a.; (5) acetabular a.; (6) acetabular branch of gluteal inferior a.; (7) anastomosis between inferior gluteal a. and obturator a.; (8) iliolumbar a.; (9) nourishing branch of iliolumbar a.; (10) fourth lumbar a.; (11) deep iliac circumflex a.; (12) medial pudendal a.; (13) common iliac a. (Adaptation from Prof. Dr. Paulo Rego's illustration, with permission)

4.1 Radiographs

For hip-related pain, nearly all patients will be initially evaluated with radiographs per the American College of Radiology (ACR) Appropriateness Criteria (Agten et al. 2016). However, in clinical practice, not every injury requires a radiographic examination, particularly for clinically suspected soft-tissue non-articular injuries.

Hip morphology is assessed using angles and lines that are usually visible on an AP radiograph with standardized acquisition of the entire pelvis with additional views according to each specific clinical situation (Siebenrock et al. 2003; Pedersen et al. 2004; Kalberer et al. 2008; van der Bom et al. 2011; Tannenbaum et al. 2014; Hellman et al. 2016). In contrast to CT or MRI, CR is a two-dimensional projection of a 3D reality. Given the enormous individual variability and overlap, it is difficult to precisely define the thresholds between what is normal and pathological regarding hip shape (Tönnis 1976; Tönnis 1987).

4.1.1 General Technical Considerations

For the pelvis AP radiograph, the legs must be 15° internally rotated to compensate for femoral antetorsion. The central beam is centred to the midpoint between the upper border of the symphysis and a line connecting the two ASIS.

Main technical factors to consider include (1) ***Conical projection*** (Tannast et al. 2014) (the closer an object is located to the X-ray source, the more lateral it will be projected), (2) ***Film-tube distance*** (Tannast et al. 2007; Clohisy 2008): should be around 120 cm (increasing film-tube distance the apparent acetabular anteversion increases), (3) ***Centring and direction of the x-ray beam*** (Tannast et al. 2007) (the sacrococcygeal joint should be located 1–3 cm from the superior aspect of the pubic symphysis) and (4) ***pelvic orientation*** (Siebenrock et al. 2003; Tannast et al. 2014) (orientation can vary in three dimensions: obliqueness, rotation and tilt).

4.1.2 Views and Basic Technique (Table 5)

Supine pelvic radiographs are preferred by some authors because they can be directly compared to CR performed intraoperatively or at follow-up during early rehabilitation and restricted weight bearing (Tannast et al. 2007). On the other hand, in clinical entities where acetabular evaluation is of paramount importance (such as Pincer FAI and developmental hip dysplasia (DDH)),

Table 5 Summary of technical details and imaging purposes of several radiographic projections of the hip and pelvis

	Position	Hip flexion	Knee flexion	Foot position	X-ray beam	Usefulness
AP pelvis	Supine/standing	0°	0°	15°–20° internal rotation	Centred to midpoint between: upper border of PS and a line connecting both ASIS	Basic radiographic evaluation for HPS, total hip arthroplasty or trauma; assessment of NSA, acetabular coverage/depth/inclination, head sphericity, JSW
Lauenstein	Supine	45–70° flexion + 45° abduction	45°	Parallel to the table	Hip-centred: vertically to the FH	Assessment of the anterosuperior coverage of the FH, assessment of the anterosuperior FHN junction
Lauenstein (variant)	Supine + 45° lateral rotation to the side of interest	45–70° flexion, no abduction	45°	Parallel to the table	Hip-centred: vertically to the FH	Assessment of the anterosuperior coverage of the FH, and of the anterosuperior FHN junction
Frog-leg lateral	Supine	45° External Rotation	30°-40°	United plantar soles (if bilateral)	Pelvis-centred	Evaluation of the anterior and posterior FHN contour, sphericity of the femoral head, joint congruency
Cross table lateral view	Supine	0°	0°	15°–20° internal rotation	Parallel to the table + oriented at 45° to the limb	Evaluation of the anterior and posterior FHN contour
False profile (Lequesne)	Standing + back tilted 65° to the "wall"	0°	0°	Parallel to the detector	Hip-centred	Assessment of the anterior coverage of the FH, quantification of posteroinferior JSW
Ducroquet	Supine	90° flexion + 45° abduction	90°	45° abduction	Hip-centred	Assessment of the anterosuperior FHN junction
Dunn 45°	Supine	45° + 20° abduction	90°	Neutral	Perpendicular and centred midway to the PS and the ASIS	Assessment of the anterosuperior FHN junction
Dunn-rippstein	Supine	90° flexion + 20° abduction	90°	Neutral	Perpendicular and centred midway to the PS and the ASIS	Assessment of the anterosuperior FHN junction, femoral antetorsion, anterior and posterior FHN contour

AP anteroposterior, *ASIS* anterior superior iliac spines, *FHN* femoral head-neck, *PS* pubic symphysis, *α* alpha, *HPS* hip preserving surgery, *NSA* neck-shaft angle, *JSW* joint space width, *FH* femoral head

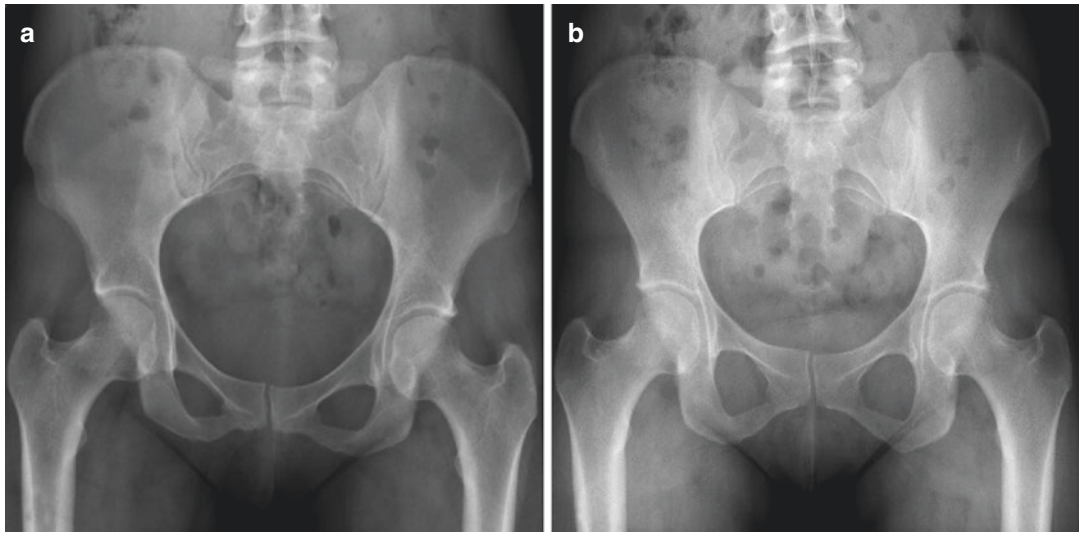

Fig. 4 (**a**, **b**) AP radiographs of the pelvis obtained in the (**a**) supine and (**b**) weight-bearing positions in the same patient. In B the sacrum becomes more vertical and anterior acetabular coverage is reduced. Proper positioning on an AP pelvic radiograph is recognized when: (1) femur—the greater trochanter is seen laterally and the lesser trochanter is partially superimposed on the femoral neck, (2) the obturator rings and acetabular teardrops are symmetric and (3) midsacral line aligns with the pubic symphysis

Table 6 Advantages of obtaining AP radiographs of the pelvis in the supine and standing positions

Supine radiographs	Standing radiographs
• Technically easier to obtain • Easier to perform in obese and older patients • Reproducible in the operating room • Feasible in recent postoperative setting • Most outcome studies derive from supine radiographs	• Accurate JSW and JSN measurement • Allow functional assessment of acetabular morphology, version and coverage

JSN joint space narrowing, *JSW* joint space width

Table 7 Influence of pelvic positioning (rotation and pelvic tilt) on radiographic hip parameters

No significant change with pelvic rotation and tilt	Relevant change with pelvic rotation and tilt
• LCEA • Acetabular index • Extrusion index • Sharp angle • Craniocaudal coverage	• Anterior acetabular coverage • Posterior acetabular coverage • Cross-over sign • Posterior wall sign • Retroversion index

LCEA lateral centre-edge angle

weight-bearing AP pelvic radiographs should be obtained given that they reflect functional anatomical positioning (Jackson et al. 2016) and also account for the differences in pelvic flexion-extension and acetabular version variations (Fig. 4 and Tables 6 and 7).

Axial/lateral view of the hip: Different techniques have been described (Mascarenhas et al. 2019), which are performed to answer specific questions (Table 5 and Fig. 5). The single optimal lateral radiograph for cam morphology assessment is the Dunn 45° view as the femoral head-neck asphericity is most often localized in the anterosuperior region. An AP pelvis radiograph and a Dunn 45° view are the best choice for the initial radiographic assessment of the FHN junction, as further radial imaging is usually performed when FAI is clinically suspected.

Lumbar imaging: There is no current evidence to support additional lumbar imaging when approaching hip and groin-pain, although assessment of spinopelvic (SP) parameters and lumbar pathology is increasingly recognized as important in this setting. Sagittal pelvic kinematics along with SP parameters have recently been

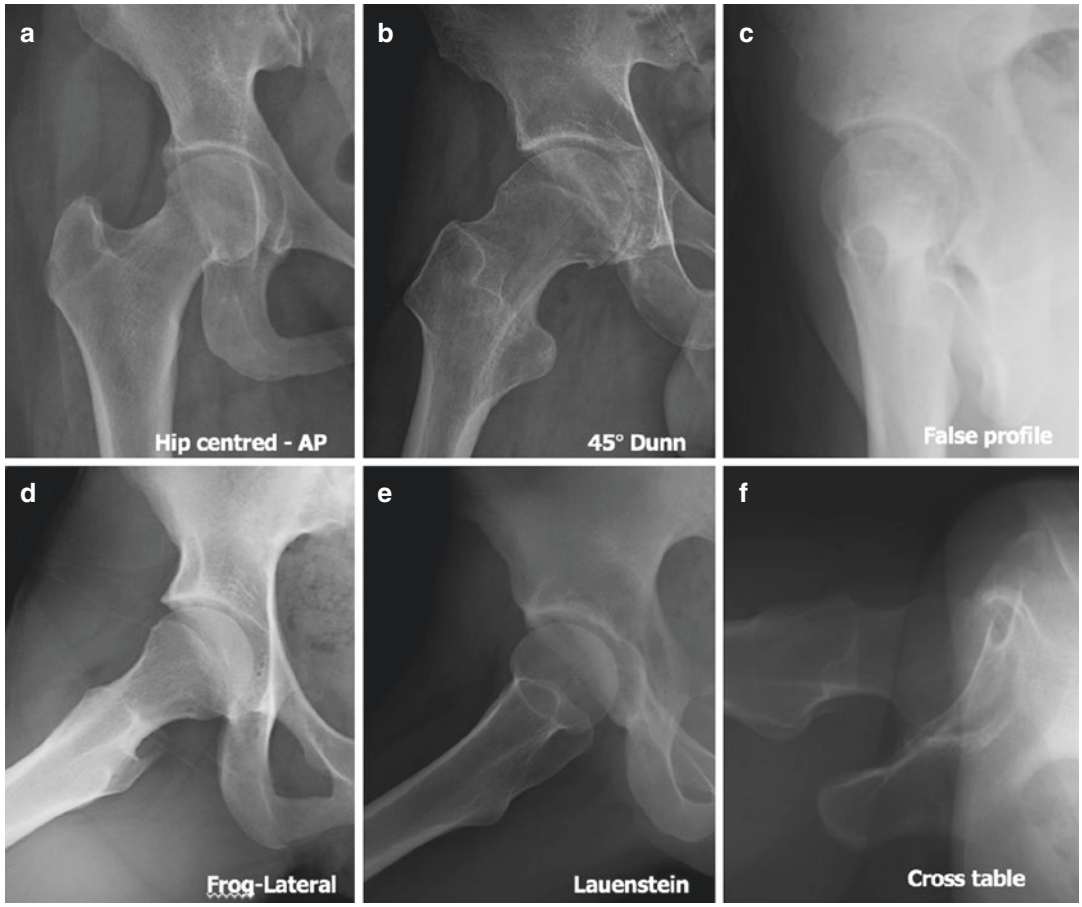

Fig. 5 (**a–f**) Most commonly used radiographic hip views: (**a**) Anteroposterior hip centred. (**b**) Dunn 45; this is the recommended lateral view as a first-line evaluation of proximal femoral morphologies, in combination with an AP view of the pelvis. It is obtained with the hip in 45° of flexion, 20° of abduction and neutral rotation. (**c**) False profile, (**d**) Frog-leg lateral, (**e**) Lauenstein and (**f**) cross-table lateral view

studied for their effect on hip function, FAI (Grammatopoulos et al. 2018; Ng et al. 2018; Mascarenhas et al. 2018a), and hip replacement (Rivière et al. 2017b). Variability in sagittal pelvic function may substantially influence impingement phenomena (Rivière et al. 2017b; Grammatopoulos et al. 2018; Ng et al. 2018; Mascarenhas et al. 2018a), but many of the spine-hip relations are still unexplored. When clinically deemed important, imaging evaluation may include a review of SP parameters and assessment for lumbar disease as a hip pain mimicker, either with a lateral lumbosacral radiograph, or by CT/MRI of the entire pelvis with multiplanar reconstructions, instead of imaging only the hip of interest (Grammatopoulos et al. 2018; Ng et al. 2018; Mascarenhas et al. 2018a).

4.1.3 Parameters

Femoral side: The most commonly described parameters to evaluate femoral morphology can be divided according to the main features that they assess: joint congruency, FH sphericity and other important parameters, such as neck orientation in the coronal (neck-shaft angle) and axial (torsion) planes (Fig. 6 and Table 8).

Acetabular side and spinopelvic parameters: Overall, the most commonly described parameters to assess acetabular morphology can be divided according to the main features that

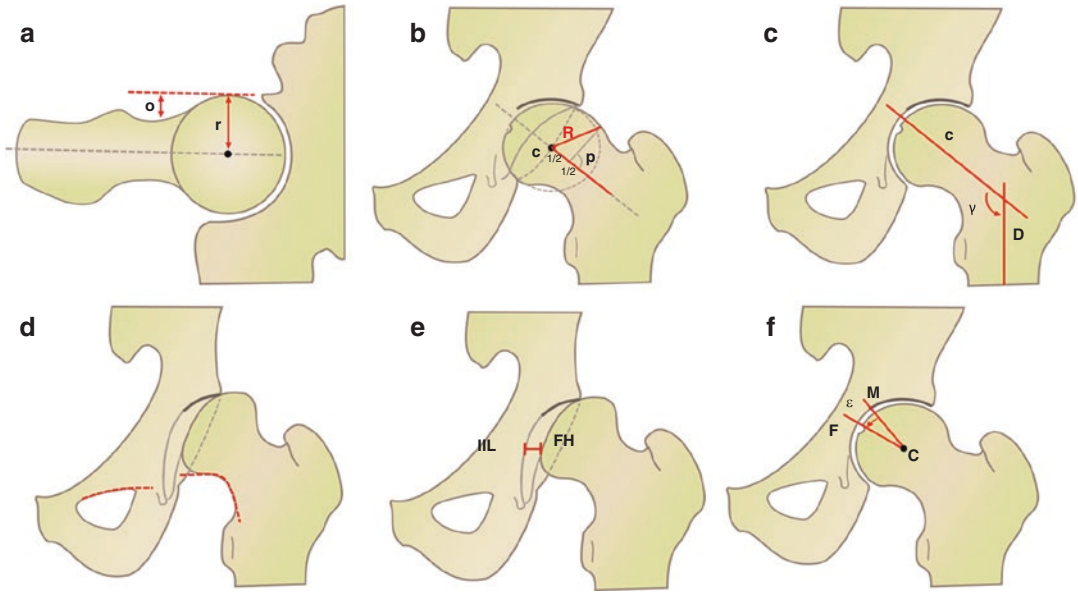

Fig. 6 (**a–f**) Imaging parameters to describe proximal femoral morphology. See Table 8 for definitions. (**a**) offset and offset ratio, (**b**) triangular index, (**c**) cervicodiaphyseal (CCD) angle, (**d**) Shenton's line, (**e**) lateralization of femoral head, (**f**) fovea angle delta

Table 8 Imaging parameters to describe femoral morphology (see Fig. 6 for corresponding illustration)

Femur and joint	Parameter	Unit	Imaging technique	Definition
Femur sphericity	Alpha angle	(°)	Axial and AP pelvis CT and MRI	Angle formed by the FHN axis and line through the centre of the femoral head and the point where the anterior (posterior) FHN contour exceeds head radius
	Pistol-grip Deformity	Qualitative	Axial and AP pelvis	Seen as bump at the FHN junction other than osteophytes from seronegative arthritis and osteoarthritis
	Asphericity and Flattening of the lateral aspect of the FH	Qualitative	Axial and AP pelvis CT and MRI	Flattening of the normal concavity of the FHN junction The head is said to be aspherical if the femoral epiphysis extended more than 2 mm outside the reference circle corresponding to a spherical head
	Offset Offset ratio	[mm] NA	Axial and AP pelvis CT and MRI	Difference (o) between the FH radius (r) and the neck radius Ratio of offset (o) to the FH radius (r)
	Femoral distance	[mm]	Axial and AP pelvis CT and MRI	The perpendicular distance between a tangent along the cortex of the FN and the point of the largest osseous deformity at the FHN junction is measured
	Triangular index	NA	AP pelvis	A perpendicular line (p) is drawn at half the head radius (r). Distance (R) is measured from the FH centre (C) to the point where p intersects the anterior FHN contour. The triangular index is positive if R > r + 2 mm
	Omega angle	(°)	Radial imaging and 3D MRI/CT	Quantifies the extent of abnormally elevated α angles, providing information on cam magnitude (defined by the radial extension of the FHN deformity)

Table 8 (continued)

Femur and joint	Parameter	Unit	Imaging technique	Definition
Joint congruency	Shenton's line	(intact/ interrupted)	AP pelvis	Interrupted if the caudal FHN contour and the superior border of the obturator foramen do not form an harmonic arc
	Lateralization of femoral head or position of the hip centre	(mm)	AP pelvis	Shortest distance between the medial aspect of the femoral head (FH) and the ilioischial line (IIL) Lateralized if greater than 10 mm
Additional findings	Cervicodiaphyseal angle or NSA	(°)	AP pelvis CT/MRI	Angle formed by FHN axis and femoral shaft axis
	Femoral torsion	(°)	Axial images over proximal/ distal femur (CT, MRI or Dunn 90°)	Angle between the longitudinal axis of the FN and the tangent at the condyles of the distal femur
	Joint space width Minimum JSW	(mm)	AP pelvis standing	JSW should be measured in the superior region of the hip joint (distance between the superior FH cortex and the acetabular sourcil). mJSW: inter-bone distance at the point of maximal narrowing
	Fovea angle delta	(°)	AP pelvis	Angle formed by a line through the medial edge of the acetabular roof (M) and the FH centre (C) and a line through the lateral border of the fovea capitis (F) and the FH centre (C). Angle ≤ 10° associated with DDH (fovea alta)
	FEAR index	(+/−)	AP pelvis	Angle formed by: (a) the central straight section of the femoral physis and (b) the most medial and lateral points of the sourcil sclerosis. Positive FEAR index if a laterally directed angle results. Painful hip with a LCEA ≤25° and FEAR index <5° is likely to be stable

AP anteroposterior, *CT* computed tomography, *DDH* developmental dysplasia of the hip, *FEAR* Femoro-Epiphyseal Acetabular Roof, *IIL* ilioischial line, *FH* femoral head, *FHN* femoral head-neck, *FN* femoral neck, *MRI* magnetic resonance imaging, *NA* not applicable

they measure: depth, coverage or orientation (Fig. 7 and Table 9). Spinopelvic parameters have been increasingly recognized as paramount on the hip-spine relationship (Table 10).

4.2 Ultrasound

Although highly dependent on operator experience, US is a valuable tool in the work-up of an athlete with hip pain and particularly for muscle and tendon disease, for both diagnostic purposes and therapeutic interventions (Hegazi et al. 2016). Physicians must have pertinent knowledge of the normal anatomy and should make judicious use of surface anatomy landmarks while using a systematic diagnostic approach. Main advantages are (1) accessibility on site at sporting events, (2) relatively low cost, (3) real-time dynamic imaging capability, as well as (4) radiation-free examination and (5) guidance of interventions such as fluid aspiration and/or substance injection (Boric et al. 2019), improving the accuracy of medication delivery (Sconfienza et al. 2019) and reported satisfaction compared to fluoroscopy-guided injections (Byrd et al. 2014).

Accurate diagnosis of hip injuries is often challenging, given the complex soft-tissue anatomy and the wide spectrum of injuries that can occur (Lungu et al. 2018). Commonly assessed structures are the iliopsoas tendon, iliopsoas bursa, iliotibial tract and joint effusion. Evaluation

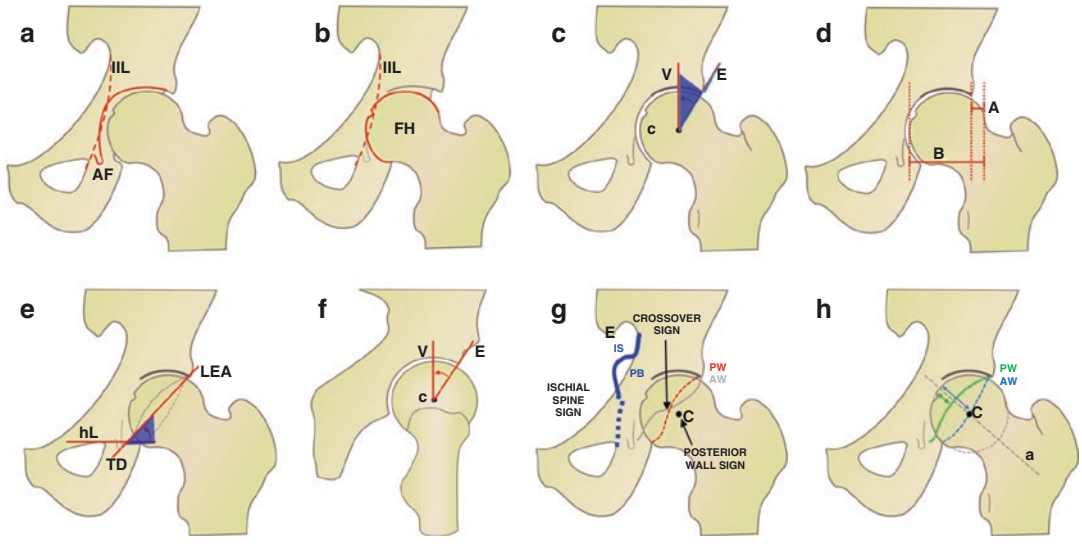

Fig. 7 (**a–i**) Imaging parameters to describe acetabular morphology. See Table 9 for definitions. (**a**) *Coxa profunda*, (**b**) *protrusio*, (**c**) lateral centre-edge angle, (**d**) extrusion index, (**e**) Sharp angle, (**f**) anterior centre-edge angle, (**g**) posterior wall sign, ischial spine sign and crossover sign, (**h**) anterior and posterior acetabular wall index

Table 9 Imaging parameters to describe acetabular morphology (see Fig. 7 for corresponding illustration)

Acetabulum	Parameter	Values	Imaging technique	Definition
Depth	*Coxa profunda*	Positive/ negative	AP pelvis	Acetabular fossa (AF) touches or crosses the ilioischial line (IIL)
	Protrusio acetabuli	Positive/ negative	AP pelvis	Femoral head (FH) touches or crosses the ilioischial line (IIL)
	Acetabular depth	mm	CT/MRI-transverse oblique image of the FN long axis	Distance between the FH centre and the line connecting the anterior/posterior acetabular rim
Coverage	Lateral centre-edge, LCEA	(°)	AP pelvis CT/MRI	Angle formed by a vertical line (v), which is perpendicular to a line connecting the teardrops, and a line through the centre of the FH (C) and the lateral bony rim of the acetabulum
	Centre-edge angle of Wiberg, W-CEA	(°)	AP pelvis	Same as previous, but using the lateral end of the sourcil, i.e. the weight-bearing area of the acetabulum, rather than the lateral rim of the acetabulum
	Acetabular inclination or Sourcil angle	(°)	AP pelvis CT/MRI	Angle formed by a horizontal line and a line through the medial and lateral edge of the acetabular roof
	Extrusion index	(%)	AP pelvis	Percentage of the FH width which is not covered by the acetabulum
	Sharp angle	(°)	AP pelvis	Angle between a horizontal line (hL) and a line connecting the acetabular teardrop (TD) and lateral edge of the acetabulum (LEA)
	Acetabular depth-width ratio (ADR)	NA	AP pelvis	The depth of the acetabulum divided by the width of the acetabulum, multiplied by 1000, presented as a ratio: (A/B)*1000
	Anterior centre-edge	(°)	False profile CT/MRI	Angle formed by a vertical line (V) and a line through the centre of the femoral head (C) and the anterior edge of the acetabulum (E)

Table 9 (continued)

Acetabulum	Parameter	Values	Imaging technique	Definition
	Coverage	(%)	CT/MRI	Technique to measure the % cover of the FH by the weight-bearing zone (pelvic position standardized relative to a specific anatomical plane)
	AASA PASA	(°)	CT/MRI	Lines through the FH centre and contralateral femoral head and tangential to the anterior (AASA) or posterior (PASA) lip of the acetabulum
Orientation	Posterior wall sign	Positive/ negative	AP pelvis	Positive if the posterior wall (PW) runs medially to centre of FH (C)
	Anterior (AWI) and posterior acetabular wall index (PWI)	–	AP pelvis	Ratio of the width of the anterior (AW)/ posterior acetabular walls (PW) measured along the FN axis (a) divided by the FH radius (r)
	Crossover sign	Positive/ negative	AP pelvis	Anterior wall (AW) crosses the posterior wall (PW)
	Retroversion index	(%)	AP pelvis	% of retroverted acetabular opening divided by entire opening
	Ischial spine sign	Positive/ negative	AP pelvis	Positive if ischial spine (IS) is projected medially to pelvic brim (PB)
	Acetabular version (1, 2 and 3 o'clock)	(°)	CT/MRI	Intersection of a perpendicular to the line between the posterior pelvic margins and a line connecting the anterior/posterior acetabular rims
Others	McKibbin index	–	CT/MRI	Sum of femoral version and the acetabular version (at 3 o'clock)

FN femoral neck, *FH* femoral head, *NA* not applicable, *MRI* magnetic resonance imaging, *CT* computed tomography, *AP* anteroposterior, *AASA* anterior sector angle, *PASA* posterior sector angle

Table 10 Spinopelvic parameters. Definition of pelvic incidence, sacral slope and pelvic tilt

Spinopelvic parameters	Parameter	Values	Imaging	Definition
	Pelvic incidence	(°)	Standing sagittal lumbosacral 3D CT or MRI	Angle between a line perpendicular to the sacral plate at its midpoint and a line from the mid-point between the axis of the two femoral heads to the centre of the sacral plate. PI = SS + PT
	Sacral slope	(°)	Standing sagittal lumbosacral	Angle formed by a line drawn parallel to the sacral plate and a horizontal reference line
	Pelvic tilt	(°)	Standing sagittal lumbosacral	Angle formed by a line from the midpoint of the sacral plate to the centre of the femoral heads and a vertical plumb line

of the acetabular labrum with US has been described. However, only the anterior part of the labrum is consistently seen, and other techniques such as MRA are far superior for detection of labral tears.

Ultrasound in FAI: Although level 2 evidence exists supporting a limited role of US in FAI, currently its use cannot be recommended as a diagnostic tool. Labral tears in patients with FAI have been found at US in 63.6% of cases (Orellana et al. 2018), with highly variable diagnostic performance (sensitivity 58–75%, specificity 25–67%, accuracy 61–75%) when compared to arthroscopy (Jung et al. 2013).

4.3 Computed Tomography

Although volumetric CT is excellent at depicting osseous morphologies, assessing osteoarthritic changes (Samim et al. 2019; Mascarenhas et al. 2019) and in virtual range of motion (ROM) 3D simulation studies (Mascarenhas and Caetano 2018; Samim et al. 2019; Mascarenhas et al. 2019), it is (1) unable to detect chondrolabral changes, (2) is associated with radiation exposure and (3) has limited value in evaluation of sports injuries. Mainly it is reserved for (1) detecting subtle fractures not visible on CR, (2) for preoperative evaluation of complex fractures and dislocations, and for the (3) diagnosis of intra-articular ossified bodies or extra-articular ossifications.

Protocol: Patient is positioned supine in the scanner with the legs in slight internal rotation. CT of the hip and pelvis should cover from the iliac crests through the lesser trochanters in thin-section acquisition/reformats (0.5–1 mm), using both bone and soft-tissue algorithm kernels (axial, sagittal and coronal planes). 3D volume-rendered reformations may also be useful.

CT arthrography (hip): Usually reserved for patients in whom MRI is contra-indicated, to appreciate the labrum and cartilage. It is performed after direct intra-articular injection of an iodinated contrast agent. Single-contrast studies are often sufficient and preferred. It involves the injection into the joint space of 10–14 mL of a low-osmolar contrast agent. Usually, no dilution is generally needed if a low to medium concentration preparation (i.e., 180–240 mg of iodine per millilitre) is used, to prevent streak artifacts observed at higher concentrations.

4.4 Magnetic Resonance Imaging

MRI is useful to evaluate intra- and extra-articular disease being the preferred imaging modality for assessment of bone and soft-tissue structures. According to the ACR, in patients with chronic hip pain, MRI should be the next imaging modality of choice when radiographs are normal (Zoga et al. 2016). Because hip/groin pain in athletes can have multiple origins, a problem-oriented imaging protocol is paramount (refer to https://www.essr.org/subcommittees/sports/ for detailed hip/groin area protocols).

Unenhanced MRI and direct MRA (dMRA) are the techniques of choice for detection of hip chondral-labral lesions, although dMRA is the best technique to study intra-articular pathology (Smith et al. 2012; Sutter et al. 2014; Saied et al. 2017). 3T MRI was reportedly equivalent to 1.5T dMRA for diagnosing labral tears and cartilage delamination, but superior for acetabular cartilage defects. Additionally, 3T MRI demonstrated similar sensitivity to 3T dMRA in the detection of acetabular labral tears, although the latter is more sensitive for the detection of acetabular chondral lesions (Smith et al. 2010; Smith et al. 2012; Saied et al. 2017; Crespo-Rodríguez et al. 2017). Indirect MRA is generally not indicated (shows overall less accuracy when compared to dMRA) (Smith et al. 2012; Saied et al. 2017).

Protocol: While evidence is lacking regarding the ideal hip MRI protocol, sequence details or comparison between protocols, the following is recommended for the assessment of a young patient with hip/groin pain (Fig. 8):

1. A fluid-sensitive sequence with a large FOV covering the whole pelvis, in the axial or coronal planes, to screen for soft-tissue and bone marrow oedema and other possible differential diagnosis
2. Unilateral hip, small FOV: should be centred in the magnetic field, high-resolution sequences of the symptomatic hip/area of interest
3. If assessing FAI: use radial imaging (either direct acquisition or 3D reformats) and fast axial sequence of the femoral condyles and femoral neck, to assess femoral torsion

MRA: When intra-articular disease is suspected, dMRA is the imaging study of choice, as both a **diagnostic** arthrography and **anaesthetic** injection can be combined into a single procedure. The main goals are (1) to achieve joint distension hence greater lesion conspicuity and (2) confirm the intra-articular origin of the athlete's pain. dMRA is superior to standard MRI for detection of labral lesions (compared sensitivity: 69–81% vs. 50%). dMRA also improves detection of ace-

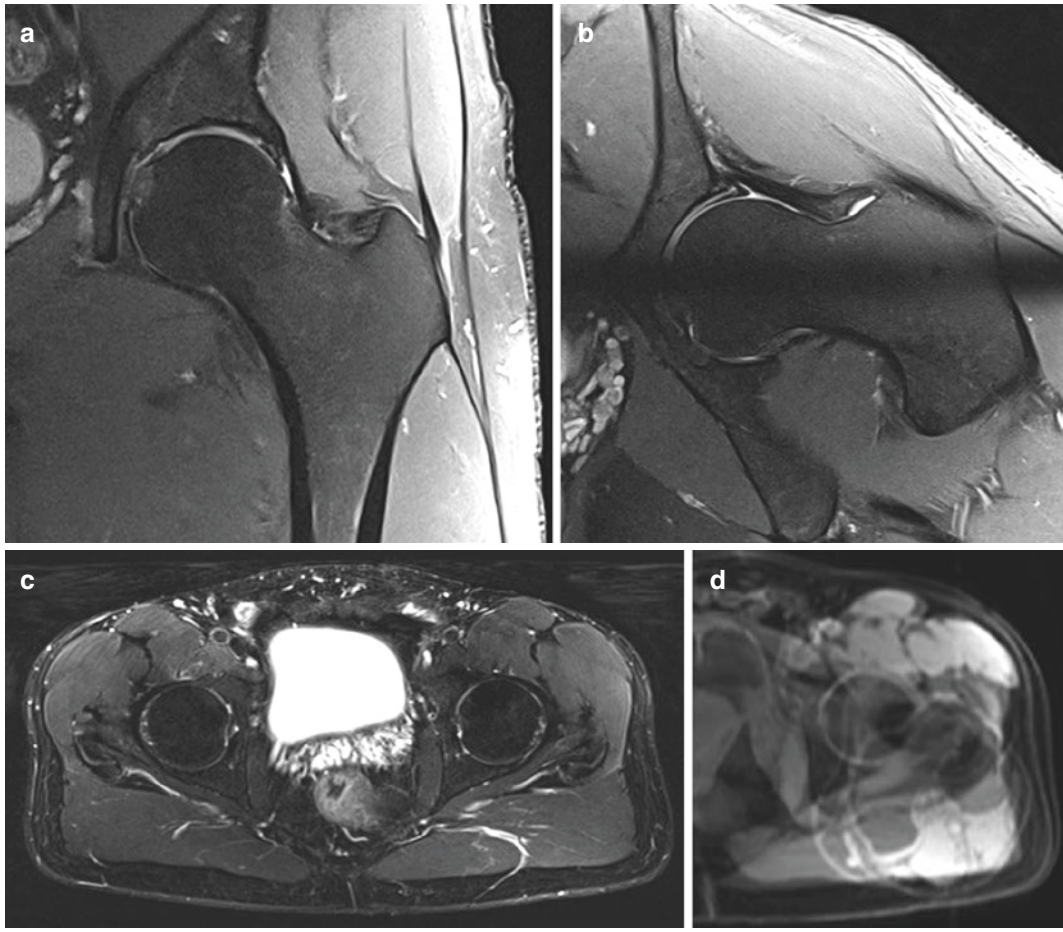

Fig. 8 (**a–d**) Sequences that should be included on the proposed routine MRI protocol for the assessment of hip and groin pain, comprise a pelvic fluid-sensitive sequence and unilateral 2D sequences (coronal, axial and sagittal are most useful). If FAI is suspected, femoral torsion assessment and radial imaging should be performed. (**a**) Unilateral FOV coronal fat-suppressed proton-density and (**b**) radial sequences might be used for hip detailed assessment. (**c**) A 2D large-FOV axial sequence of the pelvis is used to screen for other possible differential diagnosis. (**d**) Assessment of femoral torsion: different slices may be superimposed on a single image with post-processing software, making it easy to measure

tabular cartilage defects, while no advantage was found for cartilage defects on the femoral head in comparison with conventional MRI.

Technique basics: 8–14 mL of diluted gadolinium-based contrast agent (2.5 mmol/L solution or a 1:200–400 dilution in saline, depending on the contrast agent) mixed with 3 mL of anaesthetic (e.g. ropivacaine). The target zone for the needle is the centre of the femoral neck or the superolateral quadrant of the FH (preferred in a previous arthroscopy setting, because of possible adhesions between the joint capsule and the femoral neck).

Traction MRA: The main goal is to achieve joint distension and distraction, hence greater lesion conspicuity. There is evidence that dMRA with hip traction aids in the detection of cartilage delamination both at 1.5T and at 3T, by uncovering cartilage flaps that are usually less visible on the reduced FH (Llopis et al. 2008; Schmaranzer et al. 2014). It is still unclear whether traction at hip MRI should be used routinely and, if so, whether images should be obtained without and with traction or only with traction.

Technique basics: The combination of dMRA and leg traction (Llopis et al. 2008) may be

achieved by using orthopaedic traction devices (weight used for traction varies from 6 kg (Llopis et al. 2008), 8–10 kg (Suter et al. 2015) and 15–23 kg (Schmaranzer et al. 2014) and varying injected volumes of 10–14 ml to 18–27 ml.

5 Pathology

5.1 Hip Intra-articular

A combination of abnormal bony morphology, which is seen in a high percentage of athletes, and specific hip load may be related to the development of specific intra-articular hip pathologies in athletes (Heerey et al. 2019). Morphological hip shapes give rise to a continuous spectrum ranging from isolated instability to impingement with decreased mobility. Located at one end of this spectrum is DDH, and at the other is FAI. In many situations, however, there is a combination of several morphologies that may have greater or lesser clinical expression and determine the predominance of a mechanism of chondral and labral injury: instability or impingement (Tibor et al. 2013).

5.1.1 Acetabular Dysplasia and Instability (Fig. 9)

DDH is regarded as an insufficiency of contact between the articular surfaces (Wilkin et al. 2017). The surrounding soft tissues such as the labrum, joint capsule, ligaments and muscles are important static and dynamic hip stabilizers in sports. This combination usually results in a **static overload** of the acetabular roof and an instability or inability to maintain the centre of rotation of the joint fixed, resulting in lateral, superior and anterior migration of the FH. Clinically, DDH may be quite symptomatic (Wilkin et al. 2017) and has been reported as a risk factor for early-onset OA (Morvan et al. 2013). Recent advances in imaging of the dysplastic hip with CT scans have demonstrated that DDH is, in fact, a 3D deformity of the acetabulum and that multiple patterns of acetabular instability exist that may not be completely assessed on 2D imaging (Kraeutler et al. 2016).

The concept of **microinstability** is based on symptomatic hip laxity without marked subluxation. Aetiology may be either (1) traumatic (single or repetitive trauma) or (2) atraumatic (generalized laxity or DDH). Patients may feel hip unsteadiness, snapping, and/or pain during sports (Cerezal et al. 2012). Diagnosis is problematic, due to no established criteria.

Imaging:

Radiographs (AP pelvis), characterized by increased (1) inclination of the acetabular roof (acetabular inclination>13°) and/or (2) decrease in lateral and/or anterior coverage (established DDH: LCEA<20° or *borderline* DDH: 20<LCEA<25°). Additionally, (3) aspherical FH (usually "pear-shaped"), (4) *coxa valga*, (5) anteversion of the femoral neck and (6) retroversion of the acetabulum (Tibor et al. 2013) may be present.

MRI: most characteristic findings include (1) labrum hypertrophy, (2) "inside-out" acetabular cartilage lesions, (3) increased iliocapsularis-to-rectus-femoris ratio in hips with DDH (i.e. if the cross-sectional area of the iliocapsularis, measured in an axial slice through the centre of the FH, exceeds the cross-sectional area of the rectus femoris muscle, a DDH is said to be present in 89% of patients (Haefeli et al. 2015)).

– *Microinstability* suspected patients might have (1) a thickened iliofemoral ligament (anterior joint capsule) with irregularities on the undersurface of the anterior capsule, (2) an increased capsular volume, detectable during MRA and (3) larger or easier widening/distraction of a hip joint during traction MRA, suggesting hip laxity. Other findings associated with positive joint distraction were higher alpha angles, higher neck-shaft angles, smaller acetabular depths and hypertrophy of the LT (Cerezal et al. 2012).

5.1.2 Ligamentum Teres Pathology

Anatomy: The *LT* (Fig. 9) is a strong intra-articular ligament that is anatomically and biochemically similar to the anterior cruciate ligament of the knee (with an anterior and

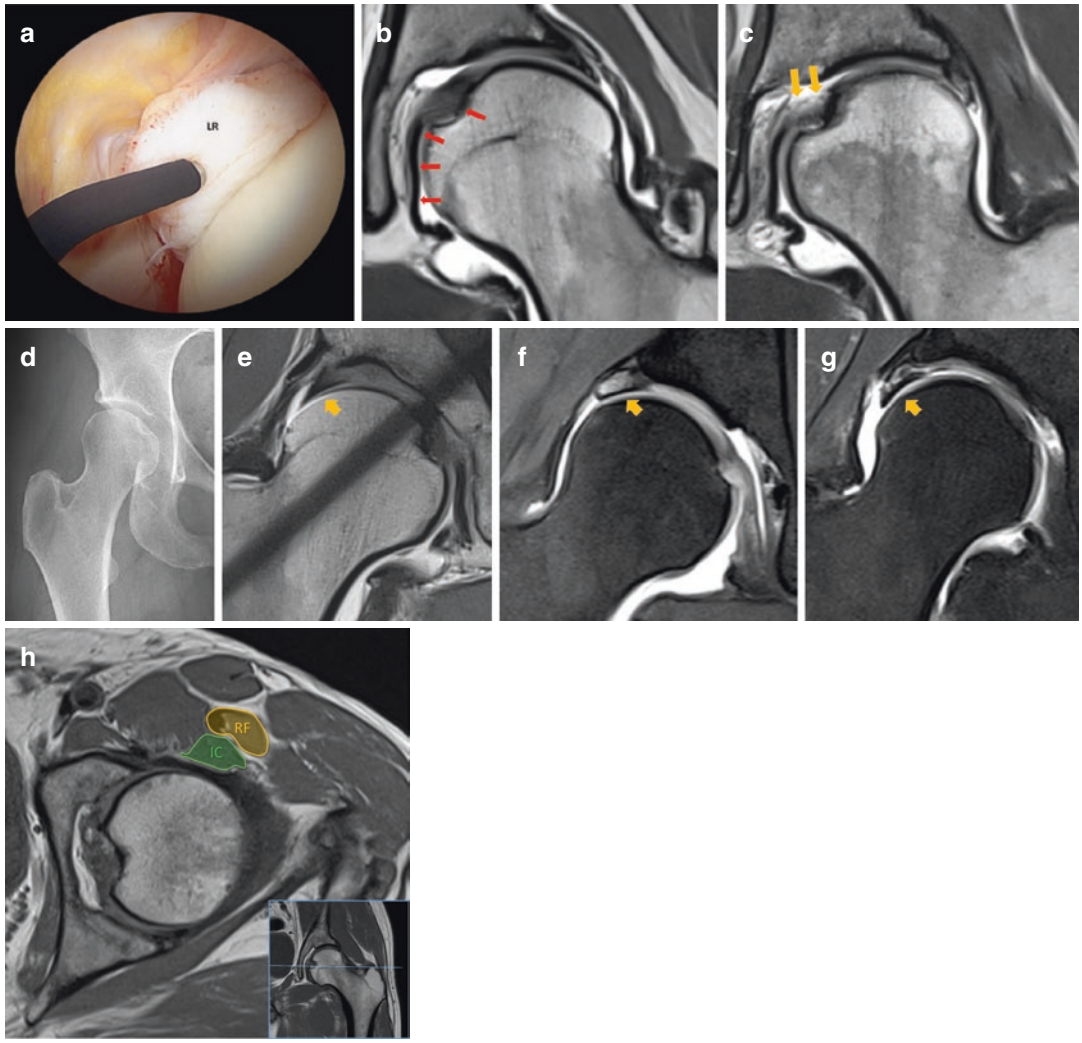

Fig. 9 (**a–h**) (**a**) Hip arthroscopic and (**b**, **c**) coronal MRA proton-density images of *ligamentum teres (LT)*. (**a**) Hypertrophic degenerated ligament (LR). (**b**) Normal hypointense LT (red arrows). (**c**) Degeneration and fraying (partial rupture) of the LT at the foveal insertion. Note the shallow acetabulum, highly located fovea, pear-shaped FH and labrum degeneration all characteristic of DDH in a 25-year-old ballet dancer. (**d**) Right hip AP radiograph on a 29-year-old ballet dancer shows characteristic DDH, with a shallow acetabulum, *coxa valga*, pear-shaped FH, decreased LCEA and increased acetabular inclination. (**e–g**) showing different stages of labral disease in DDH and microinstability, ranging from (**e**) labrum hypertrophy, (**f**) labrum hypertrophy and degeneration and ultimately leading to (**g**) tear of the capsular labral surface. (**h**) T1w axial MR image of the left hip at the level of the femoral head centre, in a 48-year-old patient with complaints of lumbar pain radiating to the hip. The contours of the rectus femoris (RF) and iliocapsularis (IC) are outlined. In this case, the cross-sectional area of the IC does not exceed that of the RF

posterior bundle). It arises from the transverse ligament and the ischial and pubic margins of the acetabular fossa. The ligament is trapezoidal at its base and runs to the FH, where it becomes progressively round or oval shaped and inserts into the *fovea capitis*. The **functions** of the LT might include: (1) intrinsic stabilizer that resists joint subluxation forces, (2) may play a role in nociception and coordination of movements, (3) provides blood supply to the developing FH and (4) helps to distribute synovial fluid within the hip joint via a "windshield wiper effect".

Why is it important?: Athletes with LT tears may develop pain and hip microinstability. When combined with sporting activities, this results in damage to the labrum and cartilage (explaining the high association rate between tears of the LT, labral tears and cartilage lesions) (Chahla et al. 2016). In symptomatic ballet dancers and mixed athletes, it was reported a prevalence of 44% LT tears per hip (compared to 21% in asymptomatic mixed athletes' population), reflecting the demands during sporting activity, particularly those sports requiring large ranges of hip motion.

Imaging: LT lesions are categorized arthroscopically as rupture (partial or complete) or degeneration. Complete rupture occurs after hip dislocation or after sudden external rotation episodes and are most commonly located near the fovea (showing a discontinuity of the ligament with lax contours).

On MRI, the normal LT is best visualized in the coronal/axial planes and has smooth borders and a homogeneous, hypointense structure on all sequences. Ligament degeneration is similar to tendons, ranging from mucoid degeneration to complete tear. MRA revealed better diagnostic performance compared with MRI regarding partial tears (increased intrasubstance signal intensity abnormality visualized on fluid-sensitive images as well as focal partial loss of continuity). For the detection of complete tears MRI and MRA imaging (67% sensitivity, 99–100% specificity) show similar good results.

5.1.3 Femoroacetabular Impingement

Concept: FAI is a motion-related clinical disorder associated with a triad of insidious onset of groin/hip pain, signs of limited motion and characteristic imaging findings (Ganz et al. 2003; Nepple et al. 2013), which results from a conflicting contact between the proximal femur and the acetabular rim (Ganz et al. 2003). This abnormal contact may ultimately lead to premature OA (Agricola et al. 2013a; Glyn-Jones et al. 2015; Mascarenhas et al. 2020a) (Table 11). FAI remains controversial in terms of true incidence, diagnosis, prognosis and management (Jung et al. 2011; Mascarenhas et al. 2016; Griffin et al. 2016). With the implementation of this concept, concerns have been raised about overdiagnosis and overtreatment.

Table 11 Summarizing table of the clinical, epidemiological and joint damage characteristics of femoroacetabular impingement

	Patient characteristics					**Intra-articular damage**	
	Sex	Age	Activity	Deformity	Mechanism	Early damage	Late damage
Cam FAI	Mainly male	Young	High-level athletes; high-impact sports	"Cam-type morphology": Eccentric femoral head with laterally increasing radius	Sheering forces inside the joint and damage to the acetabular cartilage; "inclusion injury"	Acetabular cartilage delamination "Outside-in" acetabular cartilage lesions	Large, full-thickness anterosuperior acetabular cartilage defects; Labral damage with undersurface tears; femoral head cartilage lesions
Pincer FAI	Mainly female	Middle aged	Recreational athletic activity	"Overcoverage" of the femoral head: *protrusio acetabuli*, acetabular retroversion	Linear impact between acetabular rim and FHN junction; "impaction injury"	Labral damage ranging from subtle shortening and rounding to extensive labral damage	Ossified bony rim with partially ossified labrum; cartilage damage at acetabular rim; "contrecoup" posteroinferior acetabular damage

5.1.3.1 Cam Mechanism

Cam impingement is caused by extra bone formation—a cam morphology—in the anterolateral FHN junction (Ito et al. 2001) (resulting in flattening or convexity). This morphology may cause impingement against the acetabular rim, especially during flexion and internal hip rotation (Matheney et al. 2013). The abnormal contact results in shear forces at the acetabular rim (Bowman et al. 2010) and is typically accompanied by labral tears (Bedi et al. 2008) and detachment of the acetabular cartilage from the subchondral bone (Bittersohl et al. 2009; Matheney et al. 2013). Acetabular cartilage delamination (Anderson et al. 2009) has characteristically been found in the anterosuperior quadrant of the joint, corresponding to the site where the deformity is forced into the acetabulum. Clinically it is associated with limited internal hip rotation (Nötzli et al. 2002) as well as hip pain (Allen et al. 2009) and OA (Agricola et al. 2013c) (Fig. 10).

Interestingly, a cam morphology might develop during skeletal maturation as a result of high-impact sporting activities, which would be a promising preventative opportunity to avoid the formation of this morphology and subsequent hip OA (Agricola et al. 2014; Mascarenhas et al. 2017).

5.1.3.2 Pincer Mechanism

Pincer impingement is caused by overcoverage of the acetabulum relative to the FH (either global or focal overcoverage). The hypothesis proposed by Ganz et al. (2003) states that the femoral neck causes an abnormal linear contact against the acetabulum during terminal motion of the hip. Initially, labral damage is the main characteristic as it might be crushed between the acetabular rim and the femoral neck (Fig. 11). When there are repetitive episodes of impingement, chondral damage might gradually develop throughout the acetabulum in a small, thin marginal strip (Beck et al. 2005). The relationship between pincer FAI and OA (Giori and Trousdale 2003; Bardakos and Villar 2009; Anderson et al. 2009; Gosvig et al. 2010; Nicholls et al. 2011; Agricola et al. 2013b) is still not clear, as even when overcoverage is symptomatic it seems to be protective in relation to advanced chondral aggression (Agricola et al. 2013b).

5.1.3.3 Diagnosis (Fig. 12)

Definition: There is no consensus regarding FAI preoperative diagnostic assessment and FAI case definition. The clinical concept of FAIS has been recently defined as a triad of: (1) symptoms, (2) physical signs and (3) imaging findings (Ganz et al. 2003; Sankar et al. 2013b; Griffin et al. 2016). This term and its definition build on the definitions of FAI from Ganz et al. (2003) and Sankar et al. (2013a) to ensure that there is a distinction between patients with FAIS and those with cam or pincer morphology but no symptoms.

Symptoms: The primary symptom of FAIS is motion-related or position-related pain in the hip or groin (Ganz et al. 2003), although it may also be felt in the back, buttock or thigh. In addition to pain, patients may also describe clicking, catching, locking, restricted ROM or giving way (Philippon et al. 2007; Ayeni et al. 2012; Nepple et al. 2014).

Signs: There is often a limited ROM, typically restricted internal rotation in flexion (Freke et al. 2016). Hip impingement tests usually reproduce the patient's typical pain, although the most commonly used test, flexion adduction internal rotation (FADIR), is sensitive but not specific (Reiman et al. 2015). With further and gradual internal rotation, hip pain is usually elicited (Shanmugaraj et al. 2018). When FAIS is suspected, it is important to examine gait, leg control, muscle tenderness and the FABER distance (flexion abduction external rotation).

Imaging (Mascarenhas et al. 2020a): Although paramount to diagnose FAIS, imaging assessment remains non-standardized with no consensus on which imaging modalities and parameters should be routinely assessed (Kassarjian 2019; Mascarenhas et al. 2019). Assessment should be based on radiographs (minimum required are AP pelvis and a Dunn 45°) and MRI in selected cases (Fig. 12). **Imaging goals** are: (1) to diagnose associated soft-tissue damage, (2) to detect early or focally advanced OA and (3) to assess patho-

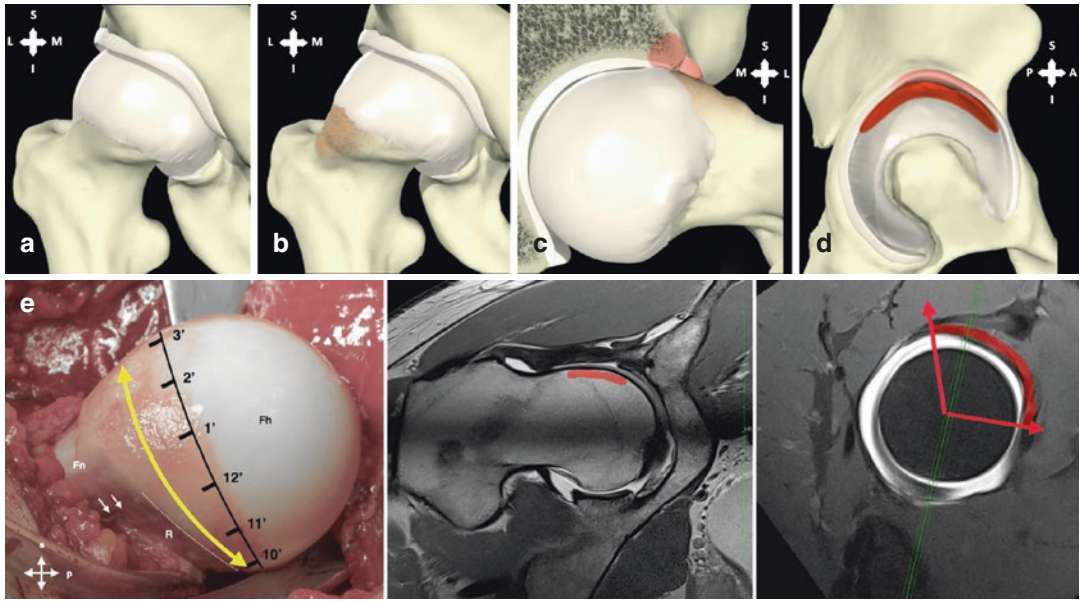

Fig. 10 (**a–e**) A schematic representation of the hypothesized mechanism of cam FAI. (**a**) Normal spherical femoral head and acetabulum, which is congruent with the femoral head, provides the hip a wide range of motion. (**b**) cam morphology can cause (**c**) Cam impingement against the acetabular rim, especially during flexion and internal rotation of the hip leading to a typical pattern of (**d**) acetabular chondrolabral damage anterosuperiorly. (**e**) dMRA examination and corresponding surgical hip dislocation procedure in a former 35-year-old elite soccer athlete. Sagittal fat-suppressed proton-density sequence (right image), corresponding radial proton-density-weighted sequence (middle image) and surgical hip dislocation caption (left image). Red curved line represents cam morphology assessed on the radial image at 1:00 o'clock and corresponding deformity in the sagittal plane extending from 11:30 to 3:00, later confirmed by direct observation. *dMRA* direct arthro-magnetic resonance, *FAI* femoroacetabular impingement

logic FAI hip morphologies. The differentiation or quantification of cam (femoral side), pincer (acetabular side) and their frequent combination is done on the basis of a predominance of either a femoral or an acetabular abnormality (Ganz et al. 2003; Pfirrmann et al. 2006; Mascarenhas et al. 2016; Griffin et al. 2016) (Table 12).

The radiologist should not state that abnormal signs and parameters are indicative of FAI/FAIS in an asymptomatic patient (as a substantial proportion of the general population have FAI-related morphology (Frank et al. 2015). Although these may be mentioned in the radiological report, interpretation should be undertaken in conjunction with the clinical history and physical examination (Frank et al. 2015; Mascarenhas et al. 2016; Mascarenhas et al. 2018b) (Fig. 12).

Diagnostic injections: A common clinical problem lies in determining whether pain (or surrogate symptoms) is really arising from the hip or from other structures in the groin and hip region. Frequently, image-guided local anaesthetic injections are useful in helping to resolve this situation (Kivlan et al. 2011; Khan et al. 2015), as they have both diagnostic and therapeutic value. Pain relief following a local anaesthetic injection would support a FAIS diagnosis, when the other diagnostic criteria are met (Griffin et al. 2016). Relief with an intra-articular injection was 90% accurate for predicting the presence of intra-articular findings during arthroscopy (Byrd and Jones 2004) (no relief is a negative predictor of short-term outcome following FAI surgery (Ayeni et al. 2014)).

Final conclusions (Mascarenhas et al. 2020a): Considering previously mentioned parameters and ongoing questions, some authors try to define what is normal and what is abnormal, also suggesting possible combinations of morphology

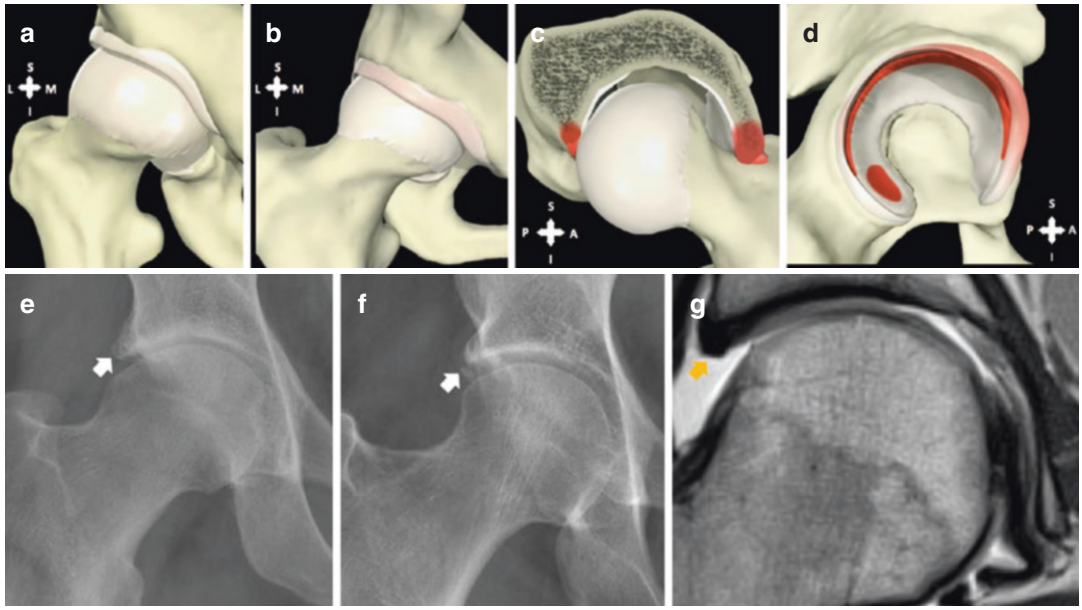

Fig. 11 (**a–g**) Schematic representation of the hypothesized mechanism of pincer FAI. (**a**) Normal spherical femoral head and acetabulum, which is congruent with the femoral head, provides the hip a wide range of motion. (**b**) A pincer deformity can cause pincer impingement against the femoral neck, (**c**) especially during terminal flexion of the hip leading to (**d**) a typical pattern of circumferential acetabular cartilage damage. (**e**) Acetabular rim ossification and (**f**) labral ossification associated with acetabular overcoverage, findings usually seen in Pincer FAI. (**g**) MRA of the right hip of a female 26-year-old field hockey player, same athlete as in (**f**), revealing (1) a small sized globular labrum with (2) peripheral cartilage thinning and (3) overcoverage of the acetabulum

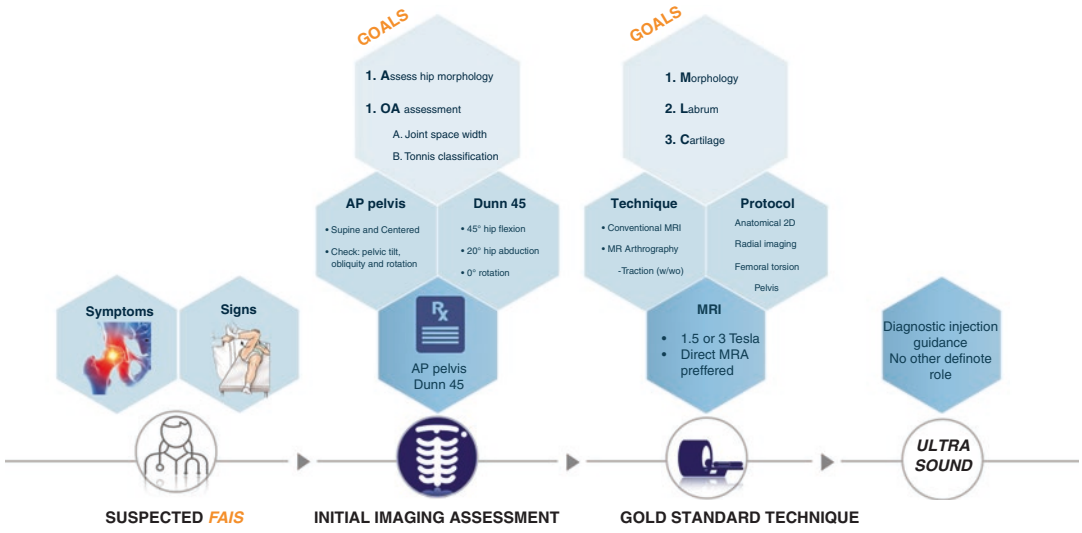

Fig. 12 Diagnostic pathway assessment for FAIS (Mascarenhas et al. 2020a, b)

that characterize classically and recently described pathological entities (Sutter and Pfirrmann 2017) (Tables 13 and 14).

5.1.3.4 Association Between FAIS and Sport Activities

Genetics, sex and physical activity influence

Table 12 Criteria proposed for classifying pincer and cam morphology in a research/clinical trial setting (regardless of the symptomatic state) (Mascarenhas et al. 2020a, b)

Imaging classification criteria for hip morphology			
Cam morphology *(1 or more)*		**Values**	**Technique**
Osseous convexity of the FHN junction		+	Radiography *(preferably AP pelvis and Dunn 45°)* CT or MRI *(with radial imaging)*
Alpha angle		*≥60°*	
FHN offset[a] *FHN offset ratio*[a]		<8 mm *≤0.15*	*Radiography (cross-table view)* CT or MRI *(with radial imaging)*
Pincer morphology		**Values**	**Technique**
Global pincer *(1 or more)*	*Protrusio acetabuli*	+	Radiographs *(standardized AP pelvis)*
	W-CEA	≥40°	
	W-CEA[a] Acetabular index[a]	≥35° <0°	
Global retroversion *(all criteria)*	Cross-over sign	+	Radiographs *(standardized AP pelvis)*
	Posterior wall sign	+	
	Ischial spine sign	+	
Focal pincer[b] *(1 or more)*	Cross-over sign	+	Radiographs *(standardized AP pelvis)* *Confirmation with CT or MRI recommended*
	Acetabular version	<0°	CT or MRI (*corrected for tilt on coronal plane and rotation on the axial plane)*

FHN femoral head-neck, *W-CEA* Wiberg centre-edge angle, *COS* cross-over sign, *CT* computed tomography, *MRI* magnetic resonance imaging

[a]Both measurements necessary to satisfy this criterion

[b]Corresponding to cranial retroversion in non-dysplastic hips

whether or not a cam morphology develops (Nepple et al. 2015). Accordingly, a strong association between sports and the development of FAIS exists, with high-level male athletes having 2–8 times more likelihood in developing a cam-type morphology (Nepple et al. 2015). Specifically, the prevalence of cam morphology is as high as 89% in athletes participating in activities that result in impact loading of the hip as compared to only 9% in non-athletic controls (Sutter and Pfirrmann 2017).

1. **Activity Type**:
   (a) Weight-bearing impact sports: High-level athletes participating in activities that require high flexion together with rotational movements of the hip (hockey, basketball, and possibly soccer) are at an increased risk of physeal abnormalities that result in a cam morphology at skeletal maturity (e.g. ice hockey players are 4.5 times more at risk than skiers).
   (b) Extreme and supraphysiologic hip motion: High-level athletes requiring beyond physiologic hip joint range of motion may not exhibit the typical hallmarks of FAIS but rather develop a type of atypical hip impingement (resembling that of Pincer-type) that is associated with ballet dancing, ice skating or martial arts.
2. **Activity Level**: A dose–response relationship exists; elite soccer players who practiced more than three times a week before the age of 12 years were 2.6 times more likely to have a cam morphology than players that practiced three times or less.
3. **Window of "increased-**risk**":** particularly between the age of 12 years and the closure of the growth plate, athletes with previously normal hips may develop a cam-type morphology of the proximal femur, as this morphology mainly develops when the proximal femoral growth plate is open. Prevention of potentially serious conditions such as cam morphology is a major sports medicine priority, although currently there is no recommendation on how and when to adjust athletic activities (Sutter and Pfirrmann 2017).

Table 13 Possible combinations of morphology and angular parameters that characterize pathological entities

	Normal	Dysplasia	*Cam* FAI	*Pincer* FAI
Acetabular inclination	0–10°	>10°	Variable	<0°
Lateral centre-edge	25–30°	<20°	Variable	>35°
Alpha angle	<55°	Variable	>60°	Variable
Retroverted acetabulum	Absent	Up to 1/3 of patients	Variable	Frequent
Femoral version	15–20°	Mostly anteverted	Variable	Variable

Table 14 Overview of most relevant femoral and acetabular parameters, notes and recommendations for research and clinical practice

Parameter	Measurement values to consider	Preferred measurement method	Notes and recommendations
Alpha angle	• >60° indicates cam morphology (at any location around the anterosuperior FHN junction)	• Radial imaging • AP pelvic radiograph and Dunn 45° view	• State measurement location • Measure and report where maximal deformity is noted around the FHN junction
Neck-shaft angle	• AP Pelvic radiograph: 120–135° • CT: 120–140°	• AP pelvic radiograph • CT and/or MRI in the coronal femoral neck plane	• Hip rotation and femoral torsion influence assessment • Vary with sex and age
Femoral torsion	• 13 ± 10° (Reikeras method)	• CT or MRI	• Clearly define measurement method
W-CEA	• <20°: undercoverage • 20–25°: *borderline* undercoverage • 25–39°: normal coverage • ≥40°: overcoverage	• AP pelvic radiograph	• Clearly define whether W-CEA or LCEA is measured • Represents superior and lateral coverage
Acetabular index	• >13°: undercoverage • <0°: overcoverage	• AP pelvic radiograph	• Represents acetabular inclination
Protrusio acetabuli	• Present or absent	• AP pelvic radiograph	• Represent a qualitative sign of global overcoverage • Always pathological
Cross-over sign **Posterior wall sign** **Ischial spine sign**	• Present or absent	• AP pelvic radiograph	• Represent qualitative signs of version • COS indicative of Focal Pincer (acetabular retroversion) • When all signs are present indicative of Global Pincer (global retroversion)
Acetabular version	• Cranial version < 0°: Focal retroversion	• CT or MRI	• Clearly define measurement method • Indicative of Focal Pincer (acetabular retroversion)

COS cross-over sign, *CT* computed tomography, *FHN* femoral head-neck junction, *LCEA* lateral centre-edge angle, *MRI* magnetic resonance imaging, *W-CEA* Wiberg centre-edge angle

5.1.4 Labrum Pathology

5.1.4.1 Anatomy and Imaging Description

The labrum (Fig. 13) is a fibrocartilaginous structure, usually with a triangular cross section (morphology can vary widely) inserted in the osseous acetabular rim (Seldes et al. 2001). The articular or internal surface is in continuity with the acetabular cartilage and the capsular or external surface is attached to the articular capsule. Inferiorly, the labrum is in continuity with the transverse ligament. The labral vascular supply arises from a periacetabular vascular ring with radial branches that course over the capsular surface of the labrum. As it has its own inner-

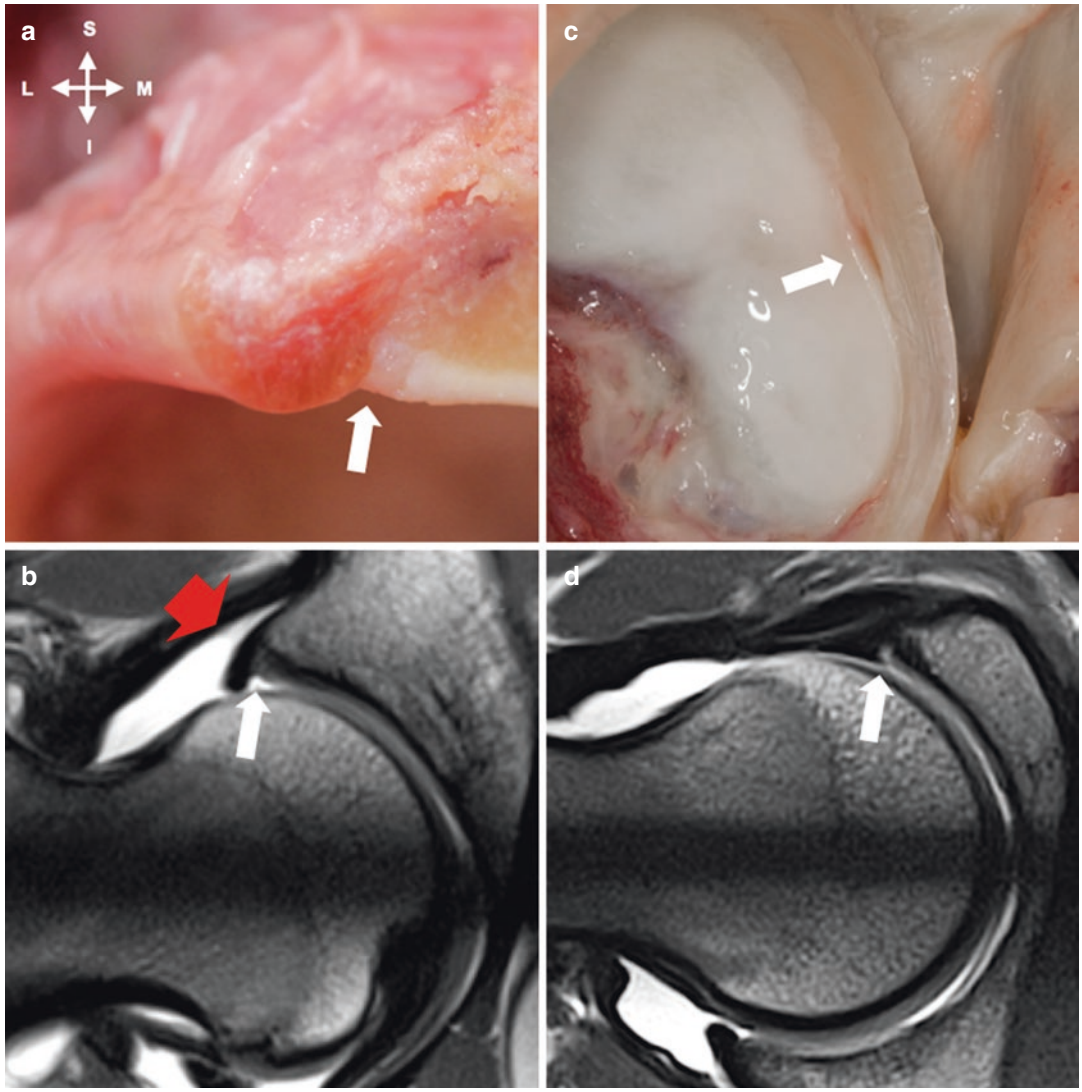

Fig. 13 (**a–d**) (**a**) Macrophotography of the acetabular labrum section. There is a normal depression in the chondrolabral transition and the continuity of the labral tissue with the bone and cartilage surface (arrow). (**b**) Radial proton-density MRA image of the same groove as in (**a**) (arrow) at the postero-superior quadrant. A peri-labral recess is also shown (red arrow). This variant should not be confused with labrum rupture. (**c**) Detail of the anterior articular surface where we frequently observe a more pronounced depression in the chondrolabral continuity (arrow). (**d**) Radial proton-density MRA image of the same recess as in (**c**) (arrow) at an anterior position. *S* superior; *I* Inferior; *M* medial; *L* lateral, *MRA* arthrography magnetic resonance imaging

vation (coming from the obturator nerve; both proprioceptors and nociceptors), when injured the labrum can be an important source of pain (Seldes et al. 2001) and also might explain the decreased proprioception and pain in an athlete with a torn labrum. Like the knee meniscus, the labrum may have the greatest healing potential at the peripheral capsulo-labral junction (Seldes et al. 2001).

Localization: Use either (1) the clock-face method, where 3 o'clock corresponds to anterior and 12 o'clock to a superior position, regardless of laterality of the hip (Blankenbaker et al. 2007), or the (2) a geographic zone classification system

modified from the acetabular zone method described by Ilizaliturri Jr. et al. (2008).

5.1.4.2 Normal Variants (Fig. 13)

Reflect variations of the normal anatomy with no clinical consequences, found in up to 25% of patients at arthroscopy. **Types:** (1) *Perilabral recess*: at the capsular surface of the labrum, between the joint capsule and the labrum. It is present circumferentially with variable depths and usually easily distinguishable from a labral tear. (2) *Sublabral recesses*: found arthroscopically (18–22%) at any location (Saddik et al. 2006), although typically found at the 4 o'clock position or most frequently (48%) at a posteroinferior location at the insertion of the transverse ligament. It is a well-defined cleft between the labrum and the acetabular hyaline cartilage with smooth edges, no signs of inflammation and no labral instability on probing.

5.1.4.3 Labral Tears (Fig. 14)

General considerations: Known causes are direct trauma, capsular laxity, FAI and instability. A combination of the dynamic movements performed in sport and the high prevalence of altered bony hip morphology, in particular cam morphology, is believed to place athletes at greater risk (Agten et al. 2016). Isolated labral tears at an anterior position have been associated with iliopsoas impingement (Blankenbaker et al. 2007). About half of all labral tears are full-thickness tears.

In individuals without pain, a labral tear prevalence per person of 56% was reported while in persons with pain prevalence was 64% (Heerey et al. 2019). Specifically, in sports (such as football, golf and tennis), it appears that athletes do not have a higher prevalence of labral tears than non-athletic individuals regardless of pain status, highlighting a potential discordant relationship between tears and pain (hence only to be consid-

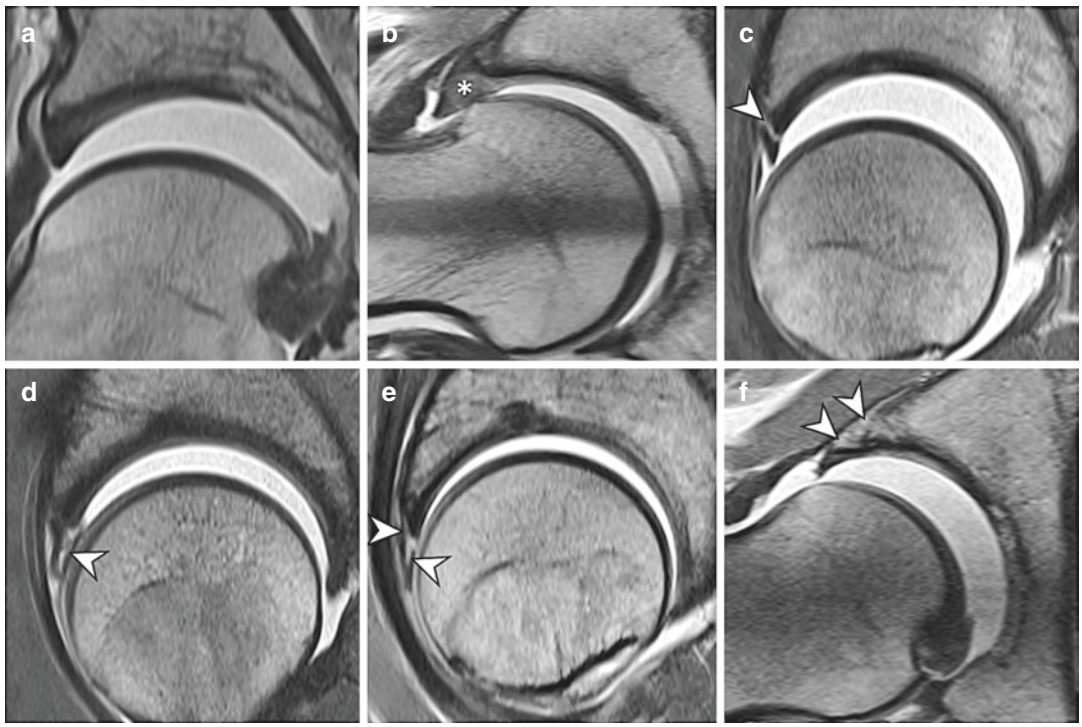

Fig. 14 (**a–f**) Classification of labrum damage patterns (traction MRA). (**a**) Normal labrum; (**b**) intrasubstance labrum degeneration (*); (**c**) labral-chondral separation (=labral detachment) (arrowhead); (**d**) intrasubstance labrum tear (arrowhead); (**e**) complex labrum tear (labral-chondral separation and intrasubstance labrum tear) (arrowheads); (**f**) labral ossification (arrowheads). *MRA* arthrography magnetic resonance imaging

ered relevant with an adequate patient history and suggestive clinical examination).

Localization: anterosuperior quadrant (84–86%; lower compressive elastic and lower tensile modulus compared with other parts of the labrum, favour tears in this location), posterosuperior (16%), anteroinferior and posteroinferior tears (rare) (Sutter et al. 2014).

Differential diagnosis: A recess (1) is located at the base of the labrum, (2) is linear in shape (labral tears may extend into the labral substance), (3) has smooth edges (unlike labral tears, that often have irregular borders), (4) do not extend through the full-thickness of the labrum and (5) are not associated with paralabral cysts.

Imaging and Classification (Fig. 14): Typically, in pincer-type FAI the labrum shows thinning, intrasubstance fissuring, and fraying, while in cam-type FAI there is usually a chondrolabral avulsion. Superior labral tears are best identified on dedicated coronal images, whereas anterosuperior labral tears are best seen on sagittal and/or axial oblique images. Posterior or anterior tears are typically most conspicuous on axial oblique images. Several surgical and MRI-based classifications for description of labrum lesions have been proposed (Czerny et al. 1996; Seldes et al. 2001; Beck et al. 2005). Due to the weak agreement between these classifications, imaging assessment of the acetabular labrum may instead focus on an accurate descriptive report (Schmaranzer et al. 2017; Mascarenhas et al. 2020a) (Table 15).

5.1.5 Cartilage Pathology

5.1.5.1 Anatomy and Imaging Description

Hyaline cartilage consists of four discrete layers: superficial, transitional, deep and calcified. The volume of chondrocytes is highest in the transitional and deep layers, and the orientation of collagen changes at each level. A tidemark between the deep and calcified layers acts as a barrier to vascular penetration.

5.1.5.2 Normal Variants (Fig. 15)

- *Supraacetabular fossa* (10% of individuals): anatomic variant located in the acetabular roof (12 o'clock), probably representing an age-related developmental morphologic variation. Type 1: defect in the subchondral bone and cartilage, filled with joint fluid; Type 2: defect only in the subchondral bone, filled with cartilage (Dietrich et al. 2012).
- *Superior acetabular roof notch* (17% of men and 22% of women on radiographs): sharply delineated, more longitudinally, fluid- or fat-filled pit in the medial aspect of the acetabular roof (Agten et al. 2016).
- *Stellate lesion* (or stellate crease): area of the acetabular roof without cartilage coverage, located more medially than a supraacetabular fossa. Some authors believe it is a residuum of a healed supraacetabular fossa or a healed roof notch (Philippon et al. 2014).

Table 15 Recommended descriptors of labral injury (Mascarenhas et al. 2020a, b), based on inferential evidence (Schmaranzer et al. 2014; Saied et al. 2017; Crespo-Rodríguez et al. 2017)

Parameters	Description	MRI findings
Location/extent	Quadrant description	**Primary findings:** • Increased intra-substance signal intensity • Surface irregularity, truncation, or diminutive appearance • Linearly increased signal intensity traversing the substance of the labrum or at the chondrolabral junction • Contrast material extending into the tear defect (MRA) **Secondary findings:** • Adjacent cartilage abnormalities • Paralabral cyst formation • Adjacent bone oedema
Shape and width	Triangular/round; mm	
Calcifications and ossifications	Location and Size	
Lesion patterns	1. Intrasubstance labrum degeneration	
	2. Intrasubstance labral tear	
	3. Labral-chondral separation (= labral detachment)	
	4. Complex labral tear (both intrasubstance tear and labral-chondral separation)	
	5. Labral ossification	

MRI magnetic resonance imaging, *MRA* arthrography magnetic resonance imaging

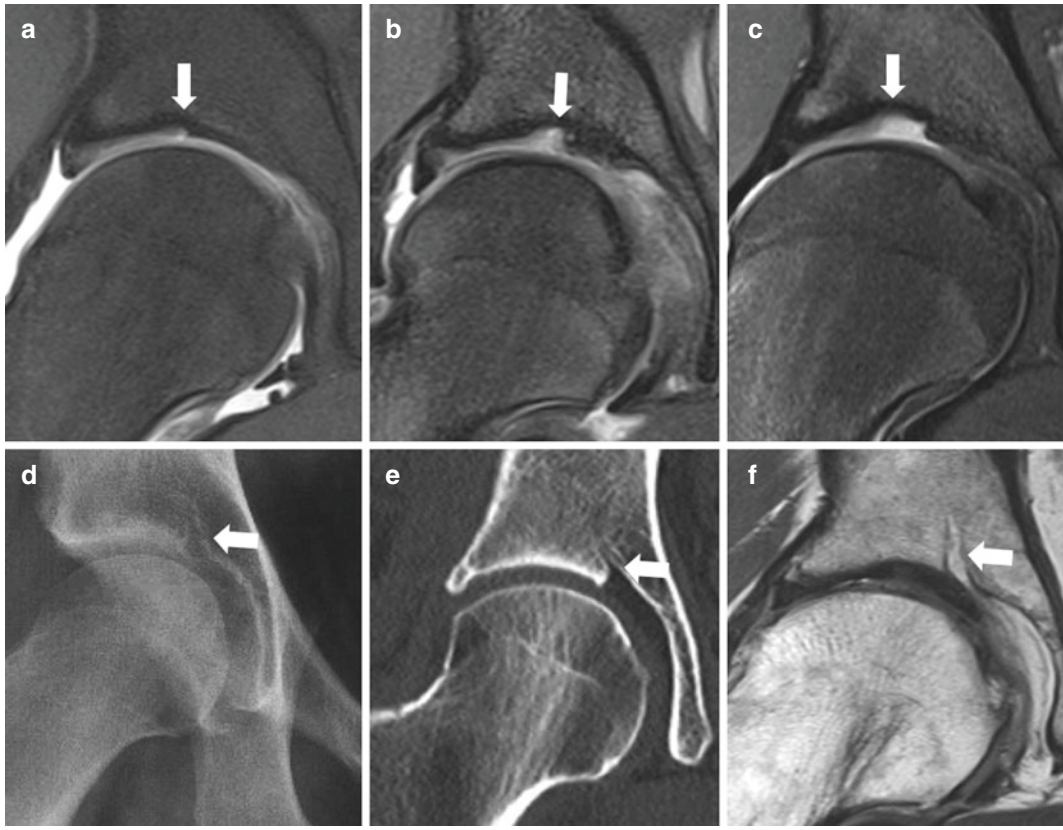

Fig. 15 (**a-f**) (**a–c**) Coronal proton density fat-supressed images with supraacetabular fossa examples with varying degrees and depth. (**d–f**) Superior acetabular roof notch seen on (**d**) radiograph, (**e**) CT and (**f**) MRI (fat-filled superior acetabular roof notch)

5.1.5.3 Cartilage Injury

General considerations: Cartilage defects are commonly seen in athletes, both symptomatic (25–40% of athletes, as opposed to 64% of all symptomatic populations) and asymptomatic (10% of athletes and 12% of all asymptomatic populations) (Heerey et al. 2019). Thus, it could be considered that cartilage defects might contribute to hip-related symptoms and reduction in function, with a trend highlighting a greater prevalence of acetabular chondral lesions observed in symptomatic individuals. Paradoxically, articular cartilage is deficient of neural and vascular supply, rendering it unable to produce pain, reflecting the variable relationship seen between cartilage defects and pain. Conceptually, injury to the articular cartilage affects joint homeostasis, in addition to biomechanical and neuromuscular function. This alteration in joint function combined with athletic activity may accelerate hip joint degenerative change, which is known to occur more frequently in retired athletes.

In athletes, cartilage damage can either result from (1) direct impact injury or (2) underlying bone deformities (Kaya et al. 2016). Cam morphologies lead to cartilage delamination (in 44–52% of FAI cam cases), most often located anterosuperiorly adjacent to labral tears (Anderson et al. 2009). Conversely, acetabular overcoverage may have some protective effect against cartilage delamination, although cartilage lesions are found in the posteroinferior quadrant of Pincer-type FAI patients. Parafoveal cartilage defects posterosuperiorly on the FH have been described in active patients with cam-type FAI participating in activities requiring repetitive, fast and forceful hip flex-

ion (American football, soccer, hurdles and martial arts) (Zaltz and Leunig 2012).

Imaging: Cartilage assessment can be performed with multiple imaging modalities.

- *Radiographs* demonstrate secondary signs of cartilage loss, such as decreased JSW, subchondral sclerosis and marginal osteophyte formation.
- *MRI*: imaging technique of choice. Given the high signal-to-noise ratio and contrast, 2D or 3D gradient-echo or FSE proton density-weighted sequences are the basic imaging techniques used in clinical practice. Additionally, 3D imaging is useful for cartilage volume and thickness measurements.
- *dMRA:* for detecting cartilage disease the sensitivity/specificity may be as high as 79%/94%, respectively (Crespo-Rodríguez et al. 2017). Chondral abnormalities are recognized as (1) focal signal intensity abnormality, (2) contour defects, (3) thinning compared with normal adjacent cartilage, and/or (4) gadolinium contrast material outlining the articular margins and filling surface irregularities or cartilage defects. On fat-supressed proton density and T1w MR images, low-signal intensity within the normally intermediate intensity acetabular cartilage is a helpful sign with high specificity (90–95%; although with low sensitivity, 22–74%) for cartilage delamination detection.
- *Advanced biochemically sensitive MRI techniques*—such as dGEMRIC, T2, T2* and T1ρ mapping, can distinguish subtle early cartilage matrix alterations, thereby acting as tools for early disease detection and monitoring. Despite mapping variations that mirror anatomical differences in various zones and regions of hip joint, there are still many unanswered questions including the standardized application of these techniques and cut-off values to provide an algorithmic cartilage damage-based approach to managing injury. Further evidence that address protocol issues regarding reproducible, objective, and meaningful evaluation of articular hip joint cartilage are necessary (Hemke et al. 2018).

Classification: Description of the location, surface and pattern/grade is recommended (Mascarenhas et al. 2020b) (Table 16 and Fig. 16).

Table 16 Recommended descriptors of cartilage lesions on a hip MRI study (Mascarenhas et al. 2020a, b)

Parameters	Description	Importance
Location[a]	Quadrant description	Diagnostic and surgical planning implications (Zaltz et al. 2014): • location supports a cam/pincer FAI mechanism • posterior lesions are difficult to access by arthroscopy
Surface side[a]	Acetabular or femoral	Surgical planning and prognostic implications as femoral cartilage damage is: • A poor prognostic factor • Easier to treat with open surgery than with arthroscopy
Extent[b]	Any MRI cartilage damage extending <2/>2 "hours" on the clock-face	Long-term outcome of FAIS surgery is worse if cartilage damage is greater than 60° around the clock face (Hanke et al. 2016)
Pattern[a]	*Grades:* 1. no damage 2. any cartilage damage 3. complete cartilage loss *Other descriptors:* 1. peripheral (chondrolabral junction) vs. central 2. any cartilage damage: if possible add details, such as "superficial cartilage damage" or "cartilage delamination"	Surgical planning implications: • Complete cartilage loss in the chondral-labral junction: acetabular rim trimming • Cartilage damage centrally located: cartilage repair procedure

MRI magnetic resonance imaging, *FAI* femoroacetabular impingement, *FAIS* femoroacetabular impingement syndrome
[a]Recommendations based on inferential evidence
[b]Recommendations based on outcome evidence

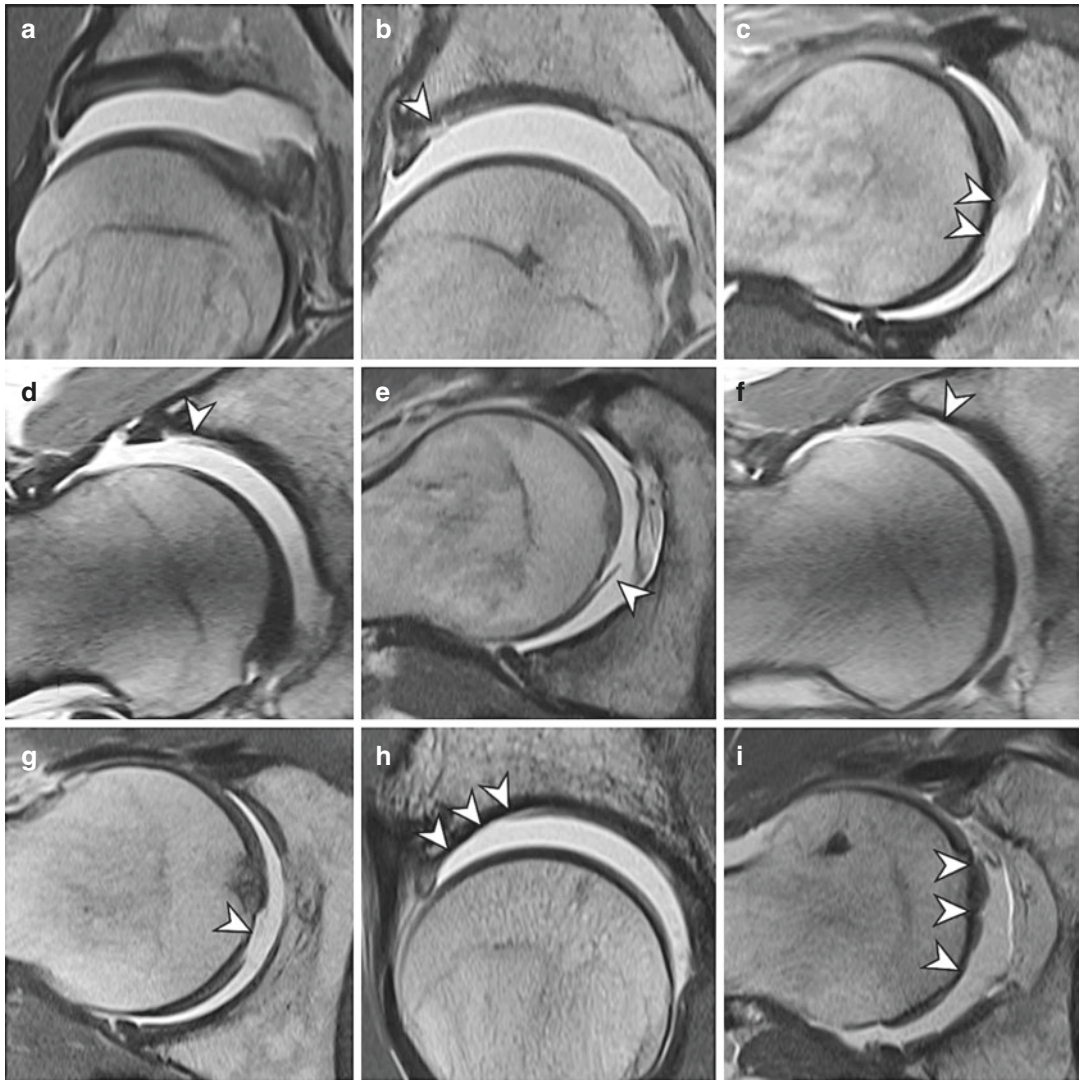

Fig. 16 (**a–i**) Classification of femoroacetabular cartilage damage patterns (traction MRA). (**a**) **Grade 1**: no damage (normal cartilage thickness). **Grade 2**: any cartilage damage, (**b**) focal acetabular and (**c**) femoral partial-thickness cartilage lesion (arrowheads). **Grade 2**: any cartilage damage, (**d**) acetabular cartilage delamination involving the chondral-labral junction and (**e**) femoral cartilage delamination (arrowheads). **Grade 3**: complete cartilage loss, focal full-thickness (**f**) acetabular and (**g**) femoral cartilage lesion (arrowheads). **Grade 3**: complete cartilage loss, diffuse full-thickness (**h**) acetabular and (**i**) femoral cartilage lesion (arrowheads). *MRA* arthrography magnetic resonance imaging

5.1.6 Hip Osteoarthritis

General considerations: Hip OA is not commonly seen in athletes who are currently active at an elite/professional level, even if they have hip and groin pain. The prevalence of hip OA in asymptomatic senior athletes appears similar to that of older non-athletic populations (17% vs. 15%). However, after retirement elite male athletes have a greater prevalence of OA and likelihood of undergoing hip arthroplasty (odds ratio = 2.5) (Gouttebarge et al. 2015). Interestingly, radiographic early hip OA may be seen in younger athletes regardless of the presence or absence of pain, highlighting a discordant relationship between radiographic features observed in early hip OA and pain in active athletes.

What is OA?—It is the most frequently occurring chronic joint disease worldwide (Hawker and Stanaitis 2014). Clinically it is characterized by pain, stiffness and loss of function (Hawker and Stanaitis 2014), and on a tissue level by loss of cartilage, osteophyte formation, subchondral sclerosis and cyst formation (Wang et al. 2016). OA has a detrimental impact on quality of life and represents an increasing economic burden to health systems (Turkiewicz et al. 2014) (both direct and indirect costs).

The lack of a precise definition of the disease has made it difficult to determine the prevalence of OA. There is often a discrepancy between the clinical presentation and the radiographic evidence of OA. In research, the commonly used definitions of hip OA include (1) "symptomatic OA" (ACR criteria) (Hunter et al. 2011), (2) "radiographic OA" (quantified by the Tonnis or Kellgren and Lawrence scale (Kellgren et al. 1963)) or (3) total joint replacement as a result of OA (Hunter et al. 2011).

How to assess?—An AP pelvic radiograph with a standardized technique should be preferably used for measuring joint space width (JSW) and joint space narrowing (JSN) (Fig. 17). Radiographic measurements of JSW and JSN are currently the best way to assess structural progression and disease severity. (Lane et al. 2015). Alternative projections (e.g. false profile) can evaluate JSW/JSN in locations other than the superior aspect of the joint and, when combined with an AP view, may increase sensitivity to detect structural alterations (Maheu et al. 2005). Tönnis classification represents current practice in HPS, although evidence supports that the "minimum JSW" may be preferable compared to the other classification systems (Table 17).

However, considering that several studies used radiographs and these are insensitive to early cartilage damage, the real disease prevalence in athletes may be underestimated. The use of imaging methods with greater sensitivity to early features of OA may be important for identifying athletes at risk of progression to hip OA.

5.2 Hip Peri-articular Pathology

5.2.1 Greater Trochanteric Pain Syndrome

What is it?—Greater trochanteric pain syndrome (GTPS) refers to the clinical manifestation of dis-

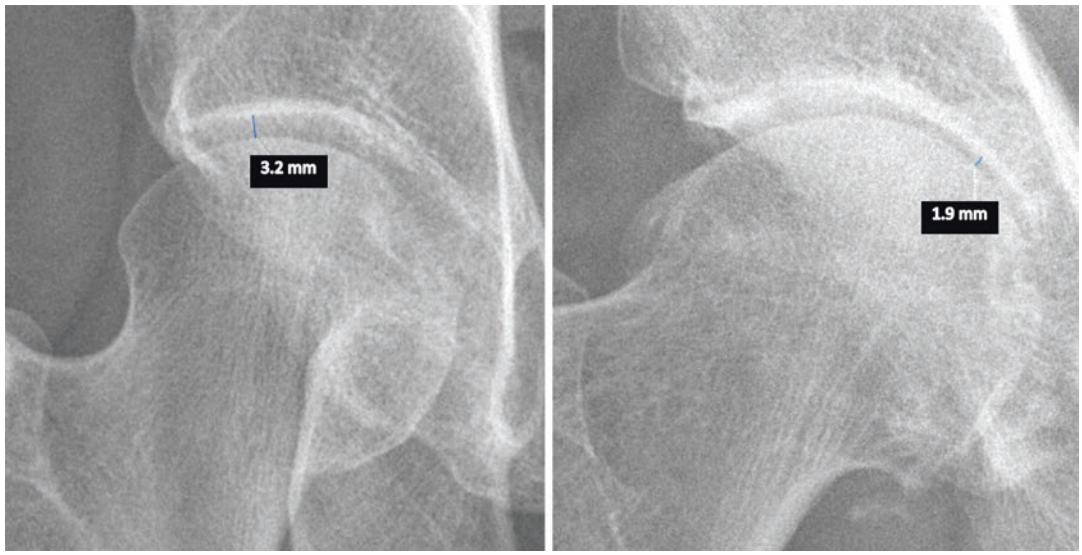

Fig. 17 Examples of measurement of minimum joint space width. This measurement should be carried out in an AP pelvic or hip-centred radiographs. Joint space width should be measured where maximal joint space narrowing is observed, preferably at the weight-bearing region of the hip joint

Table 17 The Tönnis and the Kellgren and Lawrence classifications of osteoarthritis (Busse et al. 1972; Schiphof et al. 2008)

	Tönnis	Kellgren and Lawrence
Grade 0	No signs	No features
Grade 1	Slight narrowing of joint space, slight lipping at joint margin, slight sclerosis of femoral head or acetabulum	Doubtful narrowing of joint space and possible osteophytic lipping
Grade 2	Small cysts, increased narrowing of joint space, moderate loss of femoral head sphericity	Definite osteophytes and possible narrowing of joint space
Grade 3	Large cysts, severe narrowing or obliteration of joint space, severe deformity of femoral head, avascular necrosis	Moderate multiple osteophytes, definite narrowing of joint space, some sclerosis and possible deformity of bone ends
Grade 4	–	Large osteophytes, marked narrowing of joint space, severe sclerosis and definite deformity of bone ends

ease about the GT, presenting with lateral hip pain and focal tenderness on palpation. Abnormalities of the hip abductor tendons (namely *gluteus minimus* (Gmin) and *gluteus medius* (Gmed) tendon) and the GT bursa are the most common aetiologies. It is a common cause for lateral hip pain in active middle-aged women and an increasingly recognized entity in athletes, mainly runners and ballet dancers (Nawabi et al. 2014; Cruz et al. 2019).

What causes it?—The main cause is usually a tendinopathy resulting from chronic repetitive microtrauma of the abductors followed by iliotibial band (ITB) hypertrophy, and, to a lesser extent, abductor tendon tears and degeneration (especially the Gmed and Gmin). GTPS also includes (1) trochanteric bursitis, (2) calcific tendinosis and (3) *coxa saltans*. Two or more of these findings may be found jointly. Paratendinopathy is the earliest manifestation (fluid-like signal intensity superficial to the tendons on MR) (Boric et al. 2019).

Anatomy (Hirschmann et al. 2017)**:** The *GT* has four facets: the anterior, lateral, posterior and superoposterior facets. The Gmin tendon inserts on the anterior facet. The Gmed tendon has two attachments: the anterior (attaches broadly on the lateral facet) and the posterior portions (narrower attachment on the superoposterior facet). *Bursae*: (1) subgluteus minimus bursa (between the Gmin tendon/anterior facet), (2) the subgluteus medius bursa (between the Gmed tendon/lateral facet) and (3) trochanteric bursa (superficial to the posterior facet and deep to the gluteus maximus muscle).

Imaging (Boric et al. 2019):

- *Radiographs:* usually normal, although calcifications adjacent to the GT may be seen.
- *US*: Sonopalpation is useful for reproducing pain. *Tendinopathy* is defined by tendon thickening and heterogeneous hypoechogenicity. *Peritendinous hyperaemia* may be demonstrated at Doppler. *Enthesopathy* is manifested by bony irregularity at the GT facet insertion. Anechoic defects within the tendon are consistent with tendon tears (partial or full-thickness).
- *MRI:* gluteal *tendinopathy* is characterized by tendon thickening and increased intrasubstance signal intensity on T2-weighted images, with peritendinous oedema representing *paratendinopathy*. A focal defect in tendon fibres suggests a partial-thickness *tear*. In the setting of complete tendon tear, there is often (1) retraction of torn fibres with fluid and/or granulation tissue filling the tear defect, (2) a "bald" GT facet sign when there is complete absence of the Gmed or Gmin tendon insertions, similar to the shoulder rotator cuff.

5.2.2 Snapping Hip

What is it?—It is characterized by sudden painful, audible snapping around the hip, typically seen in young athletic adults. Painful symptoms are reproduced with specific

movements, most frequently moving the hip from a frog-leg position to a neutral position (Boric et al. 2019).

What causes it?—Two forms: (1) intra-articular (due to intra-articular disease) and (2) extra-articular causes (these are further divided into external and internal types) (Boric et al. 2019).

1. **Internal snapping hip syndrome** (or iliopsoas snapping) (Agten et al. 2016; Hegazi et al. 2016):
   (a) Caused by sudden movements of the iliopsoas tendon over either (1) the iliopectineus eminence, (2) the FH, (3) a paralabral cyst or (4) the medial aspect of the iliac muscle. It can be accompanied by an iliopsoas tendinopathy and/or bursitis. When the leg is brought into extension, the tendon moves smoothly into a position in contact with the pubic bone.
   (b) Can be asymptomatic. Symptomatic cases most commonly occur with activities or sports that require significant hip ROM, such as dance, soccer, hockey and football.
   (c) **Imaging**: dynamic US can show in real time the sudden displacement of the referred tendons over the underlying structure or pathological structure. US and MRI can reveal iliopsoas tendinopathy and iliopsoas bursitis.
2. **External snapping hip syndrome** (including iliotibial band snapping) (Agten et al. 2016; Boric et al. 2019):
   (a) Involves lateral structures such as the ITB and the *gluteus maximus* muscle. Snapping occurs as these structures move over the GT during hip flexion and extension. The underlying cause could be a thickening of the posterior part of the ITB and the anterior part of the *gluteus maximus*.
   (b) Athletes, particularly runners, dancers, soccer players and weight lifters, may experience popping movements of the ITB or the *gluteus maximus* muscle over the GT during full hip extension.
   (c) **Imaging**: It is usually a clinical diagnosis and seldom requires imaging. US can show in real time the sudden displacement of the ITB or the *gluteus maximus* muscle over the GT and fluid in the trochanteric bursa. Other US findings are a hypoechoic and thickened ITB at the level of the GT. MRI can also reveal reactive fluid within the trochanteric bursa from repetitive mechanical snapping, between the Gmed tendon and the *gluteus maximus* muscle/iliotibial band, sometimes extending posteriorly around the GT.

5.2.3 Extra-articular Hip Impingement Syndromes

5.2.3.1 Deep Gluteal Pain Syndrome (and Piriformis Syndrome)

What is it (Hernando et al. 2015; Kizaki et al. 2020)**?—**The deep gluteal pain syndrome (DGPS) definition comprises three characteristics: (1) non-discogenic, (2) sciatic nerve pain and (3) entrapment in deep gluteal space (DGS). Common and underdiagnosed causes are fibrovascular bands and entrapment related to the external rotator muscles. Piriformis syndrome can be classified as a subgroup of DGPS (Fig. 18).

Anatomy (Hernando et al. 2015)**:** The DGS is the cellular and fatty tissue located between the middle and deep gluteal aponeurosis, not clearly visible on MR, limited by (1) *posteriorly*: *Gluteus maximus* muscle, (2) *inferiorly*, continues into and with the posterior thigh, (3) *laterally* it is demarcated by the *linea aspera* and the lateral fusion of the middle and deep gluteal aponeurosis layers extending up to the *tensor fasciae lata* muscle via the iliotibial tract, (4) *anteriorly* by the posterior face of the femoral neck and the GT and (5) *medially* comprised of the greater and minor sciatic foramina.

Diagnosis (Kizaki et al. 2020): The general diagnostic pathway for DGPS is composed of (1) clinical history (posterior hip pain, radicular pain, and difficulty sitting for 30 min), (2) physical examination (tenderness in deep gluteal space, positive seated piriformis test, and positive Pace sign), (3) imaging tests (pelvic radiographs,

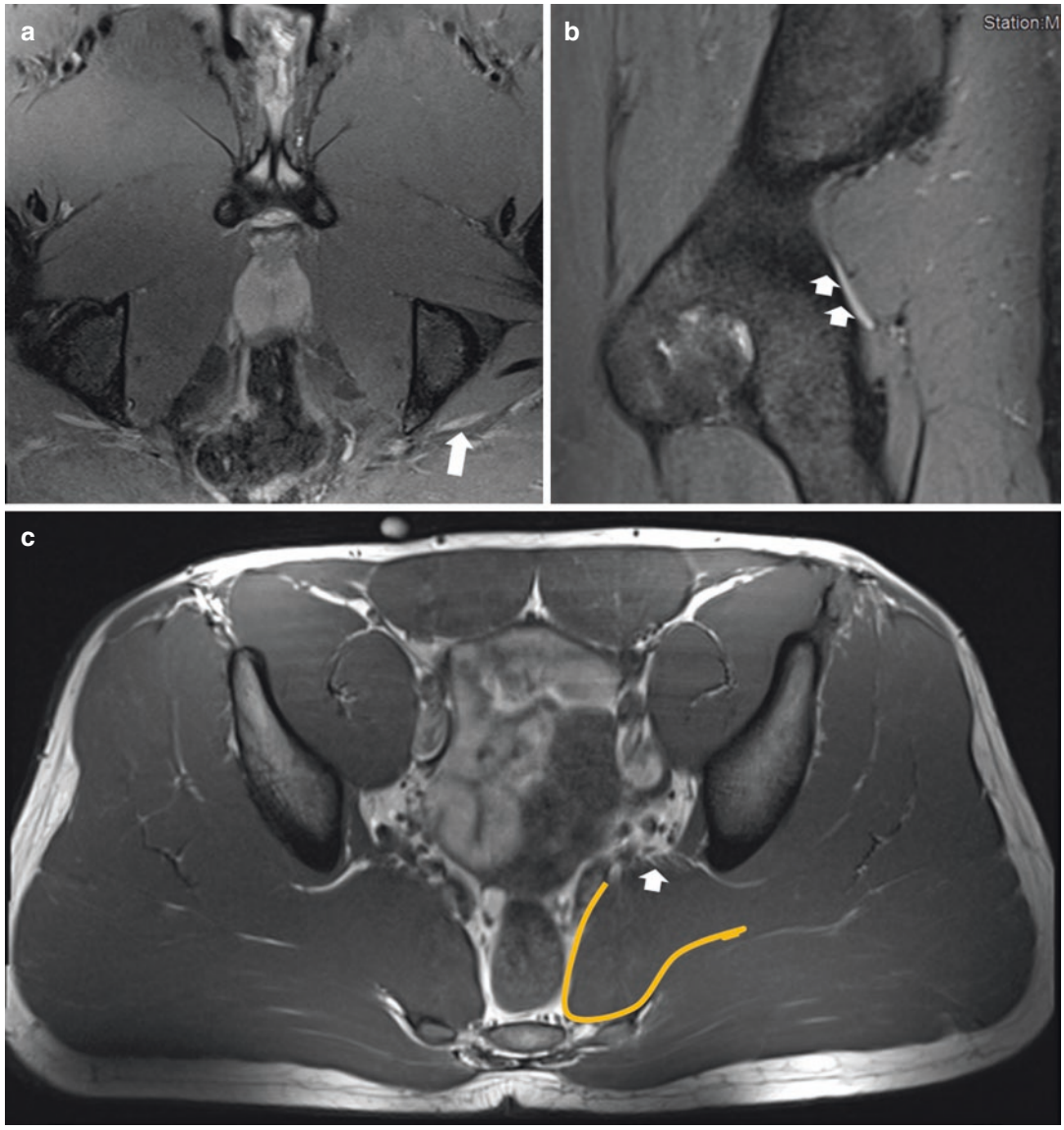

Fig. 18 Male soccer player, 28 years old. Bilateral piriformis hypertrophy (piriformis syndrome), symptomatic on the left. (**a**) Axial oblique PD Fat-Sat and (**b**) sagittal PD Fat-Sat show oedema and enlargement of the left sciatic nerve (white arrows), entrapped beneath an enlarged piriformis muscle. (**c**) Pelvis T1w shows bilateral hypertrophic piriformis muscle (orange curved line) with the enlarged sciatic nerve (white arrow)

pelvic MRI, and spine MRI) and (4) local imaging guided injections (perineural injections with corticosteroid and local anaesthetic have both a diagnostic and therapeutic function).

Imaging: The sciatic nerve/subgluteal space is not routinely scoped during hip arthroscopy, and therefore a preoperative diagnosis of sciatic nerve entrapment on MRI is necessary. *MRI* is the diagnostic procedure of choice and may substantially influence management of these patients. MRI may identify (1) anatomical muscle or tendons variations and (2) sciatic nerve abnormalities, such as signal changes. The normal sciatic nerve is a well-defined oval structure, isointense to adjacent muscle tissue (T1w). On T2-weighted or short tau inversion recovery images, the normal sciatic nerve is isointense or mildly hyperintense to muscle and hypointense to regional

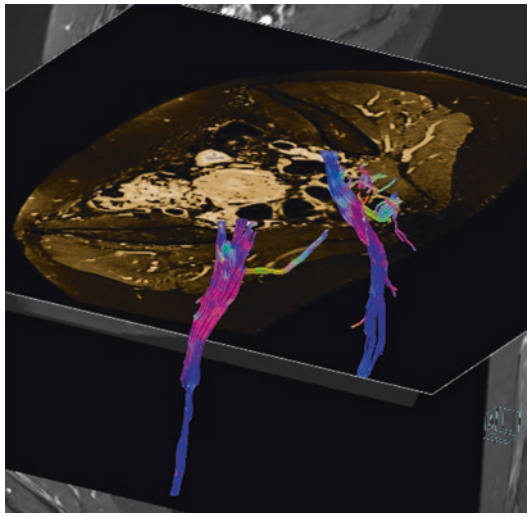

Fig. 19 Female non-athlete, 48 years old. MR tractography showing altered parameters and enlarged right sciatic nerve in the deep gluteal space (middle and distal segments)

vessels, with clearly defined fascicles separated by interposed lower signal connective tissue (Hernando et al. 2015).

MR neurography: The use of high resolution and high field strength equipment revealed excellent anatomic capability to demonstrate sciatic neuritis and entrapment. *Diffusion tensor imaging and diffusion tensor tractography* of the sciatic nerve (Fig. 19) have shown promising capabilities in patients with suspected entrapment (Hernando et al. 2015; Nakano et al. 2017; Kizaki et al. 2020).

5.2.3.2 Ischiofemoral Impingement

What is it?—It is a form of atypical, extra-articular hip impingement defined by hip pain related to narrowing of the space between the ischial tuberosity and the femur (Singer et al. 2015). In asymptomatic elite gymnasts, however, a narrowed ischiofemoral space (IFS) and oedema in the *quadratus femoris* (QF) muscle are frequent findings, often bilaterally.

What causes it?—The aetiology is multifactorial including (1) anatomical variants (of the proximal femur or pelvis; e.g. *coxa valga*), (2) hip or pelvic/spinal instability, (3) muscle imbalance (e.g. abductor/adductor), (4) overuse or extreme hip movements, (5) ischial tuberosity/hamstring enthesopathies, (6) trauma, (7) iatrogenic conditions and (8) tumours (Singer et al. 2015).

Anatomy: The IFS lies between the ischial tuberosity and the lesser trochanter. The quadratus femoris space (QFS) lies between hamstring tendons and lesser trochanter.

Diagnosis (Singer et al. 2015): based in suggestive clinical presentation and MRI findings (Table 18 and Fig. 20). MRI signal abnormalities are present within the IFS in 9.1% of asymptomatic patients.

- *Clinical presentation* (Hernando et al. 2016): Pain in the DGS, often on dynamic movement, radiating to the groin, buttock and hip region. Clicking and locking is also described. Physical examination is imprecise and often difficult to interpret.
- *Imaging* (Hernando et al. 2016): MRI is the diagnostic procedure of choice as it may substantially influence clinical management (best assessed on axial views). Dynamic MRI utilizing a full range of rotation will help to confirm impingement (see Table 18 for characteristic findings).
- *Injection test of the IFS*: paramount in many cases as it has both a diagnostic and therapeutic function.

5.2.3.3 Subspine Impingement

What is it?—It is an osseous and/or soft-tissue impingement due to a mechanical conflict following an altered position or morphology of the AIIS which impacts the distal femoral neck and FHN junction particularly during hip flexion (clinical-radiologic diagnosis) (Nakano et al. 2017).

Anatomy: The AIIS (origin of the direct tendon of the *rectus femoris* muscle and the tendon of the *iliocapsularis* muscle) may have a variable morphology (based on the relations between the AIIS and the anterosuperior acetabular rim). *Types* described: (1) type I (normal)—a smooth ilium wall between the AIIS and the acetabular rim; (2) type II—AIIS extends to the level of the rim; (3) type III—AIIS extends distally to the

Table 18 Peri- and extra-articular hip impingement syndromes

	Clinical characteristics	Physiopathology	Radiologic findings
Deep Gluteal Pain Syndrome	• Men = women, typically >40 years • Cx confused with lumbar and intra- or extra-articular hip diseases • Sitting pain with the absence of lumbar spine pathology on imaging • Active piriformis test and seated piriformis test stretch	• Multifactorial aetiology of sciatic nerve entrapment through its subgluteal path. • **Causes**: iatrogenic (30%; previous injection/intervention), piriformis syndrome (26%), trauma (15%), non-piriformis (hamstring, obturator internus) muscle pathology (14%), skeletal injury and entrapment (7%), endometriosis (6%), and vascular compression (2%) • First-line therapy includes injection and physiotherapy	• Image-guided injections(US or CT/MRI guided) are a useful tool to diagnose and treat this syndrome. • MRI, MRN and MR tractography. • Typically morphological muscle/tendons anomalies (namely piriformis syndrome), fibrovascular bands and sciatic neuritis. • Neural alterations: (1) Neural enlargement, (2) loss of the normal fascicular appearance, (3) increased perifascicular and endoneural signal intensity on fluid sensitive sequences
Ischiofemoral impingement	• ↑ Women, 50–55 y.o. (range 11–77) • Pain in the deep gluteal region, ↑ ER-EX-AD • Positive ischiofemoral impingement test, and long stride walking test	• Multifactorial aetiology • Reduced IFS or QFS with quadratus femoris muscle impingement • Quadratus femoris muscle injury with variable severity	• QF muscle: oedema ± fatty atrophy ± tear • Narrowed IFS (cut-off of ≤15 mm, a sensitivity/specificity/accuracy of 76.9%/81.0%/78.3%, respectively) • Narrowed QFS (cut-off of ≤10.0 mm results in sensitivity/specificity/accuracy of 78.7%/74.1%/77.1%, respectively) • Sciatic neuritis
Subspine AIIS impingement	• ↑ Men, 15–30 y.o., sports active ≈ FAI • Groin/anterior pain ↑ Forced FL • Positive impingement test	• Acute or chronic pain due to repeated microtrauma to the RF insertion in the AIIS → apophysis, osseous or tendinous avulsion **Aetiology**: • Extra articular (AIIS hypertrophy or elongation; primary or, secondary to trauma, acetabular retroversion or post-PAO) • Intra-articular (morphological alteration in the subspinal space)	• Osseous abnormality of the AIIS or subspinal space (deformity or excessive elongation, with caudal extension at or below the acetabular rim level) • Heterotopic ossifications in the path of the *rectus femoris* muscle • Ganglion cysts in the femoral neck in a more distal location than seen in FAI. • Fracture of the acetabular rim, focal chondrolabral damage
Iliopsoas impingement	• 25–35 y.o. • Groin/anterior pain, ↑ FL and prolonged sitting	• Excessive contact of the iliopsoas tendon over the labrum, particularly with EX movements • Signs of FAI may be absent	• MRI/MRA • Lesion of anterior labrum (3 o'clock position)
Trochanteric-pelvic impingement	• Men = women, 15–40 y.o. • Posterolateral pain, ↑ EX and ABD • Positive "gear stick" sign	• Morphological alteration of the femoral proximal epiphysis of multifactorial aetiology → abnormally high position of the GT with respect to the femoral head, *coxa vara* • Hypermobility or hyperlax (without morphological alterations)	• Radiographs: AP pelvis and hip • Typical morphological alterations; (1) *coxa vara*, *magna*, *brevis* or *plana*, (2) high position of GT ± DDH

Cx clinical features, *FL* flexion, *EX* extension, *ABD* abduction, *AD* adduction, *ER* external rotation, *IFS* ischiofemoral space, *QFS* quadratus femoris space, *GT* greater trochanter, *PAO* periacetabular osteotomy, *AIIS* anteroinferior iliac spine, *MRN* MR neurography, *DDH* developmental hip dysplasia, *MRI* magnetic resonance imaging, *MRA* magnetic resonance arthrography, *yo* years old, *RF* rectus femoris, *AIIS* antero-inferior iliac spine, *AIIS* antero-superior iliac spine, *FAI* femoracetubular impingement

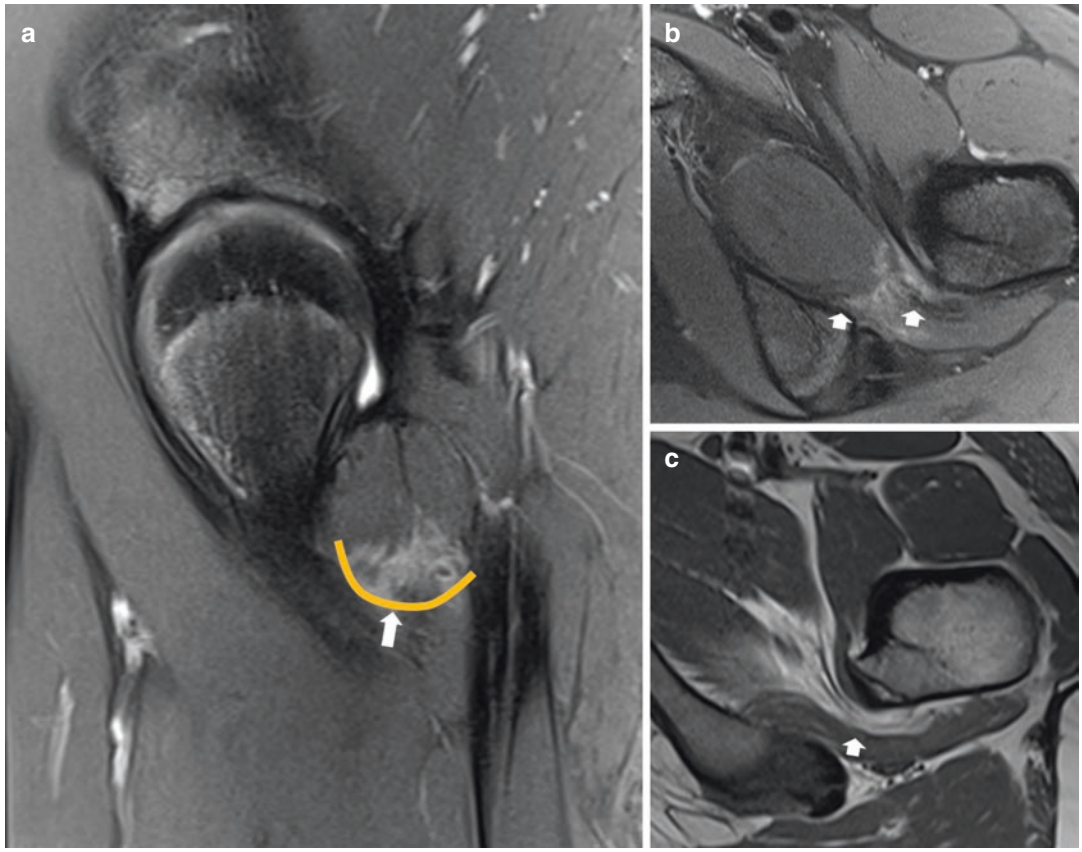

Fig. 20 (**a**–**c**) Ballet male dancer, 32 years old. Symptomatic ischiofemoral impingement. (**a**) Sagittal PD Fat-Sat. Moderate oedema (orange line and white arrow) with fatty atrophy of the *Quadratus femoris* muscle. (**b**) Axial PD Fat-Sat and (**c**) T1w show narrowed IFS (around 14 mm) and borderline QFS (10 mm) (white arrows). No sciatic neuritis or hamstring changes were depicted

acetabular rim. Type II and III variants are associated with a decrease in hip flexion and internal rotation, although they may be asymptomatic (Hetsroni et al. 2013).

Diagnosis (Fig. 21): Conjunction of characteristic clinical and imaging findings (Galeano et al. 2018).

– *Clinical Presentation*: anterior hip or groin pain aggravated with certain sporting activities such as the ball-kicking/speed-running when playing soccer. Sometimes it unilaterally affects the dominant leg.

Imaging

- Radiographs: AP pelvis radiograph, hip Lequesne's false profile and three-dimensional CT play important roles since they allow the orthopaedic surgeon to perform an adequate preoperative evaluation.
- MRI/MRA role is detecting associated intra-articular pathology as fractures of the acetabular rim and focal chondrolabral lesions are similar to the ones visible in the pincer type of FAI (see Table 18 for characteristic findings).

5.3 Pelvis

5.3.1 Stress Fractures

General considerations: Stress fractures (SF) are caused by mechanical overload of bone and comprise a spectrum of bone strain, stress reaction and true stress fractures. They occur when

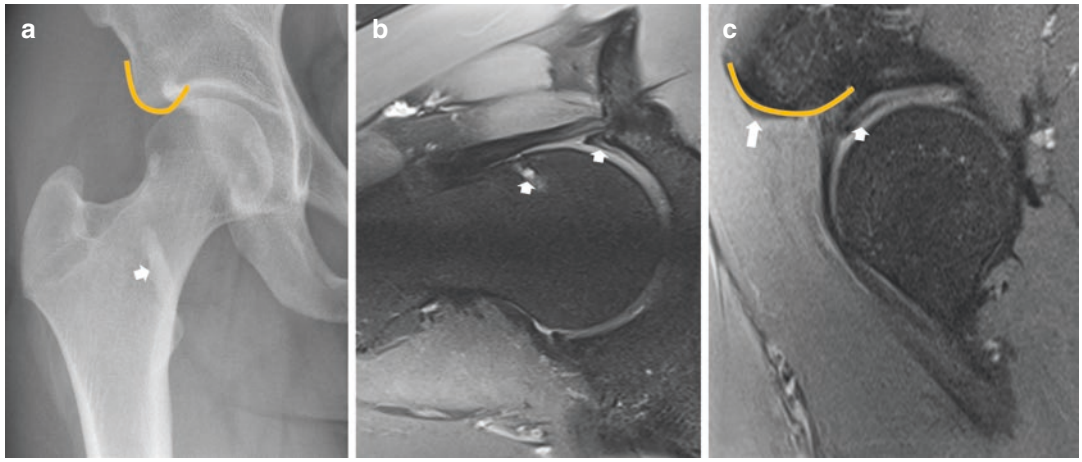

Fig. 21 (**a–c**) Male soccer player, 25 years old. Right subspine impingement. (**a**) Right AP hip radiograph showing a prominent AIIS (orange line) with caudal extension below the acetabular rim level (type 3). Also, heterotopic ossifications are seen in the path of the *rectus femoris* muscle (white arrow). (**b**) Radial fat-supressed proton density at 2 o'clock. Associated ganglion cysts in the femoral neck and acetabular chondral delamination is seen (white arrows). (**c**) Sagittal fat-supressed proton density. Osseous abnormality of the AIIS, deformed and with excessive elongation (orange curved line) with acetabular cartilage delamination (small white arrow)

repetitive mechanical stresses are applied to bone, none of which intense enough to cause an acute fracture. Although in reality both mechanisms often coexist in athletes (e.g. young females with osteopenia) (Marshall et al. 2018), conceptually SF can be divided in

1. *Fatigue fractures*: mainly seen in young, active individuals, when supraphysiologic repeated stress is applied to a bone with normal elastic resistance.
2. *Insufficiency fractures*: more commonly seen in the elderly population, caused by repeated mechanical stress, within the normal physiologic range, applied to a bone with diminished elastic resistance (most commonly due to osteoporosis).

Stress fractures are more common in women, athletes and military recruits, and usually occur in weight-bearing bones. SF of the femur and pelvis account for approximately 4.2–48.0% and 1.3–5.6% of SF in athletes, respectively (Liong and Whitehouse 2012). They may occur anywhere in the pelvic region and femur, but predominate in the proximal femur, sacrum and inferior pubic ramus (Table 19). Certain activities, such as running, are associated with a high incidence of these lesions. Furthermore, osteoporosis, previous irradiation of the pelvis, the "female athlete triad" (low energy availability, with or without disordered eating, menstrual dysfunction and low bone mineral density), corticoid therapy, total hip replacement and spinal instrumentation are factors associated with pelvic SF (Peh et al. 1996; Vavken et al. 2008; Miller et al. 2015).

Femoral neck stress fractures (predominantly of the fatigue type) (Fig. 22) are particularly worrisome, as they can progress to complete fractures with dislocation and result in avascular necrosis of the FH. When these fractures involve the tension (lateral) side of the femoral neck the risk is higher, as opposed to compression (medial) side fractures (Marshall et al. 2018). Some of these lesions are uncommon and require a high level of suspicion for adequate diagnosis (e.g. sacral fractures in young female runners (Major and Helms 2000)). In older patients, stress fractures (predominantly of the insufficiency type) commonly involve the sacrum and pubic rami, in one or both sides of the pelvis (Figs. 23 and 24). The supraacetabular region, ilium and pubic rami are other occasional locations of stress fractures.

Imaging Assessment

- *Radiographs:* useful in first-line assessment and for differential diagnosis, although they are inaccurate in the initial demonstration of stress lesions. Radiographic findings may not appear in every patient, and, even if they do, it may take weeks to months after the onset of symptoms (Greaney et al. 1983). Findings include: (1) focal osteopenia or blurring of bone contours, followed by (2) focal periosteal reaction and linear sclerosis or a (3) frank fracture line, usually perpendicular to the cortex and trabeculae.
  - *MRI*: gold standard technique in the assessment of stress lesions. It is both sensitive and specific to evaluate the continuum of stress response and is able to differentiate stress reactions (bone marrow oedema on fluid-sensitive sequences, associated with periosteal, endosteal and peri-osseous oedema, but no fracture line) from a stress fracture (when a fracture line becomes evident).
  - *CT* can show bony detail to a better degree and is frequently used in the evaluation of the bony pelvis and as a problem-solving tool when other techniques are equivocal. Sclerotic bands or fracture lines can easily be demonstrated with CT (Fig. 23) but it cannot show the early stages of stress lesions.
  - *Bone scintigraphy* is a very sensitive technique that can show early stress lesions, but it lacks specificity and has limited spatial resolution.

Table 19 Topographic distribution and associated sports in pelvic and proximal femoral stress injuries (Kiuru et al. 2003; Liong and Whitehouse 2012)

Location	% of cases	Associated activities
Sacrum	16,1%	Long-distance running, hockey, basketball, tennis and volleyball
Inferior pubic ramus	19,5%	Long-distance running
Superior pubic ramus	1,7%	Football
Iliac bone/ Acetabulum	2,3%	Running
Femoral neck	40,2%	Long-distance running, jumping and ballet dancing
Femoral proximal shaft	19,5%	
Femoral head	0,6%	

5.3.2 Muscles, tendons and enthesis

5.3.2.1 Apophyseal Injuries

General considerations: Apophysis are normal bony outgrowths that serve as insertion points for tendons and ligaments. They arise from a separate ossification centre, fusing to the remaining bone later in life (Table 20). Mechanical stress applied to the muscle-tendon-bone unit in the adult athlete may result in tendon tear or myotendinous lesions. In the child or adolescent, the weakest structure in this unit is the cartilaginous growth plate of the unfused apophysis, which may tear and displace as a result of traction stress, resulting in bony or cartilage avulsion.

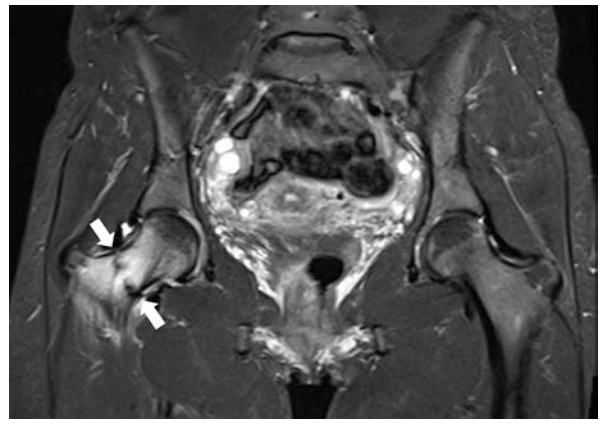

Fig. 22 Incomplete stress fracture involving the tension and compression sides of the femoral neck in a 29-year-old female trail runner. Coronal STIR image of the pelvis shows extensive bone marrow oedema in the right femoral neck, associated with cortical discontinuity and a transverse hypointense trabecular fracture line (arrows)

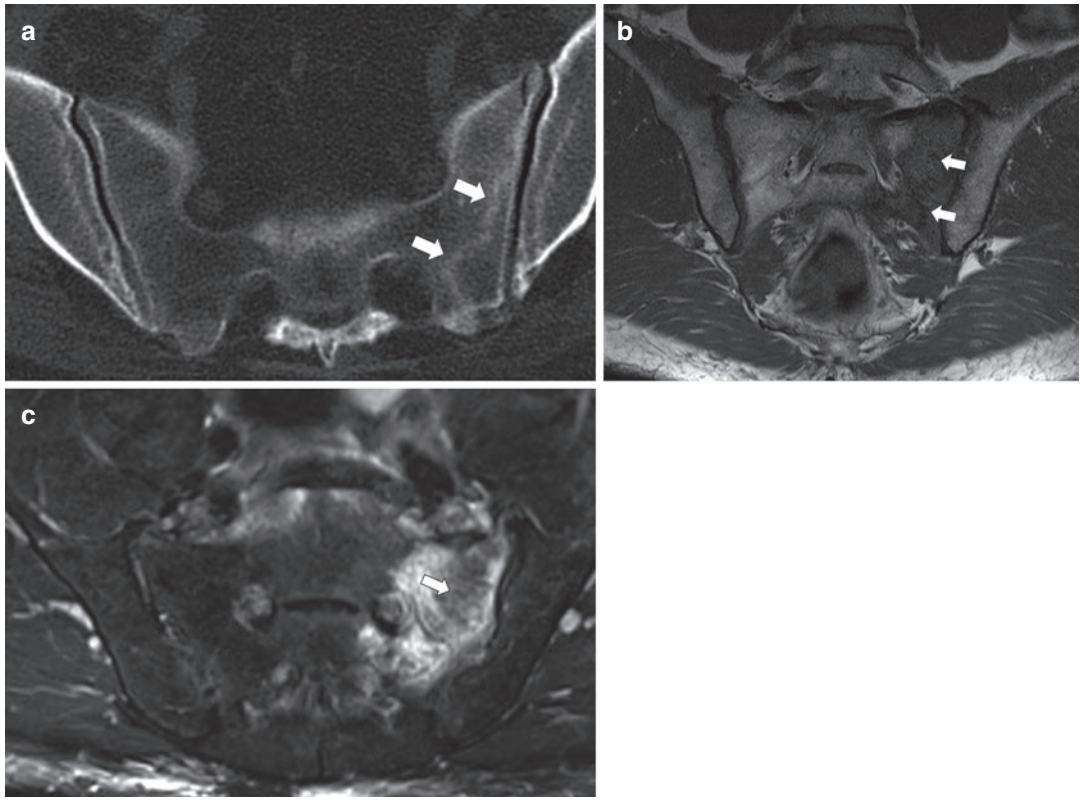

Fig. 23 (**a–c**) Stress fracture of the sacrum in a 61-year-old woman with spinal arthrodesis (not shown). (**a**) Axial oblique CT scan image reveals linear hyperdensity on the left sacral wing (arrows), paralleling the sacroiliac joint space. Arthrodesis-related abnormal distribution of loads may be a factor contributing stress. (**b** and **c**) 35-year-old non-professional athlete. (**b**) Coronal oblique T1w and (**c**) axial oblique fat-suppressed T2-weighted images show a similar stress fracture (arrows), surrounded by extensive bone marrow oedema

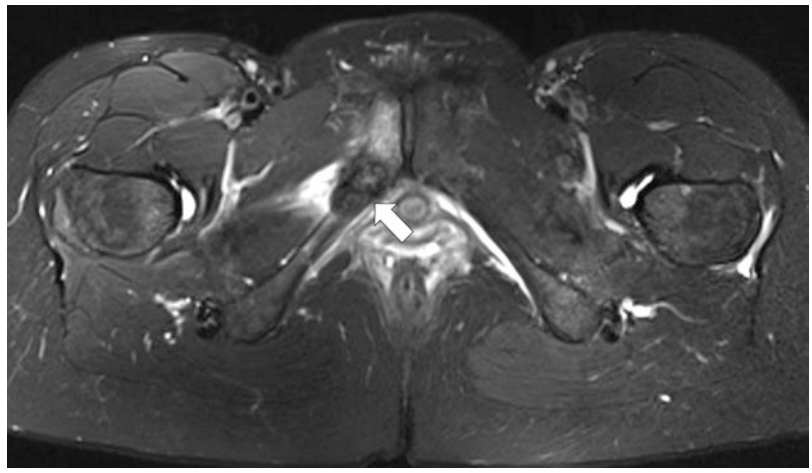

Fig. 24 Pubic ramus stress fracture in a 45-year-old non-professional athlete (long-distance runner). Axial fat-supressed T2-weighted image of the pelvis depicts a right inferior pubic ramus fracture (arrow) with surrounding bone and soft tissue oedema

Table 20 Appearance and fusion of pelvic apophyseal ossification centres (Boyd et al. 1997)

Ossification centre	Appearance	Fusion
Iliac crest	13–15y	15–17y
Anterior-superior iliac spine	13–15y	21–25y
Anterior-inferior iliac spine	13–15y	16–18y
Ischial tuberosity	16–18y	19–25y
Greater trochanter	2–5y	16–18y
Lesser trochanter	8–12y	16–18y

Apophyseal avulsion fractures are typically seen in the developing skeleton, being more prevalent in male adolescents. They usually occur after a strong sudden pull exerted on the apophysis by muscle contraction, although they may also be caused by chronic repetitive microtrauma. Intensive training further aggravates the structural imbalance at the muscle-tendon-bone unit in the young athlete, due to the combined effect of increased repetitive traction stresses and training-induced hypertrophic muscles (which place increased traction forces across the growth plate) (Boric et al. 2019). Sports that involve kicking, jumping and sudden velocity changes, such as football, rugby and sprinting, are frequently implicated.

Apophyseal avulsions are unusual in the mature skeleton and should prompt a search for an underlying cause. Avulsion of the lesser trochanter in an adult patient, in particular, should be considered a sign of metastatic disease until proven otherwise (Sanders and Zlatkin 2008).

The pelvis is a frequent location of apophyseal injury (Fig. 25). Although any pelvic enthesis can be affected, the (1) ASIS, (2) AIIS and (3) ischial tuberosities are more commonly injured (Table 21).

Diagnosis: While (1) **clinical presentation** is often diagnostic (onset is typically sudden, after the inciting event, with focal pain, swelling and gait impairment), (2) ***AP and oblique radiographs*** with contralateral comparison views are important to assess the size and degree of displacement of the avulsed fragment (Fig. 26). They may be inconspicuous however, if the apophysis is non-displaced or non-ossified, in which case US or MRI can be very helpful (Figs. 27, 28, 29, and 30). (3) ***MRI*** may show discontinuity of the apophysis, along with bone, physeal and soft tissue oedema and associated muscle and tendon injuries. (4) **CT** may have a role to better delineate bone detail in equivocal cases. Occasionally, exuberant callus formation can have an aggressive imaging appearance and be misinterpreted as neoplasm or infection (Sanders and Zlatkin 2008). A high degree of suspicion, along with a detailed clinical history and thorough anatomic knowledge should help avoid this pitfall.

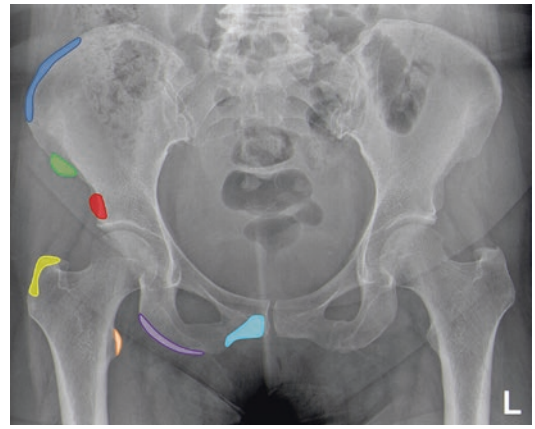

Fig. 25 AP radiograph of the pelvis depicting common and uncommon sites of apophyseal avulsion fractures: insertion of the abdominal wall muscles at the iliac crest (dark blue), insertion of the tensor fascia lata and sartorius tendons at the anterior superior iliac spine (green), insertion of the direct head of the rectus femoris tendon at the anterior inferior iliac spine (red), insertion of the gluteus medius and minimus tendons at the greater trochanter (yellow), insertion of the iliopsoas tendon at the lesser trochanter (orange), insertion of the hamstrings at the ischial tuberosity (purple) and insertion of the adductors and gracilis at the symphysis pubis (light blue)

Table 21 Prevalence and sports distribution of pelvic apophyseal avulsion injuries (Eberbach et al. 2017)

Location	Prevalence	Main associated activities
Ischial tuberosity	11–54%	Gymnastics and football
Anterior-inferior iliac spine	22–49%	Football, athletics and tennis
Anterior-superior iliac spine	19–30%	Football, athletics and gymnastics
Iliac crest	2–10%	Football, gymnastics and tennis
Pubic symphysis	0–3%	Football and fencing
Lesser trochanter	0–2%	Ball sports

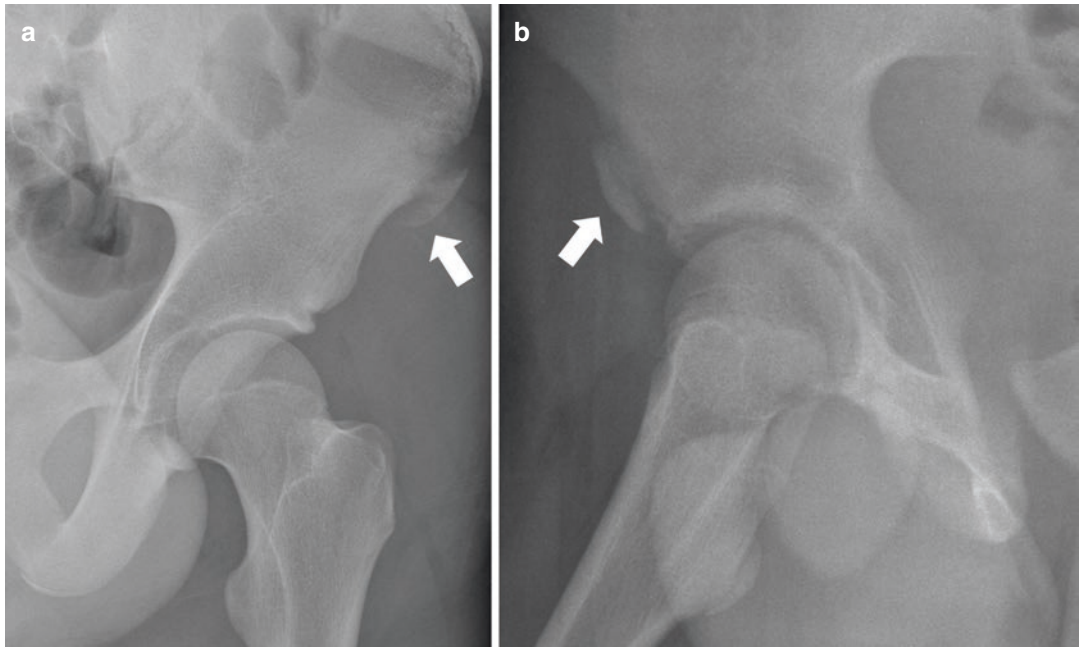

Fig. 26 (**a**, **b**) Iliac spine avulsion injuries. Oblique hip radiographs in adolescent males after (**a**) sprinting and (**b**) football injuries, depicting apophyseal avulsion fractures (arrows) of the (**a**) ASIS and (**b**) AIIS. *AIIS* anterior inferior iliac spine, *ASIS* anterior superior iliac spine

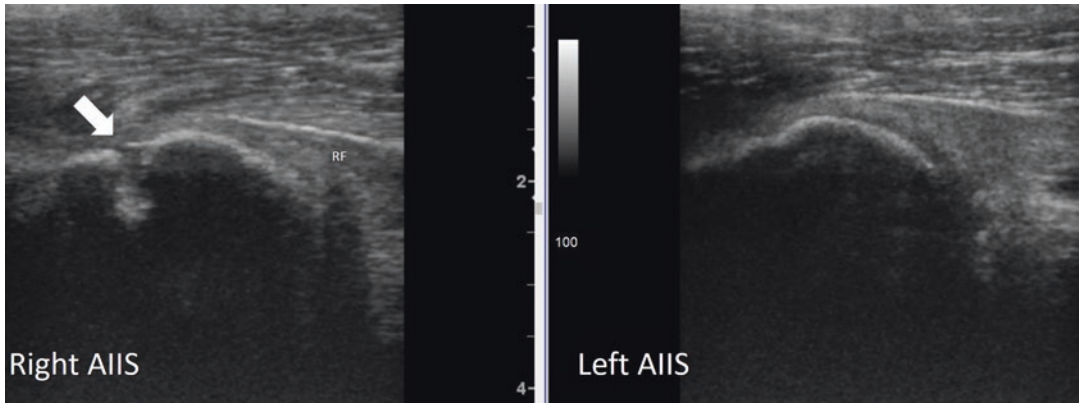

Fig. 27 14-year-old boy with anterior right hip pain after a football injury ("kicking in the air"). Longitudinal US scan of the insertion of the direct tendon of the rectus femoris (RF) on the right AIIS, evidencing apophyseal separation (arrow). The left asymptomatic side is shown for comparison. *AIIS* anterior inferior iliac spine, *US* ultrasound

Treatment is usually conservative, but when significant displacement occurs (more than 1.5–2 cm), surgery may be beneficial. Residual post-traumatic apophyseal deformity or non-union (Fig. 31) at specific locations may cause soft tissue impingement (e.g. subspine or ischiofemoral) (Calderazzi et al. 2018).

5.3.2.2 Muscle and Tendon Injuries

General considerations: Muscle lesions are the most common pelvic injuries in sports (Boyd et al. 1997; Brittenden and Robinson 2005). They can be caused by indirect (stretch-induced) or direct (contusion or laceration) trauma.

In the adult athlete, the myotendinous junction (MTJ) is a particularly vulnerable region from

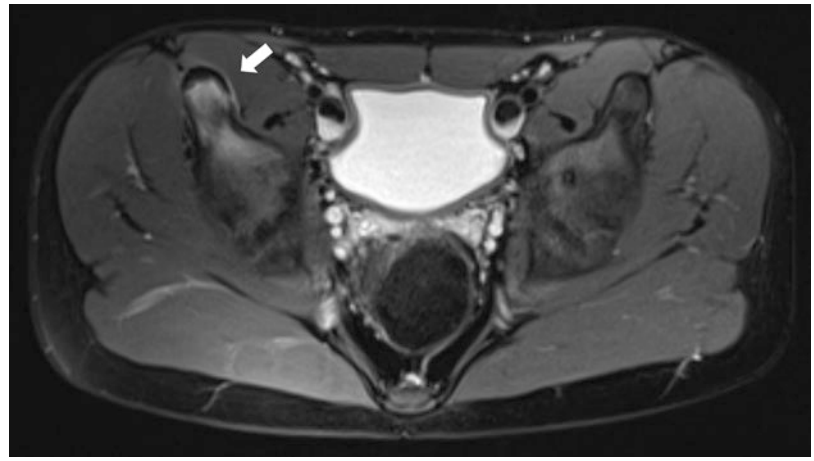

Fig. 28 15-year-old boy with anterior hip pain after a football injury. Axial fat-supressed T2w image of the pelvis shows bone and soft tissue oedema involving the right anterior inferior iliac spine (arrow), consistent with non-dislocated apophyseal avulsion

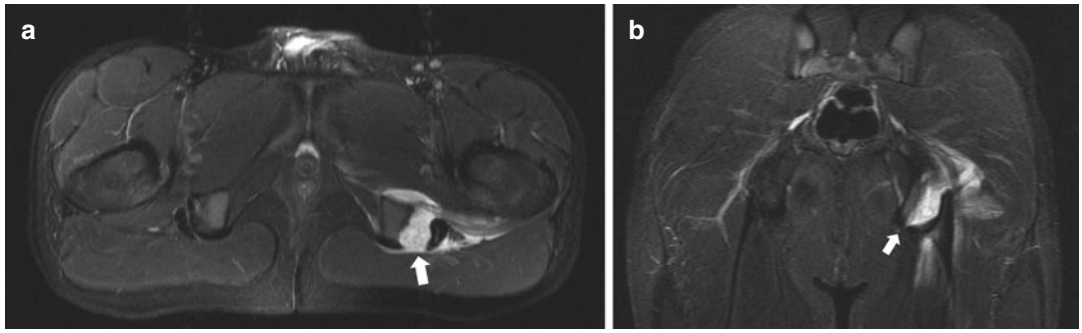

Fig. 29 (**a**, **b**) 14-year-old football player complaining of pain after a sudden pull during a match. (**a**) Axial and (**b**) coronal fat-supressed T2w images show left ischial tuberosity avulsion (arrow), with moderate dislocation of the avulsed fragment

the biomechanical standpoint, which accounts for its usual involvement in **indirect trauma**, typically after a violent contraction or an abrupt motion block. The *rectus femoris*, *biceps femoris* and *adductor longus* are most commonly involved in this type of injury (Crema et al. 2015; Agten et al. 2016). Soft tissue contusions are common in collision and contact sports. These **direct-type** injuries may occasionally result in muscle hematoma and, less commonly, compartment syndrome or myositis ossificans. In the hip and thigh region, the most frequently affected muscle by direct injuries is the *vastus intermedius*.

Delayed-onset muscle soreness (DOMS) is another common condition in sports that results from strenuous exercise of a muscle or muscle group, and presents on MRI as muscle oedema that can mimic a low-grade muscle injury. Clinical presentation is distinct and allows differentiation between the two, since pain associated with DOMS reaches a peak from 24–72 h after the inciting activity, while in muscle injury it has an immediate onset (Guermazi et al. 2017).

In contradistinction to muscle injuries, which are typically the result of a single major traumatic event, tendon lesions can present either as an overuse or as an acute injury.

Imaging: While MRI is the most sensitive and comprehensive technique to evaluate muscle injuries, US can be very useful as an adjunct, when access to MRI is limited or a fast screening is desired.

US: Muscle fibre and tendon discontinuity can be detected, along with hyperechoic hematic

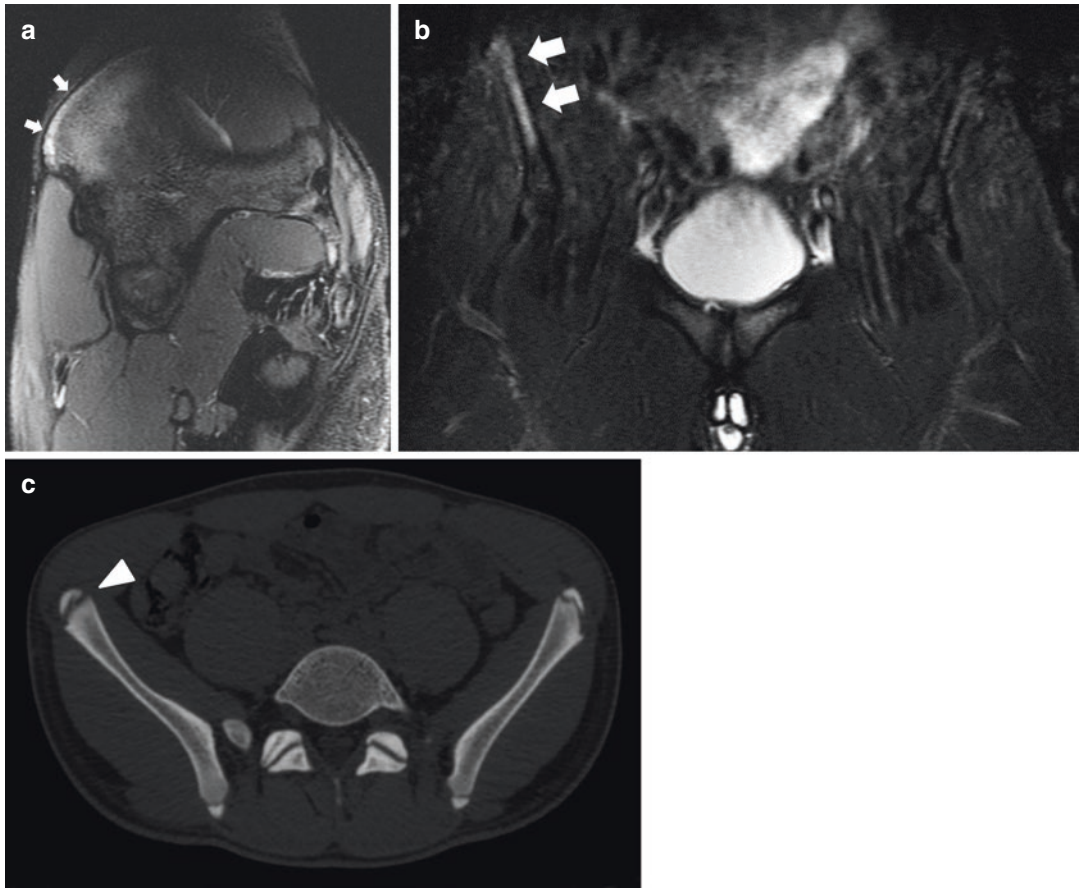

Fig. 30 (**a–c**) 16-year-old male football player boy with pain over the right anterior iliac crest. (**a**) Sagittal and (**b**) coronal fat-suppressed T2w MR images of the pelvis show bone oedema of the iliac crest apophysis and adjacent iliac bone (arrows). (**c**) Axial CT scan image confirms the diagnosis of right iliac crest apophyseal injury (arrowhead). (Case courtesy of Dr. Armando de Abreu, Porto Alegre, Brazil)

muscle infiltration, fluid collections, perifascial fluid and fascial disruption. This technique also allows comparative and dynamic assessment (active muscle contraction may help demonstrate subtle tears), and can be used to guide interventional procedures in real time.

MRI: Currently, MRI may be of value for confirming the clinical diagnosis and determining the extent of muscle injury, but so far MRI findings have not demonstrated superiority over clinical features in determining time to RTS. A combination of T1w and fluid-sensitive (fat-suppressed PD/T2 or STIR) sequences should be used. Oedema and/or fibre discontinuity should be noted, as well as the amount of fibre retraction when present.

Classification: Several systems have been developed (Cruz and Mascarenhas 2018). The most commonly used are (1) the classic three-grade system described by Takebayashi, and the more recently developed (2) Munich Consensus, (3) British Athletics Muscle Injury and (4) MLG-R classifications. Despite the continued endeavours to establish more comprehensive classification systems, the prognostic value of MRI in muscle injury is limited. The overlap in recovery times between different anatomic types of injury may be explained by a multitude of other relevant factors, such as the type of sport, the player's role in the team, his/her mental characteristics and the timing of the injury in the season (Reurink et al. 2014).

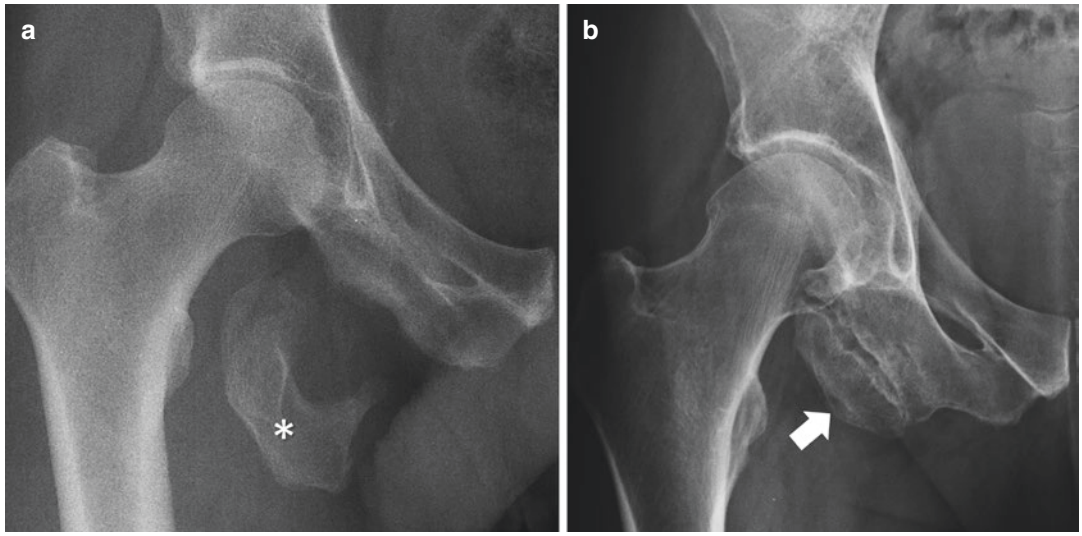

Fig. 31 (**a**, **b**) Acute and chronic ischial tuberosity avulsion injuries. (**a**) Hip AP radiograph of a male 23-year-old soccer player shows a large acutely displaced right ischial tuberosity avulsion fracture (asterisk). (**b**) Hip AP radiograph of a 58-year-old male with non-union of the ischial tuberosity (arrow), due to an old apophyseal avulsion injury

What to report: (a) the involved structure(s), (b) the location of the lesion (proximal, central or distal), (c) the anatomical site of injury (myofascial, musculo-tendinous, or intratendinous) and (d) the injury extent (percentage of cross-sectional area and longitudinal length).

How to report: As a general rule, for both MRI and US, the axial plane should be used primarily to assess muscle injuries and determine the maximum percentage cross-sectional area of fibre discontinuity, while imaging in the sagittal and coronal planes helps to evaluate the longitudinal extent and degree of retraction (Cruz and Mascarenhas 2018).

In the following paragraphs, the more typical pelvic muscle and tendon injuries in athletes are briefly reviewed, except for adductor injuries, which are discussed elsewhere in this book.

Hamstring Injuries

Anatomy: The hamstrings comprise the biceps femoris (BF), semitendinosus (ST) and semimembranosus (SM), which originate at the ischial tuberosity as a common BF-ST tendon and a separate SM tendon. Each component possesses long proximal and distal tendons and long MTJs, which, in addition to features like the high proportion of type II ("fast twitch") muscle fibres and the crossing of two joints, makes this muscle complex particularly susceptible to injury (Bencardino and Mellado 2005).

Hamstring acute lesions are very prevalent in sports (Fig. 32). They are the most common muscle injury in professional football players (37% of all muscle injuries (Ekstrand et al. 2011)), but are also frequent in other sports that involve kicking, sprinting and jumping, as well as in dancing, skiing, water skiing, and contact sports such as martial arts (Ekstrand et al. 2011; Kuske et al. 2016). Forced flexion of the hip with hyperextension of the knee is the commonly implicated mechanism.

The main injuries observed in young athletes are (1) proximal tendon avulsions (including apophyseal avulsions before skeletal maturation; Fig. 29), (2) tendon lesions, and (3) proximal MTJ injuries (Fig. 32), with or without concomitant tendon involvement. The proximal MTJ of the BF is the most frequent hamstring injury location in football (26.7%) (Crema et al. 2015). Purely muscular and myofascial injuries are less common (De Smet and Best 2000).

MRI shows similar appearance as muscle injuries in other anatomical sites. It is advocated

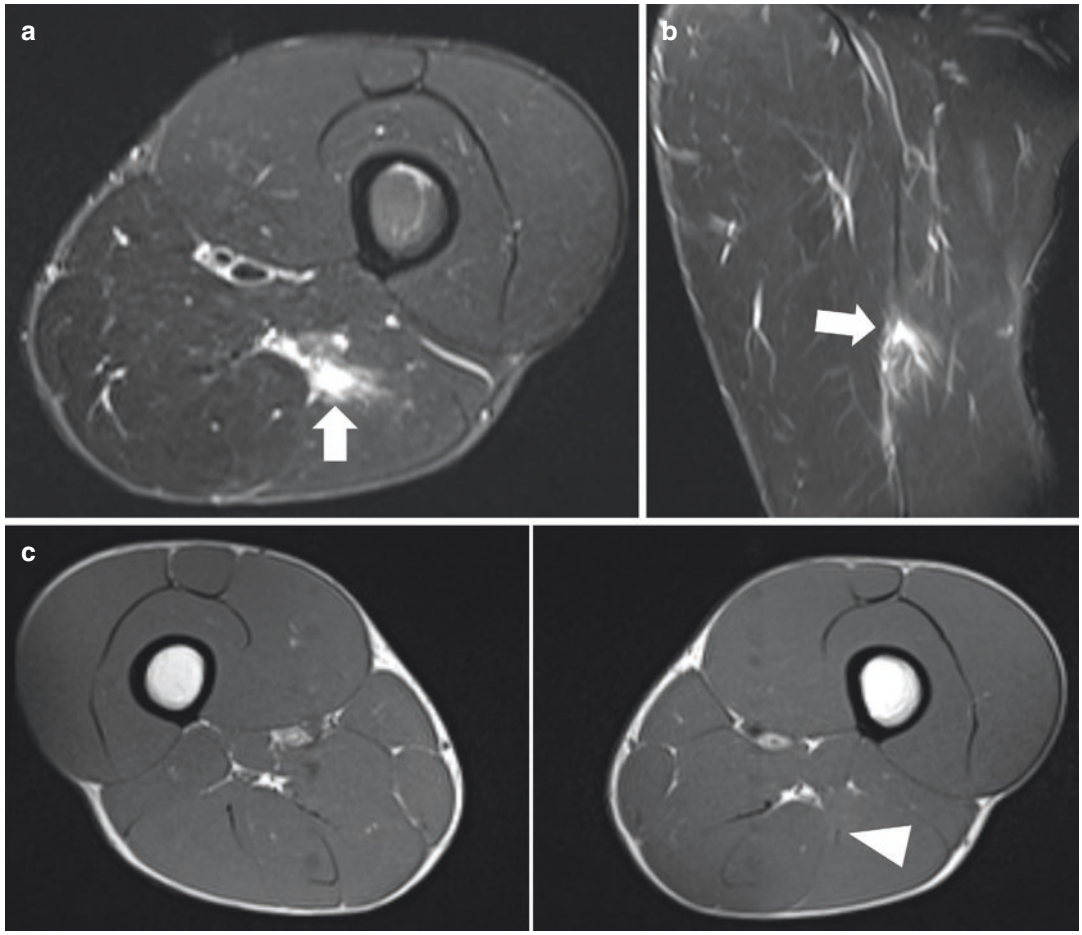

Fig. 32 (**a–c**) 27-year-old professional football player with acute posterior thigh pain during sprinting. (**a**) Axial and (**b**) coronal STIR images demonstrate a small partial myotendinous junction tear of the long head of the biceps femoris, located at the middle third of the thigh, as a fluid-like hyperintense focus (arrows) associated with muscle fascicle disruption, mild fibre retraction and fascial disruption. (**c**) Notice the involvement of the intramuscular proximal tendon (arrowhead), which appears attenuated compared with the asymptomatic contralateral side on a T1w axial MR image

ideal for detection of subtle injury, for central intramuscular tendon tears of the biceps femoris and for follow-up imaging. Due to its close anatomic location adjacent to the hamstring muscle complex, sciatic nerve entrapment is a possible complication of hamstring injuries.

Hamstring chronic tendinopathy is a frequent finding in the elderly. It manifests as tendon thickening and increased signal and peritendinous and ischial tuberosity oedema, but these appearances are also found in asymptomatic individuals (De Smet et al. 2012). In partial tears a fluid-filled defect at the tendon insertion is observed, while complete tears display detachment from the ischial tuberosity and retraction (Fig. 33).

Ischial bursitis in sports usually have a direct traumatic origin. It is visible as a fluid collection between the hamstrings insertion in the ischial tuberosity and the gluteus maximus muscle.

Proximal *Rectus Femoris* Injuries

Anatomy: RF has a complex architecture, displaying a muscle-within-a-muscle configuration (Fig. 34). It possesses two proximal tendons, a

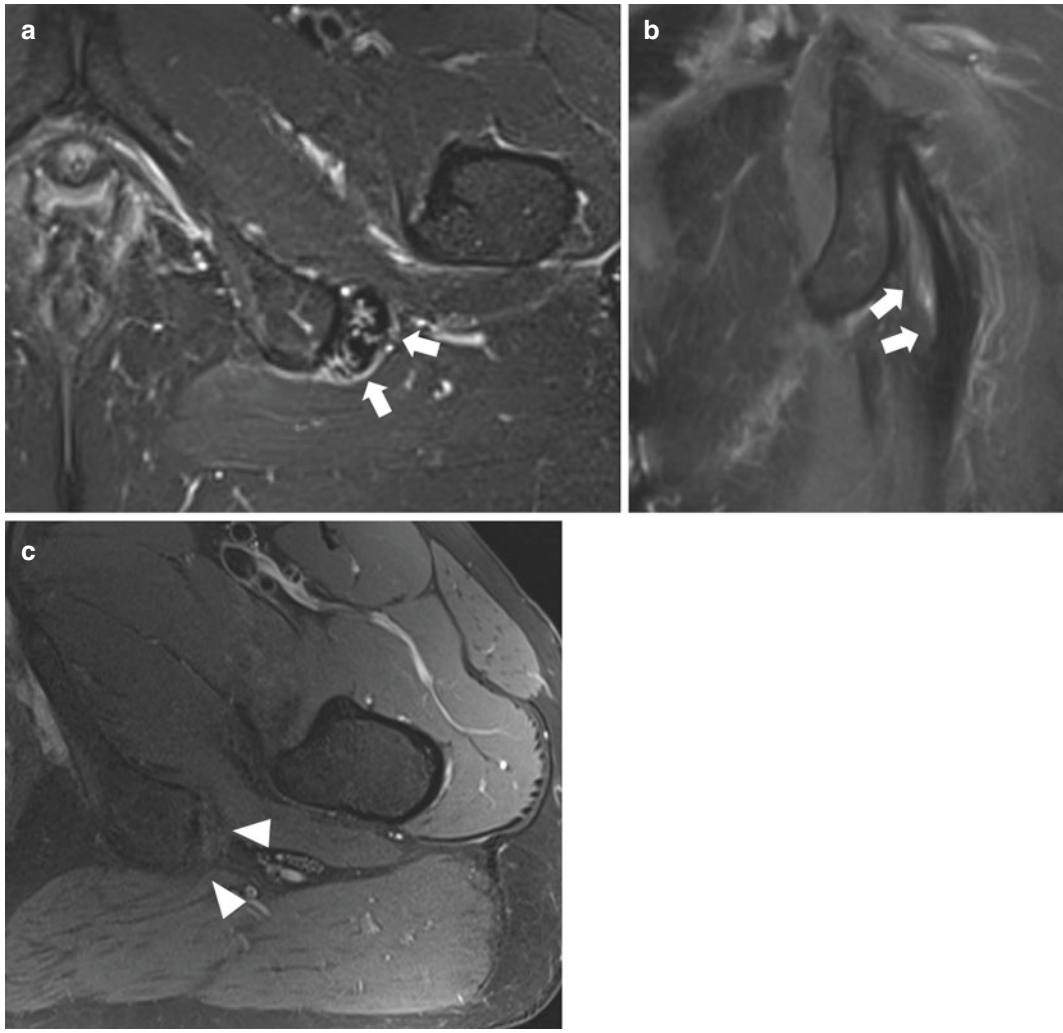

Fig. 33 (**a–c**) (**a**, **b**) 37-year-old former professional tennis player with hamstring tendinopathy. (**a**) Axial and (**b**) coronal fat-supressed T2w MR images demonstrate proximal hamstring thickening and increased tendon signal (arrows) associated with mild peritendinous oedema, representing tendinosis. (**c**) In another former athlete, axial fat-suppressed T2w MR image shows absence of the tendinous hamstring origins, consistent with hamstring avulsion. No fluid is appreciated, implying a chronic nature for this finding

direct and an indirect one. The direct tendon originates at the AIIS, while the indirect tendon originates laterally at the acetabulum. They form a conjoint tendon for a short segment, a few centimetres distal to their origin, diverging thereafter (Kassarjian et al. 2014). The direct tendon continues distally as a superficial anterior tendon that covers the proximal third of the muscle and fuses with the anterior fascia, giving rise to a peripheral unipennate muscle belly. The indirect tendon gives rise to a long intramuscular central tendon and a bipennate central muscle belly.

General considerations: RF injuries have been reported as the second or third most common muscle lesion in the lower extremity, after hamstring injuries, occurring frequently in sports such as football, rugby, basketball and other activities that involve kicking and sprinting (Ekstrand et al. 2011).

Several factors account for the high frequency and variety of RF injuries, namely (1) its structural complexity, (2) the crossing of two joints

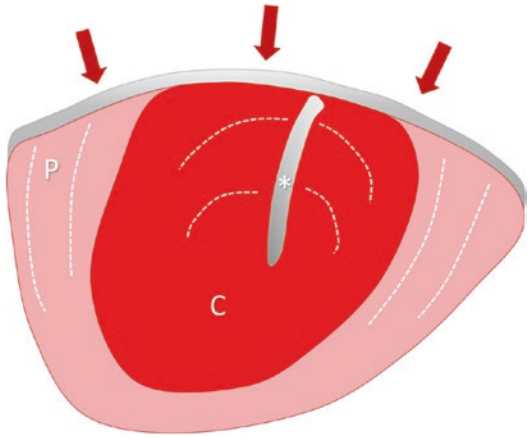

Fig. 34 Diagram illustrating the cross-sectional structure of the rectus femoris muscle in the upper third of the thigh. The muscle-within-a-muscle architecture is demonstrated. The intramuscular central tendon (*) and the bipennate central muscle belly (C) derive from the indirect tendon. The direct tendon gives rise to the peripheral unipennate muscle belly (P) and to the superficial anterior tendon (arrows) that blends with the anterior fascia. The white interrupted lines illustrate the orientation of the muscle fibres in each component of the muscle

and (3) the high proportion of type II fibres, and (4) specific biomechanical vulnerabilities associated with certain movements (e.g. running, kicking) (Kassarjian et al. 2012).

The most common injuries involve the proximal tendons (Fig. 35) and myotendinous and myofascial junctions, either of the direct head, indirect head, or both (Figs. 36, and 37).

Imaging: MRI and US features of these injuries are similar to those of other muscles and tendons. The intramuscular degloving pattern of injury, however, is unique to the RF (Fig. 38), consisting of a circumferential tear at the junction of the direct and indirect muscle bellies, partially or completely dissociating and separating the two (Kassarjian et al. 2014).

Iliopsoas Injuries

Iliopsoas tendinous and myotendinous injuries are a cause of acute and chronic groin pain in sports, typically after a forceful thigh extension

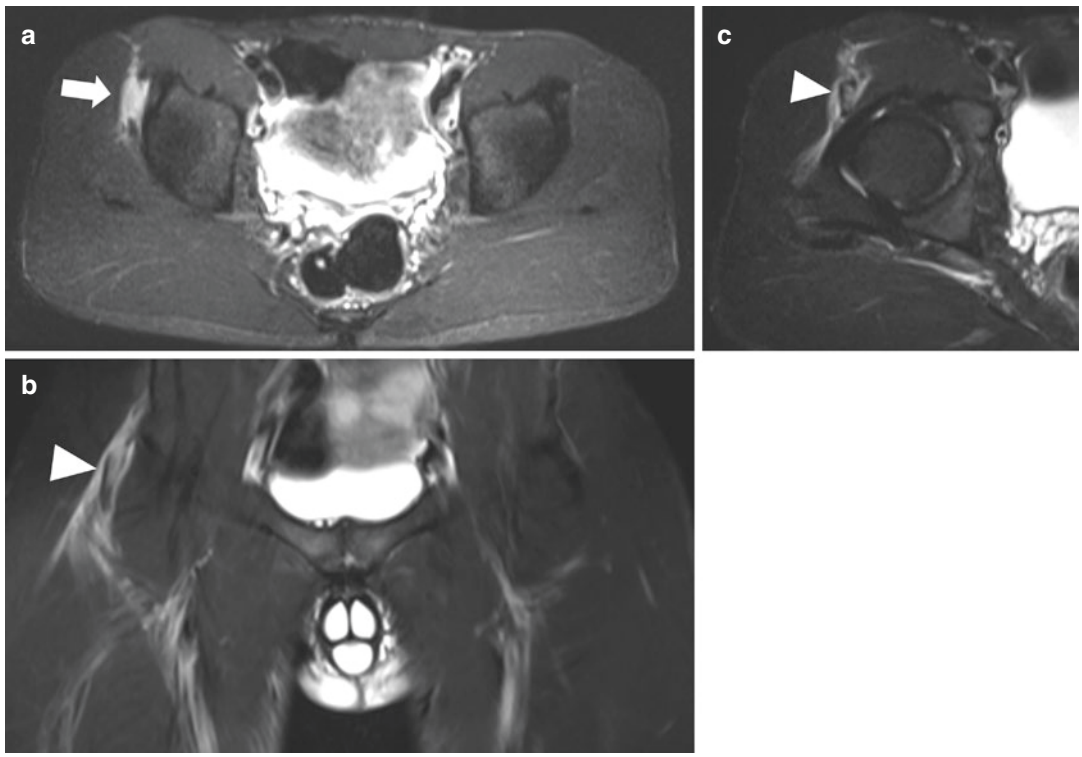

Fig. 35 (**a–c**) 20-year-old professional football player with acute injury during training. (**a**, **c**) Axial and (**b**) coronal fat-supressed T2w images show a complete tear of the indirect tendon (arrow in **a**) and a partial tear of the conjoint/direct tendon (arrowheads in (**b** and **c**) of the right rectus femoris muscle

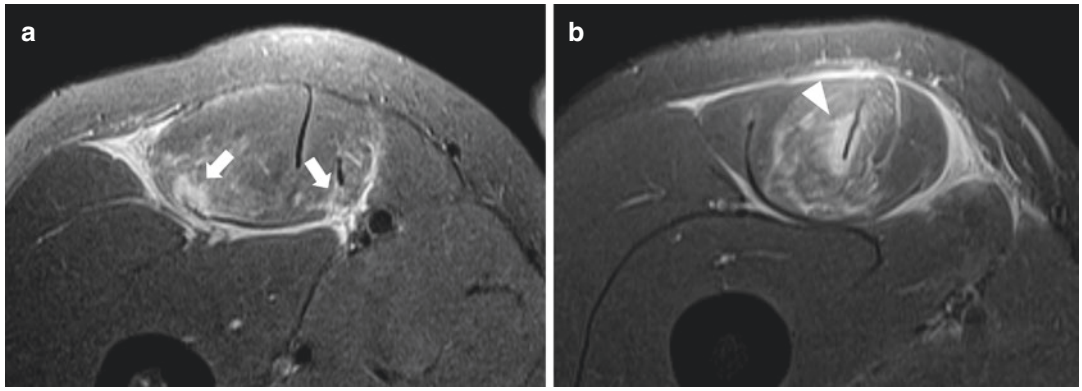

Fig. 36 (**a**, **b**) 35-year-old amateur football player with acute injury during a match. (**a**) Axial fat-supressed T2w MR image in the upper third of the thigh show myofascial posterior tears at the peripheral portion (direct head) of the rectus femoris muscle (arrows), with peripheral muscle oedema. (**b**) Axial fat-supressed T2w image in the middle third of the thigh depicts a myotendinous junction central tear (arrowhead), with central (indirect head) muscle oedema, but no tendon disruption. Abundant associated perifascial fluid is visible in both images

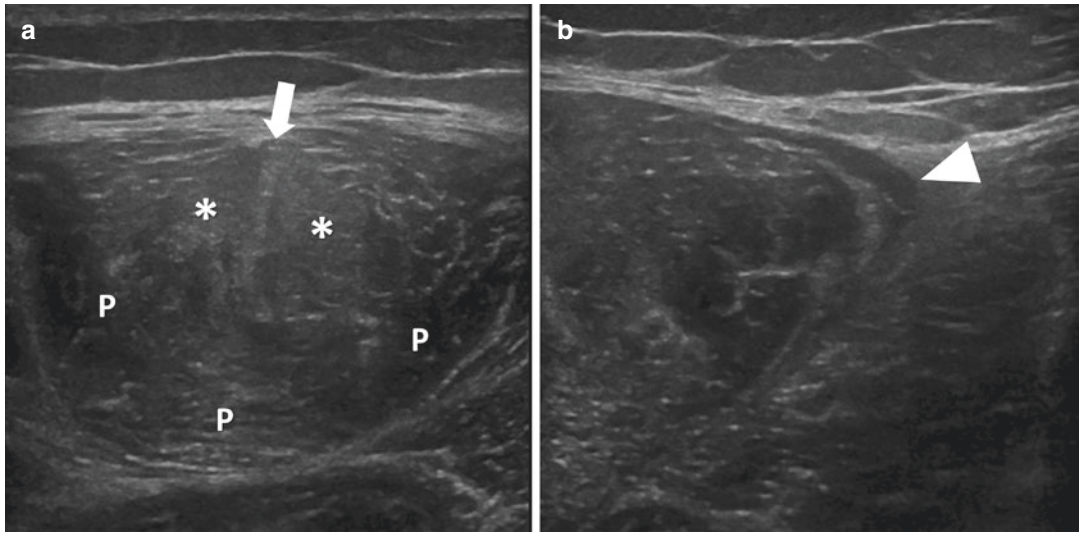

Fig. 37 (**a**, **b**) US transverse images of the anterior thigh of the patient in Fig. 36. (**a**) An ill-defined central tendon (arrow) and faint central muscle hyperechogenicity (*) are evident, consistent with injury of the central myotendinous junction. The peripheral muscle belly appears normal (P). (**b**) Perifascial fluid is demonstrated (arrowhead)

or block during flexion. They have been associated with several activities including football, basketball, tennis, hockey, running and dancing (Domb et al. 2011). Ballet dancers seem to be particularly affected, with symptomatic snapping observed in up to 58% of elite ballet dancers.

Findings of tendinopathy on MRI include thickening and increased tendon signal on T1 and T2WI. Paratendinopathy manifests as fluid tracking along the tendon (Fig. 39), and sometimes associated bursitis is observed as a distension of the iliopsoas bursa (Fig. 40). Fluid in this bursa is not always pathological, since the bursa may communicate with the hip joint. Partial tearing may manifest as focal fluid-filled tendon discontinuity or as focal oedema at the myotendinous junction or fascia (Fig. 41). Complete tears of the tendon are rarely seen in the athlete.

Iliopsoas bursitis, paratendinopathy or tendinopathy are sometimes associated with internal

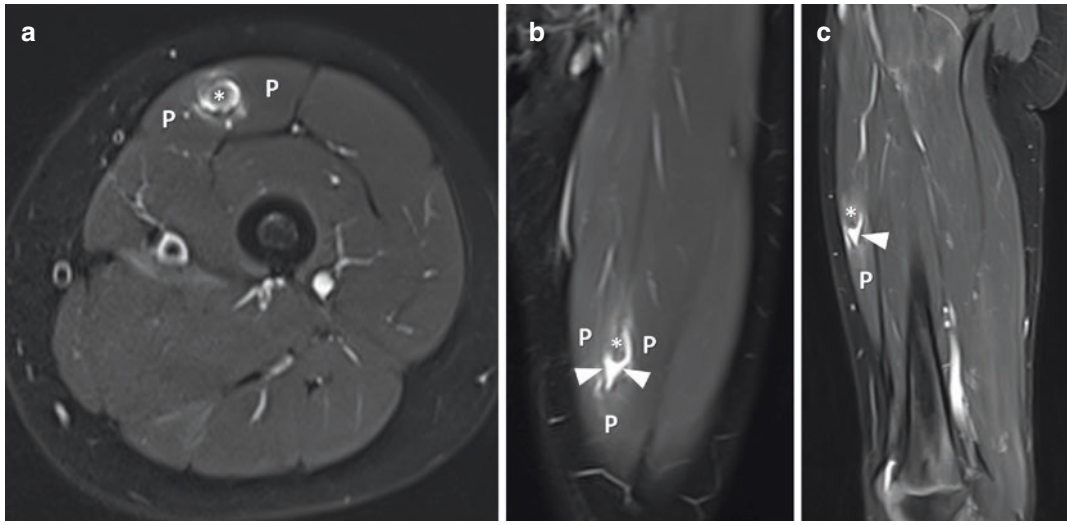

Fig. 38 (**a–c**) Intramuscular rectus femoris degloving injury. (**a**) Axial fat-suppressed T2w image shows a circumferential fluid-filled tear between the central (*) and peripheral (P) bellies of the rectus femoris muscle. (**b**) Coronal and (**c**) sagittal fat-suppressed T2w images demonstrate mild proximal retraction of the central muscle belly (*), which is separated from the peripheral belly (P) by a small amount of fluid (arrowheads)

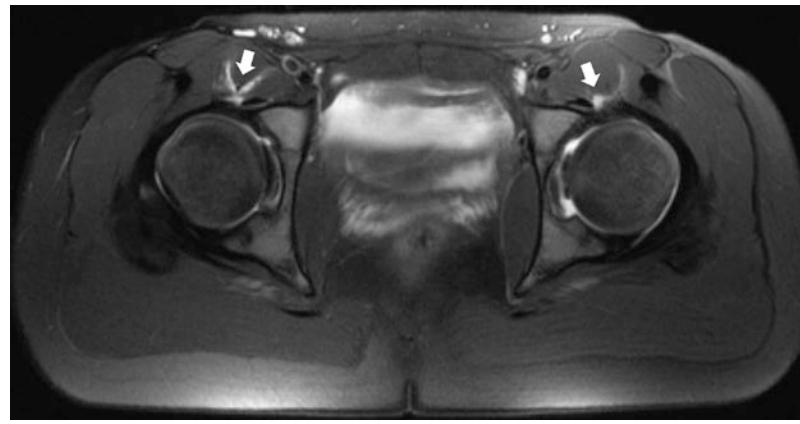

Fig. 39 Iliopsoas paratendinitis. Axial fat-supressed T2-weighted MR image shows peritendinous and perimuscular oedema (arrow). No signal changes are appreciated in the muscle or tendon

snapping hip (previously described). *Iliopsoas impingement syndrome* is another related condition, caused by chronic friction or traction of the iliopsoas tendon on the capsulolabral complex at the acetabular rim. It is more common in young adult female athletes and is associated with a distinct pattern of labral lesion in a direct anterior location, at the 3 o'clock position (Domb et al. 2011).

Proximal Iliotibial Band Syndrome

The proximal insertion of the ITB at the iliac tubercle is the location of an overuse syndrome known as the proximal ITB syndrome, which mainly involves young female long-distance runners, but may also be found in older overweight women (Sher et al. 2011).

US shows hypoechoic asymmetric thickening of the ITB enthesis, with pain elicited by local probe compression. *MRI* will show thickening and high-signal intensity on fluid-sensitive sequences at the fascial insertion on the iliac tubercle. Associated insertional bone marrow oedema and partial and complete tears may also be found (Fig. 42). The fact that hip-focused MRI frequently excludes the iliac tubercle from the

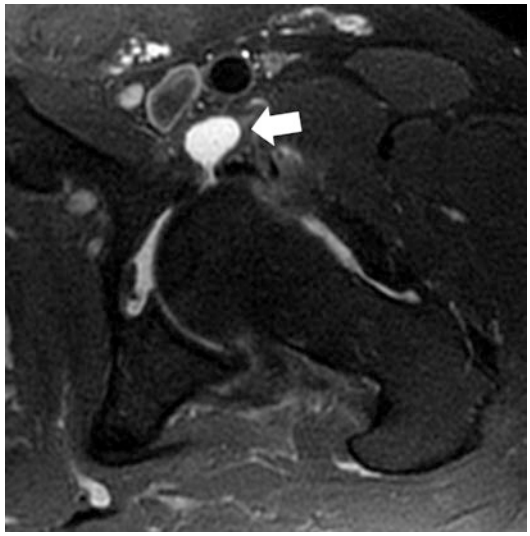

Fig. 40 Iliopsoas bursitis. Axial fat-supressed T2w image shows a distended iliopsoas bursa (arrow)

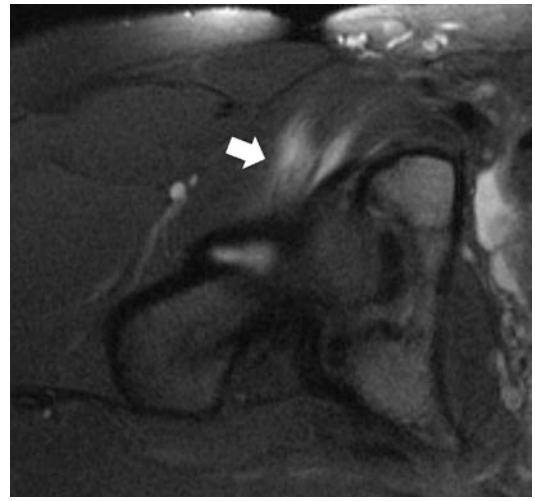

Fig. 41 Myotendinous iliopsoas partial tear. Axial fat-supressed T2w MR image shows a feathery oedema pattern at the myotendinous junction (arrow)

field of view underlines the usefulness of acquiring one large-FOV fluid-sensitive sequence of the pelvis to detect pathology beyond the hip, which may be clinically unsuspected.

Adductor Insertion Avulsion Syndrome

The adductor insertion avulsion syndrome, also known as "thigh splints", belongs to the spectrum of stress lesions of the bone. It represents a painful overuse traction periostitis at the distal insertion of the adductors in the thigh, similar to "shin splints" at the tibia (Anderson et al. 2001).

Periostitis may be present radiographically. MRI will show hyperintense linear signal in fluid-sensitive sequences at the medial femoral cortex, representing periostitis, which may evolve into a stress fracture if left untreated (Fig. 43). US may show cortical irregularity with adjacent hypoechoic soft-tissue thickening, painful to transducer pressure, in a suggestive location in the posteromedial aspect of the femur.

5.3.2.3 Nerves and Nerve Entrapment Syndromes

***General considerations*:** Several acute and chronic nerve entrapment syndromes were described in the pelvic region in athletes, involving the sciatic, obturator, femoral, posterior femoral cutaneous, lateral femoral cutaneous, pudendal, iliohypogastric, ilioinguinal and genitofemoral nerves. They may present with an unclear clinical picture, simulating or coexisting with lumbar radiculopathy, which accounts for their frequent underdiagnosis. These compressive neuropathies have been attributed to (1) fascial thickening, (2) mass effect from hernias and ganglion cysts, (3) adjacent fractures, (4) muscle hypertrophy, while (5) scarring from previous surgery or (6) trauma is also pointed out as a possible cause (Omar et al. 2008; Petchprapa et al. 2010).

Imaging *US and MR imaging* are frequently used in the work-up of peripheral neuropathies, as an adjunct to clinical examination and electrophysiologic studies. Image-guided nerve blocks are a helpful tool when a neuropathic origin of the symptoms is suspected, and are used with both diagnostic and therapeutic purposes.

US is a popular and accurate technique for the evaluation of medium and small sized pelvic nerves along their extra pelvic course, allowing dynamic studies and contralateral comparison. Proximal hypoechoic swelling of the involved nerve, fascicle enlargement and loss of fascicular pattern may be observed in entrapment neuropathies (Fig. 44).

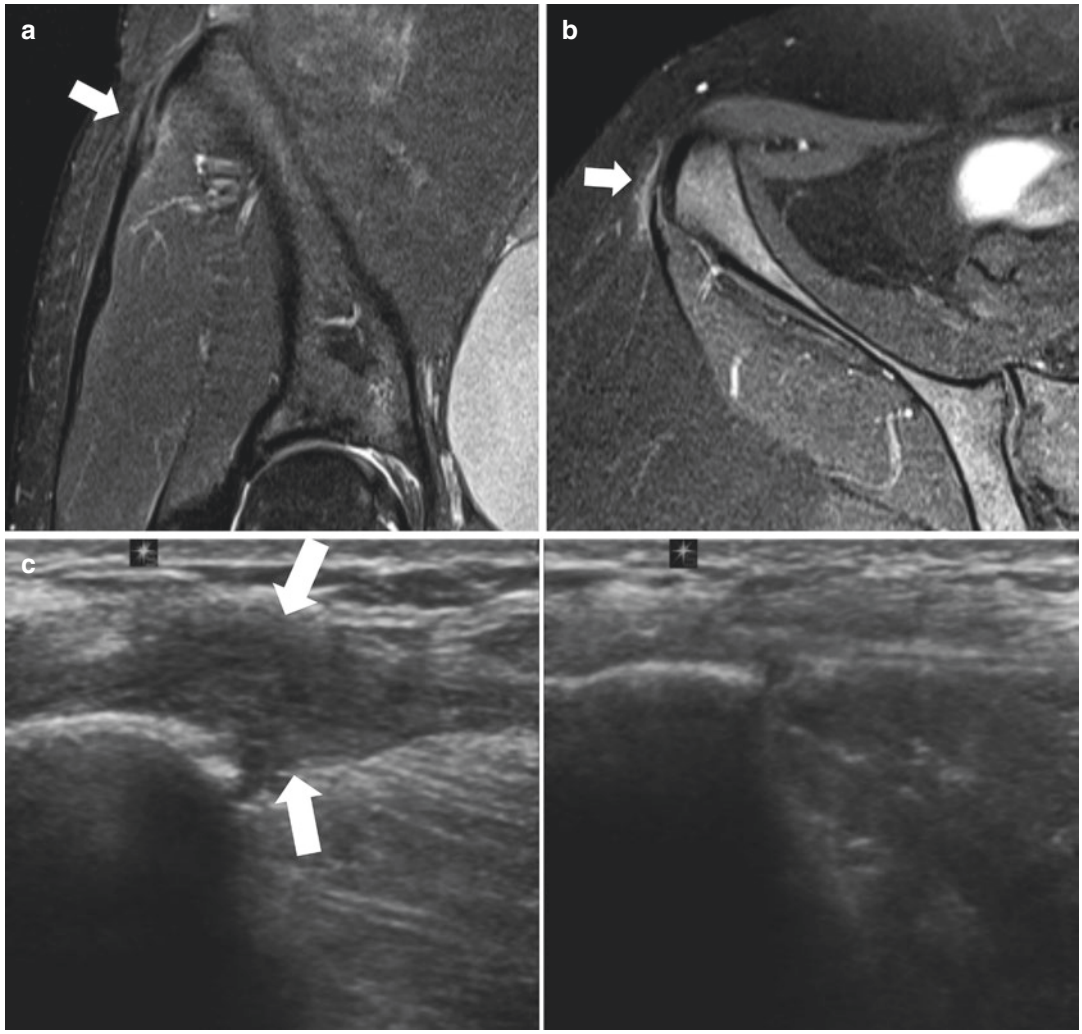

Fig. 42 (**a–c**) Proximal iliotibial band (ITB) syndrome. (**a**) Coronal fat-supressed T2-weighted MR image depicting a partial tear of the proximal ITB (arrow) in a 34-year-old female long distance runner. (**b**) Axial T2w fat-suppressed T2-weighted MR image showing a low-grade injury of the proximal ITB in an overweight non-athlete 29-year-old female, with fascial attenuation and perifascial oedema. (**c**) Longitudinal US scan of the iliac tubercle region demonstrating a marked hypoechoic thickening of the ITB insertion (arrows), which was painful to sonopalpation, in a 37-year-old female runner. The contralateral normal side is shown in the right

3-T MR neurography, in particular, is able to provide high-resolution and high-contrast anatomic images of peripheral nerves, allowing accurate assessment of size, signal and fascicular pattern, even for small nerves. Abnormal MRI features are (1) nerve enlargement (larger than the adjacent artery), (2) hyperintensity on fluid-sensitive images (Fig. 45), (3) loss of fascicular pattern, (4) fascicle swelling, (5) abnormal nerve course, (6) obliteration of perineural fat, along with (7) regional muscle denervation changes if motor or mixed nerves are affected (Soldatos et al. 2013).

Diffusion-weighted imaging and Diffusion Tensor Imaging have shown good results in the functional and quantitative evaluation of peripheral nerve pathologies, but the widespread use of these advanced techniques in clinical practice is currently limited by technical and hardware requirements (Naraghi et al. 2015) (Fig. 19).

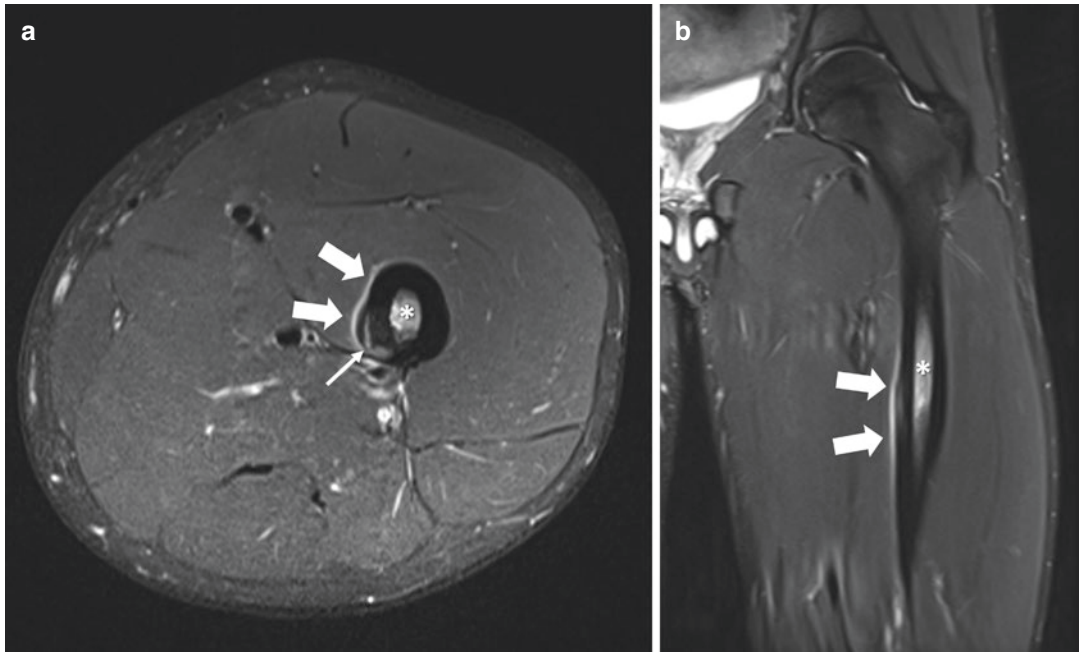

Fig. 43 (**a**, **b**) Thigh splints in a 25-year-old long-distance runner. (**a**) Axial and (**b**) coronal T2w fat-suppressed images demonstrate linear increased signal (thick arrows) at the medial cortex of the femoral diaphysis, representing periostitis. Marrow oedema (*) and increased intracortical signal (thin arrow) represent advanced stress-related changes and impending stress fracture

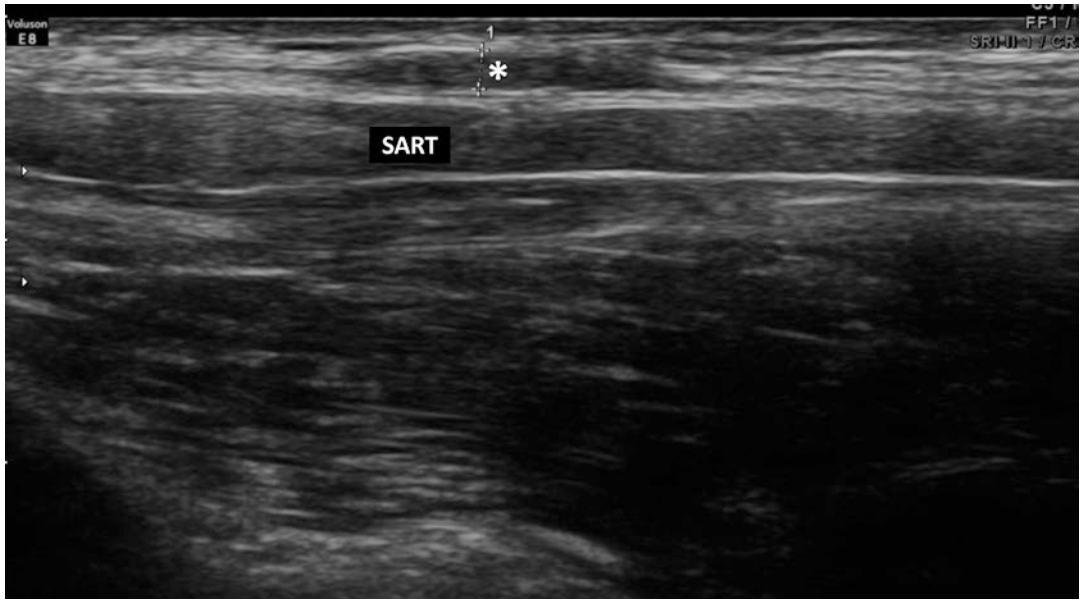

Fig. 44 Lateral femoral cutaneous neuropathy in a 37-year-old man with symptoms of meralgia paresthetica. Longitudinal proximal anterior thigh US scan shows focal hypoechoic swelling of the lateral femoral cutaneous nerve (*) below the inguinal ligament. *SART* sartorius

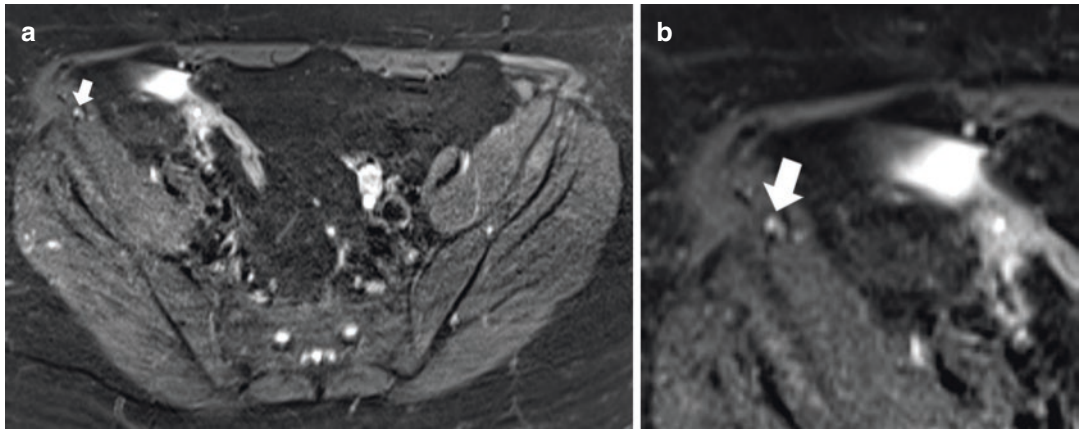

Fig. 45 (**a**, **b**) Lateral femoral cutaneous neuropathy in a 53-year-old woman with symptoms of meralgia paresthetica. (**a**, **b**) Axial fat-suppressed T2-weighted image shows thickening and increased signal of the lateral femoral cutaneous nerve (arrow) near the right anterior superior iliac spine

5.4 Sacroiliac Joints

5.4.1 General Considerations

Anatomy: The sacroiliac joints (SIJ) are the largest axial joints in the human body, linking the spine to the pelvis, with a mobility of 3° to 8° of nutation. SIJ have a central location, between the sacrum and the iliac bones. Obliquely orientated undulating joint facets provide stability to the SIJ, additionally empowered by strong ligaments (interosseous, iliolumbar, sacrotuberous, sacrospinous) and muscles, that interconnect with the lumbosacropelvic sling (Brolinson et al. 2003; Campos-Correia et al. 2019). The stability of this region is dependent upon these muscle-ligamentous relationships, and their breakdown can lead to chronic pain.

SIJ are composed of two main compartments (Fig. 46): (1) an inferior-anteriorly located C-shaped *cartilaginous compartment*, which resembles a symphysis, with hyaline cartilage firmly attached to the bone by fibrous tissue. It was formerly called "synovial portion" but, in fact, only a small part (its lower third) has a true synovial-lined joint capsule, and (2) a *ligamentous compartment (syndesmosis),* located superior-posteriorly, which contains strong interosseous ligaments (Campos-Correia et al. 2019).

Normal variants (iliosacral complex, bipartite iliac bony plate, semi-circular defect, crescent-like iliac bony plates, accessory SIJ), **intra-articular ossified nuclei** and **normal small vessels** should not be mistaken for pathology**.** Accessory SIJ (Fig. 47) are the most frequent variant (8–40%), often found between the iliac and the sacral articular sides at the posterior portion of the SIJ, from the level of the first to the second sacral foramina (Faflia et al. 1998; Campos-Correia et al. 2019).

Clinical presentation: SIJ disorders may present as low back pain or sciatica-like symptoms. For a long time, SIJ pain have been mostly assigned to spondyloarthropathies (SpA), but nowadays it is well recognized that SIJ dysfunction includes a broad differential, including (1) age- and stress-related changes, (2) fractures, (3) infection, (4) other inflammatory sacroiliitis, (5) metabolic, (6) tumours (primary or secondary), and other less common causes. It is also well established that changes on SIJ are commonly found in athletes and/or asymptomatic healthy patients and should be kept in mind. Additionally, the differential diagnosis should always include other pelvic and extra pelvic sites of pain, including the spine, hip and pubic symphysis (Brolinson et al. 2003; Campos-Correia et al. 2019).

Imaging: Interpretation of MRI findings in daily practice is dependent on the clinical context. Age, sex, clinical picture/features and laboratory data help shorten the imaging differential

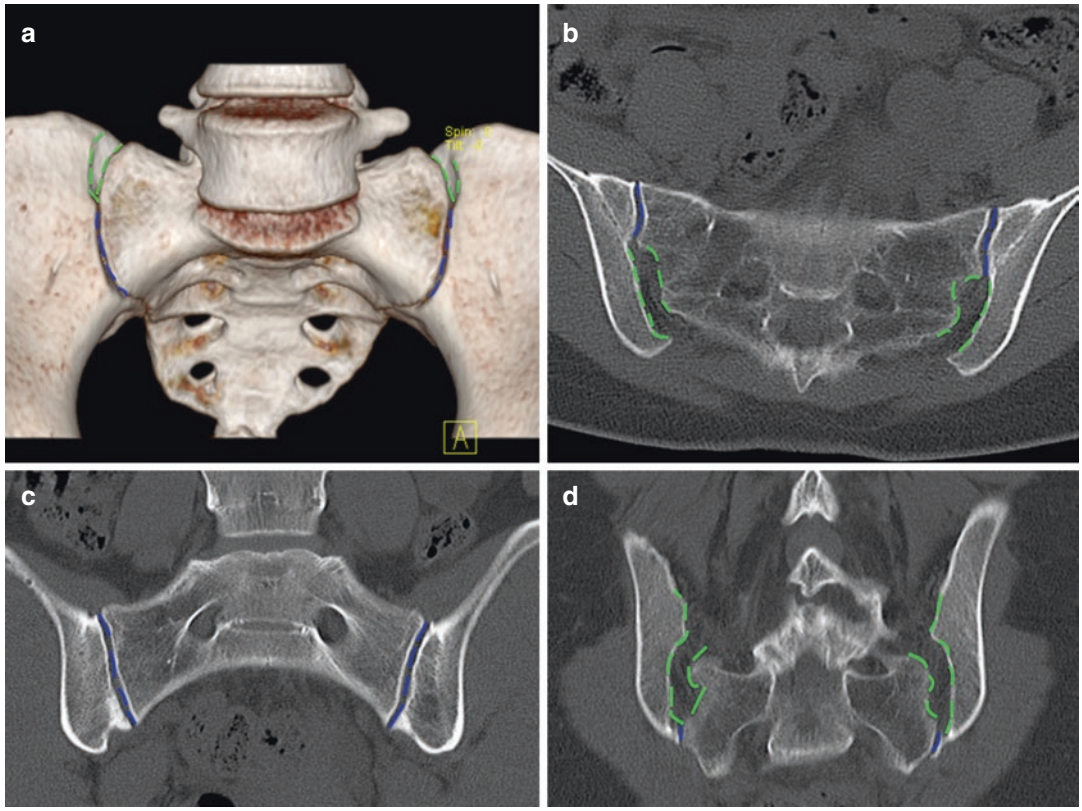

Fig. 46 (**a–d**) 33-year-old female, basketball player. (**a**) 3D volume CT image depicting the cartilaginous (blue) and ligamentous (green) components. (**b**) Axial CT image and (**c**, **d**) coronal CT images at different levels (**c**, anterior; **d** posterior) depicting the same SIJ components (cartilaginous (blue) and ligamentous (green)). Notice on (**c**) the subtle subchondral sclerosis in the lower ilium bilaterally, more conspicuous on the right side, with minor osteophytes due to mild mechanical changes

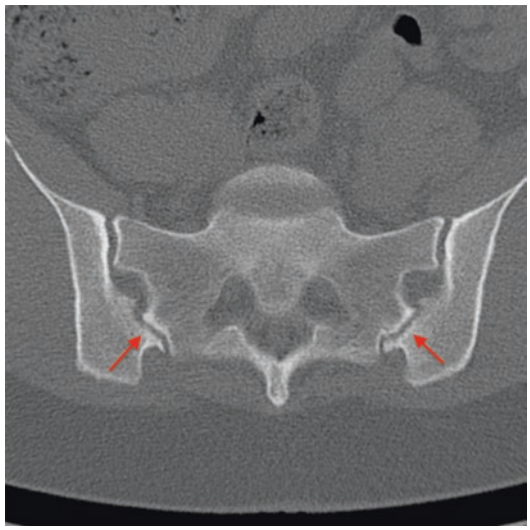

Fig. 47 Axial CT image shows bilateral accessory SIJ (red arrows), a common normal variant, which occasionally may become symptomatic

diagnosis. Prior imaging studies should always be used for comparison, when available (Campos-Correia et al. 2019).

5.4.2 Mechanical/Degenerative Changes of the SIJ: Athletes

The concept of the SIJ as a pain generator is well recognized but controversy exists due to several factors, namely: the complex anatomy and biomechanics of the SIJ and the absence of any specific clinical sign or symptom that is both sensitive and specific for the diagnosis of SIJ dysfunction (Brolinson et al. 2003).

Mechanical changes of the SIJ may account for as much as 20% of low back pain cases in the general population. The prevalence of SIJ pain among athletes is unknown and, likely, underreported because pain referral patterns are nonspecific, and often similar to spinal disease.

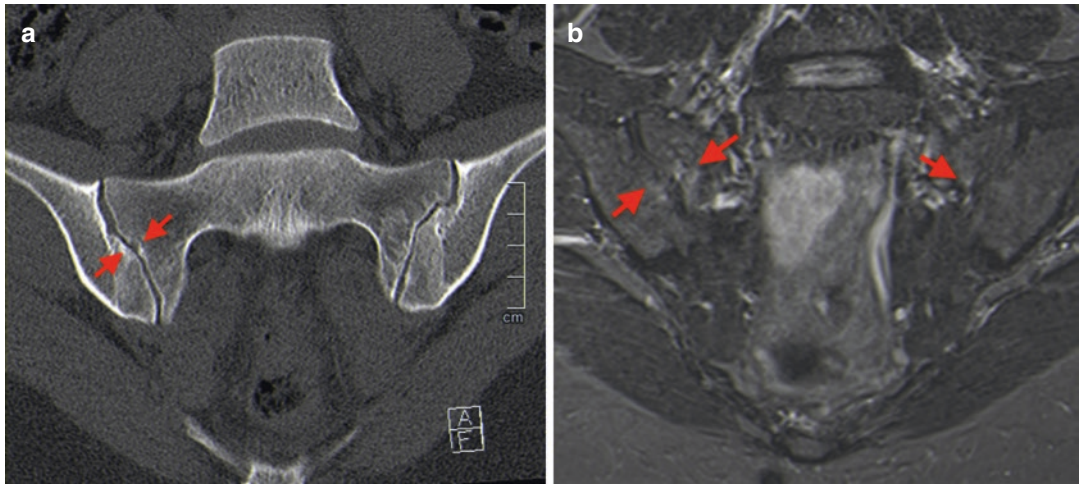

Fig. 48 (**a**, **b**) 25-year-old female, gymnast and contemporary dancer. (**a**) coronal CT image with cortical irregularity/minor erosions, subtle space joint changes and mild sclerosis more evident on the right SIJ (red arrows). (**b**) Coronal fat-suppressed T2-weighted image on the same level, depicts mild oedema foci (red arrows) surrounding these structural changes, related to mechanical, repetitive stress over the SIJ. Another focus of oedema, very subtle, is seen on the left side, probably preceding structural changes

Furthermore, 39% of individuals with SIJ dysfunction have concomitant spinal pathology. In this age range, it is also mandatory to exclude inflammatory sacroiliitis as a cause for the low back pain.

Because of the unique nature of sports' demands on the spine and pelvis, SIJ dysfunction is acknowledged in athletes. Risk factors include:

1. **Type of activity**: sports that involve (1) frequent direct or torsional impact on the axial skeleton, (2) repetitive or asymmetric loading (kicking, swinging, throwing and single leg stance) and (3) repetitive traumatic falls onto the buttocks. Hence, sports with the highest pain prevalence include football, powerlifting, basketball, gymnastics, golfing, cross country skiing, rowing, step aerobics and those that use elliptical and stair stepper machines (Figs. 48 and 49). Furthermore, runners, ice hockey or football players with cumulative repetitive torsional strain of the pelvic ring are also at risk. Rowers are at risk for SIJ dysfunction secondary to their biomechanical demands (prevalence of SIJ dysfunction in 54.1% of USA Senior National Rowing Team members reported (Brolinson et al. 2003)).
2. **Associated conditions:** inflammatory conditions, leg length discrepancy, hypermobility, scoliosis, direct trauma, pregnancy/postpartum and other biomechanical abnormalities (Saunders et al. 2018).

Imaging: Mechanical and degenerative SIJ changes can be seen on imaging, namely (1) **bone marrow oedema** (BME), not only anteriorly in the symphysis pubis, but also potentially dorsally in the SIJ (via propagation of biomechanical strain along the pelvic skeleton), (2) **erosions,** which are less common in athletes, but some studies show scarce, minor erosions in this population, (3) **fat metaplasia,** also relatively scarce in published series while ankylosis of the SIJ was not reported (Weber et al. 2019).

Low-grade BME surrounding the SIJ is present in up to 25% of asymptomatic healthy adults (Ritchlin 2018), most often (but not exclusively) located in the lower iliac bone. Potential triggers of low-grade BME in healthy individuals are mechanical or degenerative stress injury to the spine, overweight or peri/postpartum changes. To date, imaging studies cannot distinguish asymptomatic from symptomatic individuals (Weber et al. 2019).

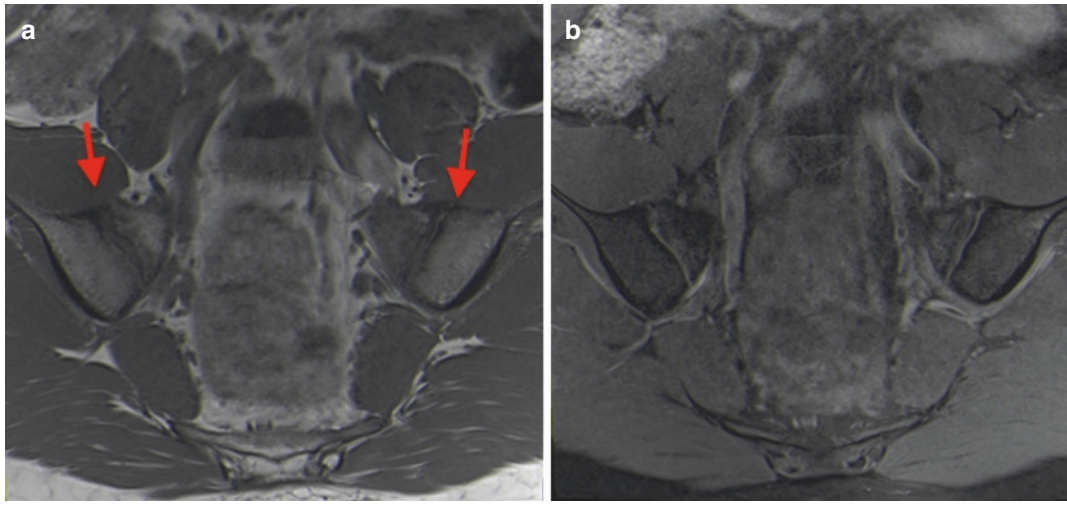

Fig. 49 (**a**, **b**) 17-year-old male, table tennis player with 3-months low back pain. (**a**) Coronal T1w image shows sclerosis, cortical irregularity and minor osteophytes in the anterosuperior part of both SIJ (red arrows). (**b**) Coronal fat-suppressed proton-density-weighted image shows scarce and very subtle oedema on the left side

Athletes may show BME fulfilling ASAS criteria (Assessment of Spondyloarthritis International Society) for active sacroiliitis, which has been reported in 30–35% of recreational runners and 41% of elite ice hockey players (mean age of 27.2 and 25.9 years, respectively) De Smet (2000). The posterior lower ilium quadrant was the single most affected for BME lesions, followed by the anterior upper sacrum. Potential mechanisms for non-specific SIJ BME in athletes are (1) partial-volume effects of presacral vascular plexus or from the deep iliac ligament insertion, (2) local axial strain or (3) anatomic SIJ joint variation encompassing lumbosacral transitional vertebral.

5.4.3 Mechanical/Degenerative Changes of the SIJs: Non-athletes

Osteoarthritis of the SIJ is a common finding in CT (appearing in 65.1% of adults and increasing with age) (Faflia et al. 1998). Moderate adaptive changes begin to occur on the iliac side as early as the third decade, especially in men. Age-related imaging features include (1) space narrowing (often mild), (2) marginal osteophytes, (3) subchondral sclerosis (more well defined and narrower than in SpA), cysts and joint vacuum phenomena (Fig. 50).

While the prevalence of degenerative changes increases with age, they can be seen in young patients, particularly if sport's active. Osteoarthritis tends to affect the iliac side more due to increased load bearing and thinner articular cartilage (Schueller-Weidekamm et al. 2014). Small erosions can also occur within the spectrum of degenerative changes in the SIJ, especially in elderly overweight women, confounding the clinical picture. BME due to osteoarthritis also occurs, particularly surrounding sclerotic areas. It tends to be mild and often is limited to the immediate subchondral area, commonly in the antero-superior part of the SIJs (Weber et al. 2019). Fat deposition is a non-specific finding, but may sometimes be seen in the degenerative setting and even in older healthy individuals. Bridging osteophytosis in osteoarthritis leads to para-articular bony ankyloses (not to be mistaken for the true intra-articular bony ankylosis seen in SpA).

5.4.4 Differential Diagnosis

The list of SIJ differential diagnosis in SIJ disorders is broad, and beyond the scope of this chapter. These are some of the most important differential diagnosis in clinical practice:

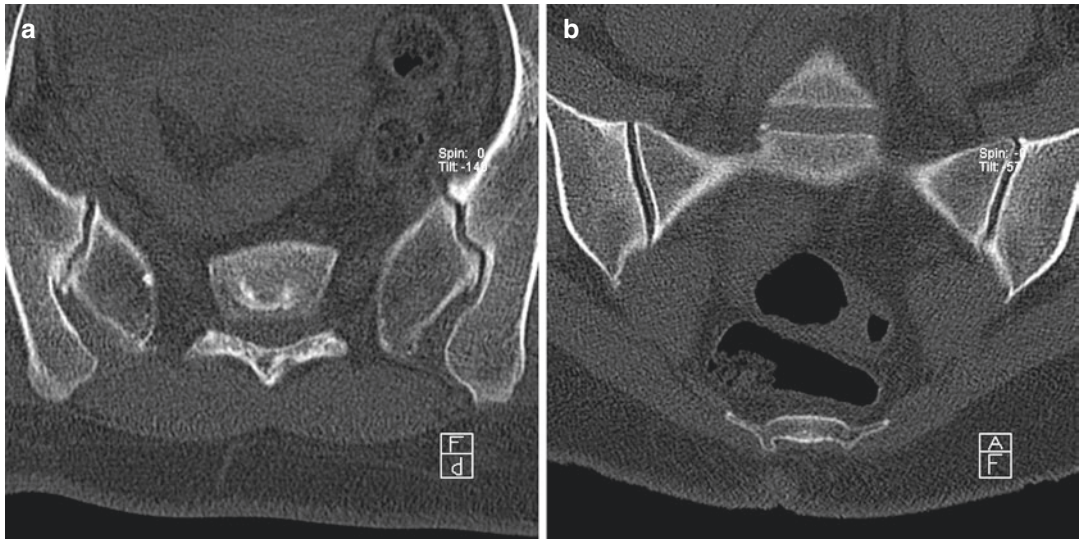

Fig. 50 (**a**, **b**) 49-year-old male with SIJs osteoarthritis. (**a**) axial and (**b**) coronal CT images show bilateral vacuum phenomenon, mild subchondral sclerosis and anterior marginal osteophytosis, with subtle cortical irregularity

Spondyloarthropathies (inflammatory sacroiliitis) (Fig. 51): SpA are a group of inflammatory entities which share overlapping clinical, imaging, genetic and therapeutic features, that are often associated with human leukocyte antigen (HLA) B27 positivity and seronegativity for rheumatoid factor (Rudwaleit et al. 2009). Based on the dominant clinical features, they can be divided into two main groups: (1) **axial SpA** (where sacroiliitis is the cornerstone) and (2) **peripheral SpA**.

A consensus organized by ASAS culminated in the definition of SIJ imaging criteria for the diagnosis of SpA (ASAS imaging arm). Sacroiliitis on imaging is defined as "definite radiographic sacroiliitis according to modified New York criteria" and/or as active sacroiliitis on MRI ("positive" MRI defined by the unequivocal presence of subchondral BME). According to ASAS criteria, the diagnosis of SpA in an adult is based on the presence of active inflammatory lesions (positive MRI "sacroiliitis" ± structural post inflammatory changes (Lambert et al. 2016)) and of at least one clinical feature of SpA (Table 22).

Even with well-established criteria, it is crucial to be aware that a wide range of conditions can pose diagnostic challenges on MRI. Even in patients with inflammatory low-back pain, it is important to consider non-inflammatory disease. It has been documented that 23–33% of patients referred for MRI due to clinical suspicion of SpA had alternative non-inflammatory conditions, and that 41–50% had normal SIJs on MRI.

Other diagnosis: Stress fractures (fatigue and insufficiency), infectious sacroiliitis, osteitis condensans ilii, diffuse idiopathic skeletal hyperostosis (DISH), hyperparathyroidism, chronic recurrent multifocal osteomyelitis (CRMO)/synovitis, acne, pustulosis, hyperostosis and osteitis (SAPHO) and gout.

6 Future Trends in Hip Imaging

The future of hip imaging will include comprehensive 3D joint imaging, performed within fractions of the time currently spent and multiparametric in nature, allowing for (1) high resolution 3D MRI acquisitions with potential for replacing MRA; (2) automated biochemical cartilage and quantitative imaging biomarkers analysis in clinical routine imaging; (3) fully automated diagnostic examinations with algorithms to diagnose and automatically quantify

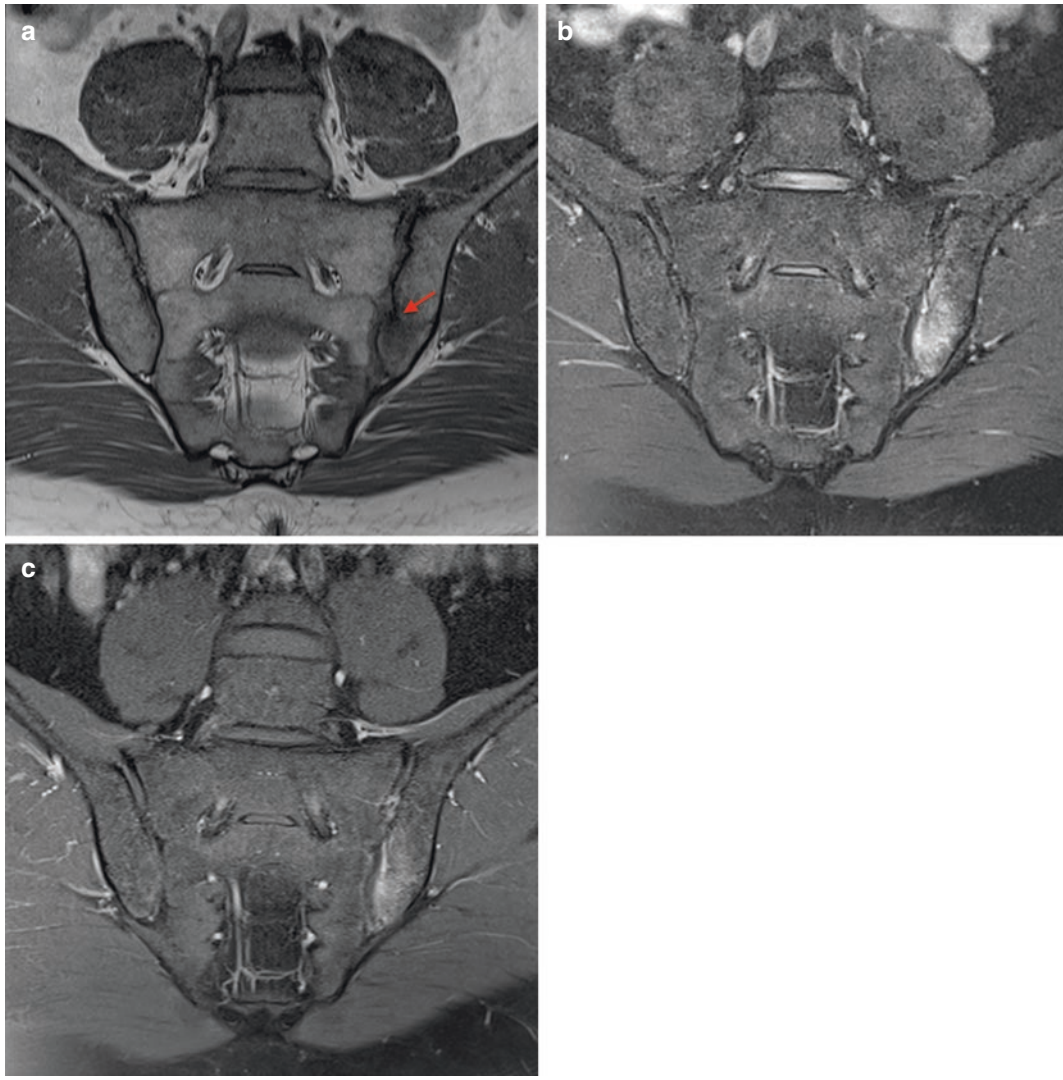

Fig. 51 (**a–c**) 33-year-old male with psoriatic arthritis. (**a**) Coronal T1 (**b**) coronal fat-suppressed proton-density and (**c**) coronal fat-suppressed post-contrast, T1w MR images depict extensive BME adjacent to the left SIJ, on the iliac side, fulfilling ASAS criteria for "positive MRI". Notice cortical irregularity and minor erosions (red arrow) seen on (**a**)

Table 22 Types of MRI lesions in the SIJ

Active inflammatory lesions	Chronic (structural) postinflammatory lesions
BME/osteitis (primary criterion)	Subchondral sclerosis
Capsulitis	Erosions
Enthesitis	Backfill
Joint space enhancement (formerly called synovitis)	Fat metaplasia
Active erosion	Bone ankylosis
Joint space fluid	Bone bud

specific biomarkers (Mascarenhas and Caetano 2018) (Fig. 52).

6.1 Artificial Intelligence

Clinical large databases in the era of value-based health care are paramount. The implementation of standardized national sports registries in conjunction with programmes tailored to radiologists

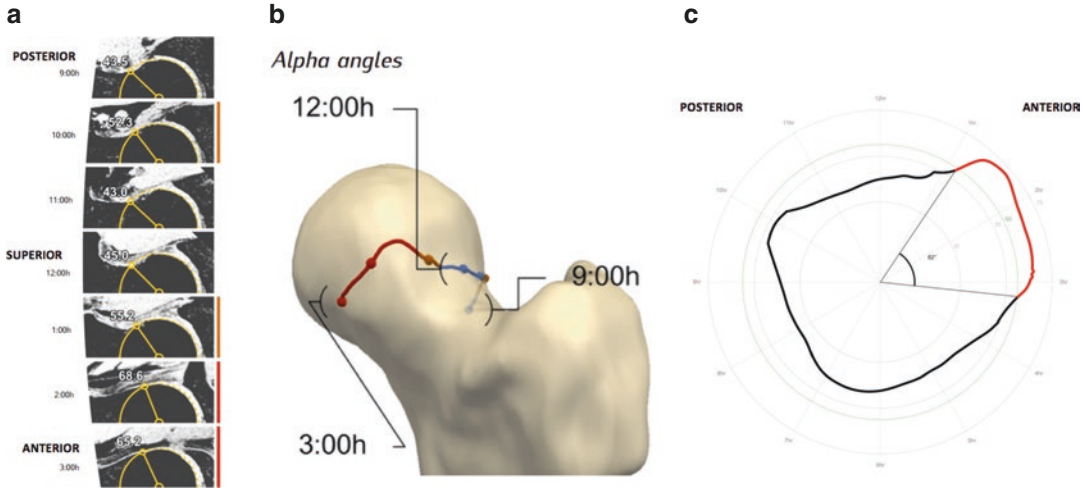

Fig. 52 (**a–c**) Automated segmentation and quantification of femoral parameters based on a 3D MRI dataset of a 25-year-old elite soccer player. (**a**) Volumetric 3D MRI alpha-angle (α°) automated measurements made at different points around the femoral head/neck junction. α° measured at 9 o'clock (posterior); 10, 11 and 12 o'clock (superior); and 1, 2 and 3 o'clock (anterior). (**b**) 3D generated model representing the radial extension of the cam deformity (orange and red line representing increased alpha angles). (**c**) Polar plot (2D) of the automated 360° α° measurements around the FHN, representing the Ω° angle and corresponding perimeter (red line) for a given α° threshold (60°). Red lines represent increased α°s for a given threshold. The Ω° is formed by two lines intersecting the centre of the femoral neck at the level of the head-neck junction. The most posterior line posteriorly intersects the point at which the α° angle begins to be abnormal beyond a best-fitting circle and the anterior line at the point where the α° angle returns to normal

and sports medicine practisers will ultimately improve patient outcomes while minimizing the economic burden.

Artificial intelligence in the sports medicine field will certainly set the new standard by automatically detecting patterns in injury data, and then using those patterns to predict RTS or enable decision making under uncertain conditions. Applications include (1) automatic image segmentation and registration; (2) computer-aided detection and diagnosis; (3) integration with healthcare big data and (4) defining "personalized" RTS prediction and treatment strategies (Syed and Zoga 2018).

6.2 Personalized Medicine and Biobanks

The original concept of precision sports medicine involves the implementation of treatment and prevention strategies that consider individual variability by assessing large sets of data, including patient information, medical imaging, and genomic sequences. Patient-based imaging data will be implemented and cross-linked to population-based data already acquired in biobanks, allowing a "tailored" decision to a specific athlete (Kooijman et al. 2016).

7 Conclusion

Innovation has been the catalyst for the transformation of hip imaging, as the arrival of new modalities and the introduction of MRI resulted in a paradigm shift from bone morphology analysis to integrated soft tissue, joint and cartilage assessment. Understanding the pathophysiology through the visualization of osseous structures and detailed depiction of soft tissues has become part of routine imaging and has had a major impact on therapeutic decision-making.

With increasing sports medicine specialization and also rising rates of overuse injuries,

major questions have still to be answered when it comes to sports injuries, namely RTS specific predictors and the role played by intense athletic activity in FAIS development. The delicate balance between early preventive measures, conservative treatment and surgical intervention has yet to be clearly defined. It is time to refine the diagnostic and therapeutical algorithm by incorporating both clinical and imaging data into the medical equation. Looking ahead, imaging and sports will continue to evolve hand-in-hand, with new problems and greater challenges.

Box 1: Standard Radiography

- Radiography is the first-line imaging modality to assess the bony hip and pelvis; it is not well suited, however, to evaluate soft tissue injuries.
- Radiographs are two-dimensional projections of three-dimensional structures, which limit their value in particular clinical settings (e.g. morphological assessment in FAI).
- Specific radiographic views may be warranted, depending on a particular clinical problem.

Box 2: Ultrasound (US)

- US is an established technique in the work-up of an athlete with hip/groin pain, particularly for suspected muscle and tendon disease.
- US is a fast, low-cost, radiation-free, widely available technique which easily allows dynamic imaging and contralateral comparison.
- US-guided injections may prove very useful in both the diagnostic (confirm the source of symptoms) and therapeutic settings.

Box 3: Computed Tomography

- CT is an excellent imaging method to assess osseous morphologies, hence useful in the evaluation of fractures and calcification/ossification although very limited in depicting soft tissues injuries.
- In athletes, CT should be used mainly as a problem-solving tool, whenever radiographic occult fractures are suspected or in pre-operative planning.
- Hip CT arthrography can be used to assess hip chondrolabral injuries particularly if MRI is contra-indicated.

Box 4: Magnetic Resonance Imaging

- MRI is a comprehensive radiation-free technique considered the gold standard imaging approach in sports, to assess both bony and soft tissue structures in the pelvis/hip region.
- MRI protocols combining hip dedicated sequences as well as sequences covering the pelvis offer the best chance of identifying all potential sources of symptoms; tailoring the MRI protocol to the specific clinical scenario is crucial to achieve the best results.
- When intra-articular disease is suspected, dMRA is the imaging study of choice, as both a **diagnostic** arthrography and an **anaesthetic** injection can be combined into a single procedure.

Things to Remember (Hip)

1. Knowledge of hip biomechanics helps in the understanding of sports-related hip disease.
2. In athletes with hip-groin pain, periarticular structures need to be imaged because many abnormalities occur outside the hip joint.
3. If radiographs are normal and clinical suspicion for stress fracture remains high, fur-

ther investigation with MRI should be sought.
4. Imaging findings described in cam-type FAI include an increased α angle, anterosuperior labral tears and anterosuperior chondral abnormalities at the chondrolabral junction.
5. Labral tears are common in athletes (both symptomatic and asymptomatic), and usually best identified on small FOV images.
6. The most common underlying cause of GTPS is *gluteus minimus* and *medius* insertional tendon disease resulting from chronic repetitive microtrauma, including tendinosis, tendon tearing and peritendinitis.

Things to Remember (Pelvis)

1. MRI is the gold standard technique to assess the continuum of stress response of bone.
2. Mechanical stress applied to the muscle-tendon-bone unit may result in tendon tears or myotendinous lesions in the adult athlete and in apophyseal avulsion the child or adolescent. This is due to the intrinsic fragility of the apophyseal growth plate in the immature skeleton, which may tear in response to traction stress.
3. Pelvic apophyseal avulsions are unusual in the mature skeleton and should prompt a search for an underlying cause (e.g. metastasis).
4. The *rectus femoris*, *biceps femoris* and *adductor longus* are the most commonly injured muscles in the pelvis and thigh.
5. MRI is useful to confirm the clinical diagnosis and determine the extent of muscle injury, but has limited prognostic value in determining recovery times.

Things to Remember (SIJ)

1. SIJ dysfunction is a well-known clinical entity in sports, with repetitive, asymmetric mechanical loading and microtrauma, leading to imaging changes, including low-grade BME and occasionally minor erosions in the SIJ in athletes.
2. BME is present in up to 25% of SIJ of healthy adults, usually low-grade and non-extensive even though a substantial proportion will fulfil ASAS criteria for a positive MRI of inflammatory sacroiliitis. Clinical correlation, including sports history, is warranted.
3. There is a broad differential diagnosis for SIJ dysfunction. When assessing active athletes, sacral fractures and SpA-related sacroiliitis must be sought. Deep (extensive) BME lesions are almost exclusively found in axial SpA patients. Other sites of pelvic (e.g.: pubic symphysis and hip) and extra pelvic (e.g.: spine) pain must be excluded.

References

Agricola R, Heijboer MP, Bierma-Zeinstra SMA et al (2013a) Cam impingement causes osteoarthritis of the hip: a nationwide prospective cohort study (CHECK). Ann Rheum Dis 72:918–923. https://doi.org/10.1136/annrheumdis-2012-201643

Agricola R, Heijboer MP, Ginai AZ et al (2014) A cam deformity is gradually acquired during skeletal maturation in adolescent and young male soccer players: a prospective study with minimum 2-year follow-up. Am J Sports Med 42:798–806. https://doi.org/10.1177/0363546514524364

Agricola R, Heijboer MP, Roze RH et al (2013b) Pincer deformity does not lead to osteoarthritis of the hip whereas acetabular dysplasia does: acetabular coverage and development of osteoarthritis in a nationwide prospective cohort study (CHECK). Osteoarthr Cartil 21:1514–1521. https://doi.org/10.1016/j.joca.2013.07.004

Agricola R, Waarsing JH, Arden NK et al (2013c) Cam impingement of the hip: a risk factor for hip osteoarthritis. Nat Rev Rheumatol 9:630–634. https://doi.org/10.1038/nrrheum.2013.114

Agten CA, Sutter R, Buck FM, Pfirrmann CWA (2016) Hip imaging in athletes: sports imaging series. Radiology 280:351–369. https://doi.org/10.1148/radiol.2016151348

Allen D, Beaulé PE, Ramadan O, Doucette S (2009) Prevalence of associated deformities and hip pain in patients with cam-type femoroacetabular impingement. J Bone Joint Surg Br 91:589–594. https://doi.org/10.1302/0301-620X.91B5.22028

Alonso-Coello P, Schünemann HJ, Moberg J et al (2016) GRADE Evidence to Decision (EtD) frameworks: a systematic and transparent approach to making well informed healthcare choices. 1: Introduction. BMJ 353:i2016. https://doi.org/10.1136/bmj.i2016

Anderson LA, Peters CL, Park BB et al (2009) Acetabular cartilage delamination in femoroacetabular impingement. Risk factors and magnetic resonance imaging

diagnosis. J Bone Joint Surg 91:305–313. https://doi.org/10.2106/JBJS.G.01198

Anderson MW, Kaplan PA, Dussault RG (2001) Adductor insertion avulsion syndrome (thigh splints): spectrum of MR imaging features. Am J Roentgenol 177:673–675. https://doi.org/10.2214/ajr.177.3.1770673

Anwander H, Beck M, Büchler L (2018) The influence of evolution on cam deformity and its impact on biomechanics of the human hip joint. J Orthop Res. https://doi.org/10.1002/jor.23863

Aprato A, Giachino M, Massè A (2016) Arthroscopic approach and anatomy of the hip. Muscles Ligaments Tendons J 6:309–316. https://doi.org/10.11138/mltj/2016.6.3.309

Ayeni OR, Farrokhyar F, Crouch S et al (2014) Preoperative intra-articular hip injection as a predictor of short-term outcome following arthroscopic management of femoroacetabular impingement. Knee Surg Sports Traumatol Arthrosc 22:801–805. https://doi.org/10.1007/s00167-014-2883-y

Ayeni OR, Wong I, Chien T et al (2012) Surgical indications for arthroscopic management of femoroacetabular impingement. Arthrosc J Arthrosc Related Surg 28:1170–1179. https://doi.org/10.1016/j.arthro.2012.01.010

Bardakos NV, Villar RN (2009) Predictors of progression of osteoarthritis in femoroacetabular impingement a radiological study with a minimum of ten years follow-up. J Bone Joint Surg 91:162–169. https://doi.org/10.1302/0301-620X.91B2

Beck M, Kalhor M, Leunig M, Ganz R (2005) Hip morphology influences the pattern of damage to the acetabular cartilage. J Bone Joint Surg 87:1012–1018. https://doi.org/10.1302/0301-620X.87B7

Bedi A, Chen N, Robertson W, Kelly BT (2008) The management of labral tears and femoroacetabular impingement of the hip in the young, active patient. Arthrosc J Arthrosc Related Surg 24:1135–1145

Bencardino JT, Mellado JM (2005) Hamstring Injuries of the Hip. Magn Reson Imaging Clin N Am 13:677–690. https://doi.org/10.1016/j.mric.2005.08.002

Bittersohl B, Steppacher S, Haamberg T et al (2009) Cartilage damage in femoroacetabular impingement (FAI): preliminary results on comparison of standard diagnostic vs delayed gadolinium-enhanced magnetic resonance imaging of cartilage (dGEMRIC). Osteoarthr Cartil 17:1297–1306. https://doi.org/10.1016/j.joca.2009.04.016

Blankenbaker DG, al E (2006) The painful hip: new concepts

Blankenbaker DG, De Smet AA, Keene JS, Fine JP (2007) Classification and localization of acetabular labral tears. Skelet Radiol 36:391–397. https://doi.org/10.1007/s00256-006-0240-z

Boric I, Isaac A, Dalili D et al (2019) Imaging of articular and extra-articular sports injuries of the hip. Semin Musculoskelet Radiol 23:e17–e36. https://doi.org/10.1055/s-0039-1688696

Bowman KF, Fox J, Sekiya JK (2010) A clinically relevant review of hip biomechanics. Arthroscopy 26:1118–1129. https://doi.org/10.1016/j.arthro.2010.01.027

Boyd KT, Peirce NS, Batt ME (1997) Common hip injuries in sport. Sports Med 24:273–288. https://doi.org/10.2165/00007256-199724040-00005

Brittenden J, Robinson P (2005) Imaging of pelvic injuries in athletes. Br J Radiol 78:457–468. https://doi.org/10.1177/036354659502300515

Brolinson PG, Kozar AJ, Cibor G (2003) Sacroiliac joint dysfunction in athletes. Curr Sports Med Rep 2:47–56. https://doi.org/10.1249/00149619-200302000-00009

Busse J, Gasteiger W, Tönnis D (1972) Eine neue Methode zur röntgenologischen Beurteilung eines Hüftgelenkes--Der Hüftwert [A new method for roentgenologic evaluation of the hip joint--the hip factor]. Arch Orthop Unfallchir 72(1):1–9. German. https://doi.org/10.1007/BF00415854. PMID: 5020681

Byrd JWT, Jones KS (2004) Diagnostic accuracy of clinical assessment, magnetic resonance imaging, magnetic resonance arthrography, and intra-articular injection in hip arthroscopy patients. Am J Sports Med 32:1668–1674. https://doi.org/10.1177/0363546504266480

Byrd JWT, Potts EA, Allison RK, Jones KS (2014) Ultrasound-guided hip injections: a comparative study with fluoroscopy-guided injections. YJARS 30:42–46. https://doi.org/10.1016/j.arthro.2013.09.083

Calderazzi F, Nosenzo A, Galavotti C et al (2018) Apophyseal avulsion fractures of the pelvis. A review. Acta Biomed 89:470–476. https://doi.org/10.23750/abm.v89i4.7632

Campos-Correia D, Sudoł-Szopińska I, Diana Afonso P (2019) Are we overcalling sacroillitis on MRI? Differential diagnosis that every rheumatologist should know—Part II. Acta Reumatol Port 44:42–56

Cerezal L, Arnaiz J, Canga A et al (2012) Emerging topics on the hip: Ligamentum teres and hip microinstability. Eur J Radiol 81:3745–3754. https://doi.org/10.1016/j.ejrad.2011.04.001

Chahla J, Soares EAM, Devitt BM et al (2016) Ligamentum teres tears and femoroacetabular impingement: prevalence and preoperative findings. Arthroscopy 32:1293–1297. https://doi.org/10.1016/j.arthro.2016.01.045

Clohisy JC (2008) A systematic approach to the plain radiographic evaluation of the young adult hip. J Bone Joint Surg 90:47. https://doi.org/10.2106/JBJS.H.00756

Crema MD, Guermazi A, Tol JL et al (2015) Acute hamstring injury in football players: Association between anatomical location and extent of injury—a large single-center MRI report. J Sci Med Sport 19(4):317–322. https://doi.org/10.1016/j.jsams.2015.04.005

Crespo-Rodríguez AM, De Lucas-Villarrubia JC, Pastrana-Ledesma M et al (2017) The diagnostic performance of non-contrast 3-Tesla magnetic resonance imaging (3-T MRI) versus 1.5-Tesla magnetic resonance arthrography (1.5-T MRA) in femoroacetabular impingement. Eur J Radiol 88:109–116. https://doi.org/10.1016/j.ejrad.2016.12.031

Cruz CA, Kerbel Y, Smith CM et al (2019) A sport-specific analysis of the epidemiology of hip injuries in National Collegiate Athletic Association Athletes from 2009 to 2014. Arthroscopy 35:2724–2732. https://doi.org/10.1016/j.arthro.2019.03.044

Cruz J, Mascarenhas V (2018) Adult thigh muscle injuries-from diagnosis to treatment: what the radiologist should know. Skelet Radiol. https://doi.org/10.1007/s00256-018-2929-1

Czerny C, Hofmann S, Neuhold A et al (1996) Lesions of the acetabular labrum: accuracy of MR imaging and MR arthrography in detection and staging. Radiology 200:225–230. https://doi.org/10.1148/radiology.200.1.8657916

De Smet AA, Best TM (2000) MR imaging of the distribution and location of acute hamstring injuries in athletes. Am J Roentgenol 174:393–399. https://doi.org/10.2214/ajr.174.2.1740393

De Smet AA, Blankenbaker DG, Alsheik NH, Lindstrom MJ (2012) MRI appearance of the proximal hamstring tendons in patients with and without symptomatic proximal hamstring tendinopathy. AJR Am J Roentgenol 198:418–422. https://doi.org/10.2214/AJR.11.6590

Dienst M (2005) Hip arthroscopy: technique and anatomy. Operat Tech Sports Med 13:13–23. https://doi.org/10.1053/j.otsm.2004.09.009

Dietrich TJ, Suter A, Pfirrmann C, Dora C (2012) Supraacetabular Fossa (Pseudodefect of Acetabular Cartilage): frequency at MR arthrography and comparison of findings at MR arthrography and arthroscopy

Domb BG, Shindle MK, McArthur B et al (2011) Iliopsoas impingement: a newly identified cause of labral pathology in the hip. HSS JRNL 7:145–150. https://doi.org/10.1007/s11420-011-9198-z

Eberbach H, Hohloch L, Feucht MJ, Konstantinidis L, Südkamp NP, Zwingmann J (2017) Operative versus conservative treatment of apophyseal avulsion fractures of the pelvis in the adolescents: a systematical review with meta-analysis of clinical outcome and return to sports. BMC Musculoskelet Disord 18(1):162. https://doi.org/10.1186/s12891-017-1527-z. PMID: 28420360; PMCID: PMC5395880

Ekstrand J, Hägglund M, Waldén M (2011) Epidemiology of muscle injuries in professional football (soccer). Am J Sports Med 39:1226–1232. https://doi.org/10.1136/bjsm.2004.014571

Faflia CP, Prassopoulos PK, Daskalogiannaki ME, Gourtsoyiannis NC (1998) Variation in the appearance of the normal sacroiliac joint on pelvic CT. Clin Radiol 53:742–746. https://doi.org/10.1016/s0009-9260(98)80316-4

Frank JM, Harris JD, Erickson BJ et al (2015) Prevalence of femoroacetabular impingement imaging findings in asymptomatic volunteers: a systematic review. Arthroscopy 31:1199–1204. https://doi.org/10.1016/j.arthro.2014.11.042

Freke MD, Kemp J, Svege I et al (2016) Physical impairments in symptomatic femoroacetabular impingement: a systematic review of the evidence. Br J Sports Med 50:1180–1180. https://doi.org/10.1136/bjsports-2016-096152

Galeano NA, Guinea NS, Molinero JG, Bárez MG (2018) Extra-articular hip impingement: a review of the literature. Radiología (English Edition) 60:105–118. https://doi.org/10.1016/j.rxeng.2018.02.002

Ganz R, Gill TJ, Gautier E et al (2001) Surgical dislocation of the adult hip a technique with full access to the femoral head and acetabulum without the risk of avascular necrosis. J Bone Joint Surg 83:1119–1124

Ganz R, Parvizi J, Beck M et al (2003) Femoroacetabular impingement: a cause for osteoarthritis of the hip. Clin Orthop Relat Res:112–120. https://doi.org/10.1097/01.blo.0000096804.78689.c2

Giori NJ, Trousdale RT (2003) Acetabular retroversion is associated with osteoarthritis of the hip. Clin Orthop Relat Res:263–269. https://doi.org/10.1097/01.blo.0000093014.90435.64

Glyn-Jones S, Palmer AJR, Agricola R et al (2015) Osteoarthritis. Lancet:1–12. https://doi.org/10.1016/S0140-6736(14)60802-3

Gosvig KK, Jacobsen S, Sonne-Holm S et al (2010) Prevalence of malformations of the hip joint and their relationship to sex, groin pain, and risk of osteoarthritis: a population-based survey. J Bone Joint Surg Am 92:1162–1169. https://doi.org/10.2106/JBJS.H.01674

Gouttebarge V, Inklaar H, Backx F, Kerkhoffs G (2015) Prevalence of osteoarthritis in former elite athletes: a systematic overview of the recent literature. Rheumatol Int 35:405–418. https://doi.org/10.1007/s00296-014-3093-0

Grammatopoulos G, Speirs AD, Ng KCG et al (2018) Acetabular and spino-pelvic morphologies are different in subjects with symptomatic cam femoroacetabular impingement. J Orthop Res 36:1840–1848. https://doi.org/10.1002/jor.22375

Greaney RB, Gerber FH, Laughlin RL et al (1983) Distribution and natural history of stress fractures in U.S. Marine recruits. Radiology 146:339–346. https://doi.org/10.1148/radiology.146.2.6217486

Griffin DR, Dickenson EJ, O'Donnell J et al (2016) The Warwick Agreement on femoroacetabular impingement syndrome (FAI syndrome): an international consensus statement. Br J Sports Med 50:1169–1176. https://doi.org/10.1136/bjsports-2016-096743

Griffin DR, Dickenson EJ, Wall PDH et al (2018) Hip arthroscopy versus best conservative care for the treatment of femoroacetabular impingement syndrome (UK FASHIoN): a multicentre randomised controlled trial. Lancet 391:2225–2235. https://doi.org/10.1016/S0140-6736(18)31202-9

Guermazi A, Roemer FW, Robinson P et al (2017) Imaging of muscle injuries in sports medicine: sports imaging series. Radiology 282:646–663. https://doi.org/10.1148/radiol.2017160267

Haefeli PC, Steppacher SD, Babst D et al (2015) An increased iliocapsularis-to-rectus-femoris ratio is suggestive for instability in borderline hips. Clin Orthop Relat Res 473:3725–3734. https://doi.org/10.1007/s11999-015-4382-y

Hanke MS, Steppacher SD, Anwander H et al (2016) What MRI findings predict failure 10 years after surgery for femoroacetabular impingement? Clin Orthop Relat Res:1–16. https://doi.org/10.1007/s11999-016-5040-8

Hartigan DE, Perets I, Yuen LC, Domb BG (2017) Results of hip arthroscopy in patients with MRI diagnosis of subchondral cysts—a case series. J Hip Preserv Surg 4:324–331. https://doi.org/10.1016/j.arth.2014.03.054

Hawker GA, Stanaitis I (2014) Osteoarthritis year in review 2014: clinical. Osteoarthr Cartil 22:1953–1957. https://doi.org/10.1016/j.joca.2014.06.018

Heerey JJ, Kemp JL, Mosler AB et al (2019) What is the prevalence of hip intra-articular pathologies and osteoarthritis in active athletes with hip and groin pain compared with those without? a systematic review and meta-analysis. Sports Med:1–22. https://doi.org/10.1007/s40279-019-01092-y

Hegazi TM, Belair JA, McCarthy EJ et al (2016) Sports injuries about the hip: what the radiologist should know. Radiographics 36:1717–1745. https://doi.org/10.1148/rg.2016160012

Hellman MD, Gross CE, Hart M et al (2016) Radiographic comparison of anterior acetabular rim morphology between pincer femoroacetabular impingement and control. Arthroscopy 32:468–472. https://doi.org/10.1016/j.arthro.2015.08.035

Hemke R, Mascarenhas V, Maas M (2018) Novel imaging techniques in rheumatic diseases. Semin Musculoskelet Radiol 22:237–244. https://doi.org/10.1055/s-0038-1641160

Hernando MF, Cerezal L, Pérez-Carro L et al (2015) Deep gluteal syndrome: anatomy, imaging, and management of sciatic nerve entrapments in the subgluteal space. Skelet Radiol 44:919–934. https://doi.org/10.1007/s00256-015-2124-6

Hernando MF, Cerezal L, Pérez-Carro L et al (2016) Evaluation and management of ischiofemoral impingement: a pathophysiologic, radiologic, and therapeutic approach to a complex diagnosis. Skelet Radiol 45:771–787. https://doi.org/10.1007/s00256-016-2354-2

Hetsroni I, Poultsides L, Bedi A et al (2013) Anterior inferior iliac spine morphology correlates with hip range of motion: a classification system and dynamic model. Clin Orthop Relat Res 471:2497–2503. https://doi.org/10.1007/s11999-013-2847-4

Hirschmann A, Falkowski AL, Kovacs B (2017) Greater trochanteric pain syndrome: abductors, external rotators. Semin Musculoskelet Radiol 21:539–546. https://doi.org/10.1055/s-0037-1606139

Hunter DJ, Arden N, Conaghan PG et al (2011) Nition of osteoarthritis on MRI: results of a Delphi exercise. Osteoarthr Cartil 19:963–969. https://doi.org/10.1016/j.joca.2011.04.017

Ilizaliturri VM Jr, Byrd JWT, Sampson TG et al (2008) A geographic zone method to describe intra-articular pathology in hip arthroscopy: cadaveric study and preliminary report. Arthrosc J Arthrosc Related Surg 24:534–539. https://doi.org/10.1016/j.arthro.2007.11.019

Ito K, Minka-II MA, Leunig M et al (2001) Femoroacetabular impingement and the cam-effect. J Bone Joint Surg 83:171–176. https://doi.org/10.1302/0301-620X.83B2.11092

Jackson TJ, Estess AA, Adamson GJ (2016) Supine and standing AP pelvis radiographs in the evaluation of pincer femoroacetabular impingement. Clin Orthop Relat Res 474:1692–1696. https://doi.org/10.1007/s11999-016-4766-7

Jónasson P, Halldin K, Karlsson J et al (2011) Prevalence of joint-related pain in the extremities and spine in five groups of top athletes. Knee Surg Sports Traumatol Arthrosc 19:1540–1546. https://doi.org/10.1007/s00167-011-1539-4

Jung JY, Kim G-U, Lee H-J et al (2013) Diagnostic value of ultrasound and computed tomographic arthrography in diagnosing anterosuperior acetabular labral tears. Arthroscopy 29:1769–1776. https://doi.org/10.1016/j.arthro.2013.07.274

Jung KA, Restrepo C, Hellman M et al (2011) The prevalence of cam-type femoroacetabular deformity in asymptomatic adults. J Bone Joint Surg 93:1303. https://doi.org/10.1302/0301-620X.93B10

Kalberer F, Sierra RJ, Madan SS et al (2008) Ischial spine projection into the pelvis: a new sign for acetabular retroversion. Clin Orthop Relat Res 466:677–683. https://doi.org/10.1007/s11999-007-0058-6

Kalhor M, Horowitz K, Beck M et al (2010) Vascular supply to the acetabular labrum. J Bone Joint Surg Am 92:2570–2575. https://doi.org/10.2106/JBJS.I.01719

Kassarjian A (2019) Hip hype: FAI syndrome, amara's law, and the hype cycle. Semin Musculoskelet Radiol. https://doi.org/10.1055/s-0039-1677695

Kassarjian A, Rodrigo RM, Santisteban JM (2012) Current concepts in MRI of rectus femoris musculotendinous (myotendinous) and myofascial injuries in elite athletes. Eur J Radiol 81:3763–3771. https://doi.org/10.1016/j.ejrad.2011.04.002

Kassarjian A, Rodrigo RM, Santisteban JM (2014) Intramuscular degloving injuries to the rectus femoris: findings at MRI. AJR Am J Roentgenol 202:W475–W480. https://doi.org/10.2214/AJR.13.10931

Kaya M, Suzuki T, Emori M, Yamashita T (2016) Hip morphology in uences the pattern of articular cartilage damage. Knee Surg Sports Traumatol Arthrosc 24:2016–2023. https://doi.org/10.1007/s00167-014-3297-6

Kellgren JH, Jeffrey MR, Ball J (1963) The epidemiology of chronic rheumatism: a symposium

Khan W, Khan M, Alradwan H et al (2015) Utility of intra-articular hip injections for femoroacetabular impingement: a systematic review. Orthop J Sports Med. https://doi.org/10.1177/2325967115601030

Kiuru MJ, Pihlajamaki HK, Ahovuo JA (2003) Fatigue stress injuries of the pelvic bones and proximal femur: evaluation with MR imaging. Eur Radiol 13(3):605–11. https://doi.org/10.1007/s00330-002-1562-4. Epub 2002 Aug 16. PMID: 12594565

Kivlan BR, Martin RL, Sekiya JK (2011) Response to diagnostic injection in patients with femoroacetabular

impingement, labral tears, chondral lesions, and extra-articular pathology. Arthroscopy 27:619–627. https://doi.org/10.1016/j.arthro.2010.12.009

Kizaki K, Uchida S, Shanmugaraj A et al (2020) Deep gluteal syndrome is defined as a non-discogenic sciatic nerve disorder with entrapment in the deep gluteal space: a systematic review. Knee Surg Sports Traumatol Arthrosc:1–11. https://doi.org/10.1007/s00167-020-05966-x

Kooijman MN, Kruithof CJ, van Duijn CM et al (2016) The generation R study: design and cohort update 2017. Eur J Epidemiol 31:1243–1264. https://doi.org/10.1007/s10654-016-0224-9

Kraeutler MJ, Garabekyan T, Pascual-Garrido C, Mei-Dan O (2016) Hip instability: a review of hip dysplasia and other contributing factors. Muscles Ligaments Tendons J 6:343–353. https://doi.org/10.11138/mltj/2016.6.3.343

Krishnamoorthy VP, Beck EC, Kunze KN et al (2019a) Radiographic prevalence of sacroiliac joint abnormalities and clinical outcomes in patients with femoroacetabular impingement syndrome. Arthroscopy 35:2598–2605.e1. https://doi.org/10.1016/j.arthro.2019.03.030

Krishnamoorthy VP, Kunze KN, Beck EC et al (2019b) Radiographic prevalence of symphysis pubis abnormalities and clinical outcomes in patients with femoroacetabular impingement syndrome. Am J Sports Med 47:1467–1472. https://doi.org/10.1177/0363546519837203

Krych AJ, King AH, Berardelli RL et al (2016) Is subchondral acetabular edema or cystic change on MRI a contraindication for hip arthroscopy in patients with femoroacetabular impingement? Am J Sports Med 44:454–459. https://doi.org/10.1177/0363546515612448

Kuske B, Hamilton DF, Pattle SB, Simpson AHRW (2016) Patterns of hamstring muscle tears in the general population: a systematic review. PLoS One 11:e0152855. https://doi.org/10.1371/journal.pone.0152855.s003

Lambert RGW, Bakker PAC, van der Heijde D et al (2016) Defining active sacroiliitis on MRI for classification of axial spondyloarthritis: update by the ASAS MRI working group. Ann Rheum Dis. https://doi.org/10.1136/annrheumdis-2015-208642

Lane NE, Hochberg MC, Nevitt MC et al (2015) OARSI clinical trials recommendations: design and conduct of clinical trials for hip osteoarthritis. Osteoarthr Cartil 23:761–771. https://doi.org/10.1016/j.joca.2015.03.006

Liong SY, Whitehouse RW (2012) Lower extremity and pelvic stress fractures in athletes. Br J Radiol 85:1148–1156. https://doi.org/10.1259/bjr/78510315

Llopis E, Cerezal L, Kassarjian A et al (2008) Direct MR arthrography of the hip with leg traction: feasibility for assessing articular cartilage. AJR Am J Roentgenol 190:1124–1128. https://doi.org/10.2214/AJR.07.2559

Lungu E, Michaud J, Bureau NJ (2018) US assessment of sports-related hip injuries. Radiographics 38:867–889. https://doi.org/10.1148/rg.2018170104

Lynch TS, Steinhaus ME, Popkin CA et al (2016) Outcomes after diagnostic hip injection. Arthroscopy 32:1702–1711. https://doi.org/10.1016/j.arthro.2016.02.027

Maheu E, Cadet C, Marty M et al (2005) Reproducibility and sensitivity to change of various methods to measure joint space width in osteoarthritis of the hip: a double reading of three different radiographic views taken with a three-year interval. Arthritis Res Ther 7:R1375–R1385. https://doi.org/10.1186/ar1831

Major NM, Helms CA (2000) Sacral stress fractures in long-distance runners. Am J Roentgenol 174:727–729. https://doi.org/10.2214/ajr.174.3.1740727

Makovicka JL, Chhabra A, Patel KA et al (2019) A decade of hip injuries in National Collegiate Athletic Association football players: an epidemiologic study using National Collegiate Athletic Association surveillance data. J Athl Train 54:483–488. https://doi.org/10.4085/1062-6050-59-18

Marshall RA, Mandell JC, Weaver MJ et al (2018) Imaging features and management of stress, atypical, and pathologic fractures. Radiographics 38:2173–2192. https://doi.org/10.1148/rg.2018180073

Mascarenhas VV, Ayeni OR, Egund N et al (2019) Imaging methodology for hip preservation: techniques, parameters, and thresholds. Semin Musculoskelet Radiol 23:197–226. https://doi.org/10.1055/s-0039-1688714

Mascarenhas VV, Caetano A (2018) Imaging the young adult hip in the future. Ann Joint 3:47–47. https://doi.org/10.21037/aoj.2018.04.10

Mascarenhas VV, Castro M, Rego PA, et al (2020a) The Lisbon Agreement on Femoroacetabular impingement imaging—Part 2: general issues, parameters and reporting

Mascarenhas VV, Castro MO, Rego PA et al. (2020) The Lisbon Agreement on Femoroacetabular Impingement Imaging-part 1: overview. Eur Radiol 30(10):5281–5297. https://doi.org/10.1007/s00330-020-06822-9. Epub 2020 Jul 17. Erratum in: Eur Radiol. PMID: 32405754

Mascarenhas VV, Rego P, Dantas P et al (2017) Cam deformity and the omega angle, a novel quantitative measurement of femoral head-neck morphology: a 3D CT gender analysis in asymptomatic subjects. Eur Radiol 27:2011–2023. https://doi.org/10.1007/s00330-016-4530-0

Mascarenhas VV, Rego PA, Dantas P et al (2018a) Can we discriminate symptomatic hip patients from asymptomatic volunteers based on anatomic predictors? a 3-dimensional magnetic resonance study on cam, pincer, and spinopelvic parameters. Am J Sports Med 46:3097–3110. https://doi.org/10.1177/0363546518800825

Mascarenhas VV, Rego PA, Dantas P et al (2018b) Hip shape is symmetric, non-dependent on limb dominance and gender-specific: implications for femoroacetabular impingement. A 3D CT analysis in asymptomatic subjects. Eur Radiol 28:1609–1624. https://doi.org/10.1007/s00330-017-5072-9

Mascarenhas VV, Rego PA, Dantas P et al (2016) Imaging prevalence of femoroacetabular impingement in symptomatic patients, athletes, and asymptomatic individuals: a systematic review. Eur J Radiol 85:73–95. https://doi.org/10.1016/j.ejrad.2015.10.016

Matheney T, Sandell L, Foucher K et al (2013) Motion analysis, cartilage mechanics, and biology in femoroacetabular impingement: current understanding and areas of future research. J Am Acad Orthop Surg 21(Suppl 1):S27–S32. https://doi.org/10.5435/JAAOS-21-07-S27

McKay CD, Tufts RJ, Shaffer B, Meeuwisse WH (2014) The epidemiology of professional ice hockey injuries: a prospective report of six NHL seasons. Br J Sports Med 48(1):57–62. https://doi.org/10.1136/bjsports-2013-092860. PMID: 24334505

Miller, Christopher C. Kaeding (eds.) (2015) Stress Fractures in Athletes_ Diagnosis and Management-Springer International Publishing 4–7

Morvan J, Bouttier R, Mazieres B et al (2013) Relationship between hip dysplasia, pain, and osteoarthritis in a cohort of patients with hip symptoms. J Rheumatol 40:1583–1589. https://doi.org/10.3899/jrheum.121544

Nakano N, Yip G, Khanduja V (2017) Current concepts in the diagnosis and management of extra-articular hip impingement syndromes. 1–8. https://doi.org/10.1007/s00264-017-3431-4

Naraghi A, Awdeh H, Wadhwa V et al (2015) Diffusion tensor imaging of peripheral nerves. Semin Musculoskelet Radiol 19:191–200. https://doi.org/10.1055/s-0035-1546824

Nawabi DH, Bedi A, Tibor LM et al (2014) The demographic characteristics of high-level and recreational athletes undergoing hip arthroscopy for femoroacetabular impingement: a sports-specific analysis. Arthroscopy 30:398–405. https://doi.org/10.1016/j.arthro.2013.12.010

Nepple JJ, Prather H, Trousdale RT et al (2013) Clinical diagnosis of femoroacetabular impingement. J Am Acad Orthop Surg 21(Suppl 1):S16–S19. https://doi.org/10.5435/JAAOS-21-07-S16

Nepple JJ, Riggs CN, Ross JR, Clohisy JC (2014) Clinical presentation and disease characteristics of femoroacetabular impingement are sex-dependent. J Bone Joint Surg 96:1683–1689. https://doi.org/10.2106/JBJS.M.01320

Nepple JJ, Vigdorchik JM, Clohisy JC (2015) What is the association between sports participation and the development of proximal femoral cam deformity?: a systematic review and meta-analysis. Am J Sports Med 43:2833–2840. https://doi.org/10.1177/0363546514563909

Ng KCG, Lamontagne M, Jeffers JRT et al (2018) Anatomic predictors of sagittal hip and pelvic motions in patients with a cam deformity. Am J Sports Med 2014:036354651875515. https://doi.org/10.1016/j.arthro.2016.01.011

Nicholls AS, Kiran A, Pollard TCB et al (2011) The association between hip morphology parameters and nineteen-year risk of end-stage osteoarthritis of the hip: a nested case-control study. Arthritis Rheum 63:3392–3400. https://doi.org/10.1002/art.30523

Nötzli HP, Wyss TF, Stoecklin CH et al (2002) The contour of the femoral head-neck junction as a predictor for the risk of anterior impingement. J Bone Joint Surg 84:556–560

Omar IM, Zoga AC, Kavanagh EC et al (2008) Athletic pubalgia and "sports hernia": optimal MR imaging technique and findings. Radiographics 28:1415–1438. https://doi.org/10.1148/rg.285075217

Orchard JW (2015) Men at higher risk of groin injuries in elite team sports: a systematic review. Br J Sports Med 49:798–802. https://doi.org/10.1136/bjsports-2014-094272

Orellana C, Moreno M, Calvet J et al (2018) Ultrasound findings in patients with femoracetabular impingement without radiographic osteoarthritis: a pilot study. J Ultrasound Med 38:895–901. https://doi.org/10.1038/nrrheum.2013.114

Pedersen DR, Lamb CA, Dolan LA et al (2004) Radiographic measurements in developmental dysplasia of the hip: reliability and validity of a digitizing program. J Pediatr Orthop 24:156–160

Peh WC, Khong PL, Yin Y, Ho WY, Evans NS, Gilula LA, Yeung HW, Davies AM (1996) Imaging of pelvic insufficiency fractures. Radiographics 16(2):335–48

Petchprapa CN, Rosenberg ZS, Sconfienza LM et al (2010) MR imaging of entrapment neuropathies of the lower extremity. Part 1. The pelvis and hip. Radiographics 30:983–1000. https://doi.org/10.1148/rg.304095135

Pfirrmann CWA, Mengiardi B, Dora C et al (2006) Cam and pincer femoroacetabular impingement: characteristic MR arthrographic findings in 50 patients. Radiology 240:778–785. https://doi.org/10.1148/radiol.2403050767

Philippon MJ, Maxwell RB, Johnston TL et al (2007) Clinical presentation of femoroacetabular impingement. Knee Surg Sports Traumatol Arthrosc 15:1041–1047. https://doi.org/10.1007/s00167-007-0348-2

Philippon MJ, Michalski MP, Campbell KJ et al (2014) An anatomical study of the acetabulum with clinical applications to hip arthroscopy. J Bone Joint Surg 96:1673–1682. https://doi.org/10.2106/JBJS.M.01502

Ranawat AS, Kelly BT (2005) Anatomy of the hip: open and arthroscopic structure and function. Oper Tech Orthop 15:160–174. https://doi.org/10.1053/j.oto.2005.06.010

Rego PA, Mascarenhas V, Collado D et al (2017) Arterial topographic anatomy near the femoral head-neck perforation with surgical relevance. J Bone Joint Surg Am 99:1213–1221. https://doi.org/10.2106/JBJS.16.01386

Reiman MP, Goode AP, Cook CE et al (2015) Diagnostic accuracy of clinical tests for the diagnosis of hip femoroacetabular impingement/labral tear: a systematic review with meta-analysis. Br J Sports Med 49:811. https://doi.org/10.1136/bjsports-2014-094302

Reurink G, Brilman EG, de Vos R-J et al (2014) Magnetic resonance imaging in acute hamstring injury: can we provide a return to play prognosis? Sports Med 45:133–146. https://doi.org/10.1136/bjsm.37.5.384

Ritchlin C (2018) Editorial: magnetic resonance imaging signals in the sacroiliac joints of healthy athletes: refining disease thresholds and treatment strategies in axial spondyloarthritis. Arthrit Rheumatol 70:629–632. https://doi.org/10.1002/art.39298

Rivière C, Hardijzer A, Lazennec JY et al (2017a) Spine-hip relations add understandings to the pathophysiology of femoro-acetabular impingement: a systematic review. Orthop Traumatol Surg Res 103:549–557. https://doi.org/10.1016/j.otsr.2017.03.010

Rivière C, Lazennec JY, Van Der Straeten C et al (2017b) The influence of spine-hip relations on total hip replacement: a systematic review. Orthop Traumatol Surg Res 103:559–568. https://doi.org/10.1016/j.otsr.2017.02.014

Rudwaleit M, Landewe R, van der Heijde D et al (2009) The development of Assessment of SpondyloArthritis international Society classification criteria for axial spondyloarthritis (part I): classification of paper patients by expert opinion including uncertainty appraisal. Ann Rheum Dis 68:770–776. https://doi.org/10.1136/ard.2009.108217

Saddik D, Troupis J, Tirman P et al (2006) Prevalence and Location of Acetabular Sublabral Sulci at Hip Arthroscopy with Retrospective MRI Review. Am J Roentgenol 187:W507–W511. https://doi.org/10.2214/AJR.05.1465

Saied AM, Redant C, El-Batouty M et al (2017) Accuracy of magnetic resonance studies in the detection of chondral and labral lesions in femoroacetabular impingement: systematic review and meta-analysis. BMC Musculoskelet Disord 18:83. https://doi.org/10.1186/s12891-017-1443-2

Samim M, Eftekhary N, Vigdorchik JM et al (2019) 3D-MRI versus 3D-CT in the evaluation of osseous anatomy in femoroacetabular impingement using Dixon 3D FLASH sequence. Skelet Radiol 48:429–436. https://doi.org/10.1007/s00256-018-3049-7

Sanders T, Zlatkin M (2008) Avulsion injuries of the pelvis. Semin Musculoskelet Radiol 12:042–053. https://doi.org/10.1055/s-2008-1067936

Sankar WN, Matheney TH, Zaltz I (2013a) Femoroacetabular impingement: current concepts and controversies. Orthop Clin North Am 44:575–589. https://doi.org/10.1016/j.ocl.2013.07.003

Sankar WN, Nevitt M, Parvizi J et al (2013b) Femoroacetabular impingement: defining the condition and its role in the pathophysiology of osteoarthritis. J Am Acad Orthop Surg 21:S7–S15. https://doi.org/10.5435/JAAOS-21-07-S7

Saunders J, Cusi M, Robinson D, Van der Wall H (2018) Sacroiliac joint dysfunction in the athlete: diagnosis and management. Curr Sports Med Rep 17:73–74. https://doi.org/10.1249/JSR.0000000000000456

Schiphof D, Boers M, Bierma-Zeinstra SM (2008) Differences in descriptions of Kellgren and Lawrence grades of knee osteoarthritis. Ann Rheum Dis 67(7):1034–6. https://doi.org/10.1136/ard.2007.079020. Epub 2008 Jan 15. PMID: 18198197

Schmaranzer F, Klauser A, Kogler M et al (2014) Diagnostic performance of direct traction MR arthrography of the hip: detection of chondral and labral lesions with arthroscopic comparison. Eur Radiol. https://doi.org/10.1007/s00330-014-3534-x

Schmaranzer F, Todorski IAS, Lerch TD et al (2017) Intra-articular lesions: imaging and surgical correlation. Semin Musculoskelet Radiol 21:487–506. https://doi.org/10.1055/s-0037-1606133

Schueller-Weidekamm C, Mascarenhas V, Sudol-Szopinska I et al (2014) Imaging and interpretation of axial spondylarthritis: the radiologist's perspective—consensus of the arthritis subcommittee of the ESSR. Semin Musculoskelet Radiol 18:265–279. https://doi.org/10.1055/s-0034-1375569

Sconfienza LM, Adriaensen M, Albano D, et al (2019) Clinical indications for image-guided interventional procedures in the musculoskeletal system: a Delphi-based consensus paper from the European Society of Musculoskeletal Radiology (ESSR)—part I, shoulder. 1–11. https://doi.org/10.1007/s00330-019-06419-x

Seldes RM, Tan V, Hunt J et al (2001) Anatomy, histologic features, and vascularity of the adult acetabular labrum. Clin Orthop Relat Res:232–240

Shanmugaraj A, Shell JR, Horner NS, et al (2018) How useful is the flexion–adduction–internal rotation test for diagnosing femoroacetabular impingement. Clin J Sport Med 1. https://doi.org/10.1097/JSM.0000000000000575

Sher I, Umans H, Downie SA et al (2011) Proximal iliotibial band syndrome: what is it and where is it? Skelet Radiol 40:1553–1556. https://doi.org/10.1016/j.clinbiomech.2008.07.011

Siebenrock KA, Kalbermatten DF, Ganz R (2003) Effect of pelvic tilt on acetabular retroversion: a study of pelves from cadavers. Clin Orthop Relat Res:241–248. https://doi.org/10.1097/01.blo.0000030508.43495.79

Singer AD, Subhawong TK, Jose J et al (2015) Ischiofemoral impingement syndrome: a meta-analysis. Skelet Radiol 44:831–837. https://doi.org/10.1007/s00256-015-2111-y

Smith TO, Hilton G, Toms AP et al (2010) The diagnostic accuracy of acetabular labral tears using magnetic resonance imaging and magnetic resonance arthrography: a meta-analysis. Eur Radiol. https://doi.org/10.1007/s00330-010-1956-7

Smith TO, Simpson M, Ejindu V, Hing CB (2012) The diagnostic test accuracy of magnetic resonance imaging, magnetic resonance arthrography and computer tomography in the detection of chondral lesions of the hip. Eur J Orthop Surg Traumatol 23:335–344. https://doi.org/10.1007/s00590-012-0972-5

Soldatos T, Andreisek G, Thawait GK et al (2013) High-resolution 3-T MR neurography of the lumbosacral plexus. Radiographics 33:967–987. https://doi.org/10.1148/rg.334115761

Stracciolini A, Casciano R, Levey Friedman H et al (2013) Pediatric sports injuries: an age comparison of children versus adolescents. Am J Sports Med 41:1922–1929. https://doi.org/10.1177/0363546513490644

Suter A, Dietrich TJ, Maier M et al (2015) MR findings associated with positive distraction of the hip joint achieved by axial traction. Skelet Radiol 44:787–795. https://doi.org/10.1016/j.arthro.2012.04.057

Sutter R, Pfirrmann CWA (2017) Update on femoroacetabular impingement: what is new, and how should we assess it? Semin Musculoskelet Radiol 21:518–528. https://doi.org/10.1055/s-0037-1606141

Sutter R, Zubler V, Hoffmann A et al (2014) Hip MRI: how useful is intraarticular contrast material for evaluating surgically proven lesions of the labrum and articular cartilage? AJR Am J Roentgenol 202:160–169. https://doi.org/10.2214/AJR.12.10266

Syed AB, Zoga AC (2018) Artificial intelligence in radiology: current technology and future directions. Semin Musculoskelet Radiol 22:540–545. https://doi.org/10.1055/s-0038-1673383

Tannast M, Fritsch S, Zheng G, et al (2014) Which radiographic hip parameters do not have to be corrected for pelvic rotation and tilt? Clin Orthop Relat Res https://doi.org/10.1007/s11999-014-3936-8

Tannast M, Siebenrock KA, Anderson SE (2007) Femoroacetabular impingement: radiographic diagnosis—what the radiologist should know. AJR Am J Roentgenol 188:1540–1552. https://doi.org/10.2214/AJR.06.0921

Tannenbaum E, Kopydlowski N, Smith M et al (2014) Gender and racial differences in focal and global acetabular version. J Arthroplast 29:373–376. https://doi.org/10.1016/j.arth.2013.05.015

Tibor LM, Liebert G, Sutter R et al (2013) Two or more impingement and/or instability deformities are often present in patients with hip pain. Clin Orthop Relat Res 471:3762–3773. https://doi.org/10.1007/s11999-013-2918-6

Tibor LM, Sekiya JK (2008) Differential diagnosis of pain around the hip joint. Arthroscopy 24:1407–1421. https://doi.org/10.1016/j.arthro.2008.06.019

Tönnis D (1987) Congenital dysplasia and dislocation of the hip in children and adults. Springer, Berlin

Tönnis D (1976) Normal values of the hip joint for the evaluation of X-rays in children and adults. Clin Orthop Relat Res:39–47. https://doi.org/10.1097/00003086-197609000-00007

Turkiewicz A, Petersson IF, Björk J et al (2014) Current and future impact of osteoarthritis on health care: a population-based study with projections to year 2032. Osteoarthr Cartil 22:1826–1832. https://doi.org/10.1016/j.joca.2014.07.015

van der Bom MJ, Groote ME, Vincken KL et al (2011) Pelvic rotation and tilt can cause misinterpretation of the acetabular index measured on radiographs. Clin Orthop Relat Res 469:1743–1749. https://doi.org/10.1007/s11999-011-1781-6

Vavken P, Krepler P (2008) Sacral fractures after multisegmental lumbosacral fusion: a series of four cases and systematic review of literature. Eur Spine J 17(Suppl 2):285–290.

Wang Y, Teichtahl AJ, Cicuttini FM (2016) Osteoarthritis year in review 2015: imaging. Osteoarthr Cartil 24:49–57. https://doi.org/10.1016/j.joca.2015.07.027

Weber U, Jurik AG, Zejden A, et al (2019) MRI of the sacroiliac joints in athletes: recognition of non-specific bone marrow oedema by semi-axial added to standard semi-coronal scans. Rheumatology (Oxford). https://doi.org/10.1093/rheumatology/kez458

Weir A, Brukner P, Delahunt E, et al (2015) Doha agreement meeting on terminology and definitions in groin pain in athletes. pp 768–774

Werner J, Hägglund M, Ekstrand J, Waldén M (2019) Hip and groin time-loss injuries decreased slightly but injury burden remained constant in men's professional football: the 15-year prospective UEFA Elite Club Injury Study. Br J Sports Med 53(9):539–546. https://doi.org/10.1136/bjsports-2017-097796. Epub 2018 Apr 24. PMID: 29691289

Wilkin GP, Ibrahim MM, Smit KM, Beaulé PE (2017) A contemporary definition of hip dysplasia and structural instability: toward a comprehensive classification for acetabular dysplasia. J Arthroplasty 32:S20–S27. https://doi.org/10.1016/j.arth.2017.02.067

Zaltz I, Kelly BT, Larson CM, Leunig M, Bedi A (2014) Surgical treatment of femoroacetabular impingement: what are the limits of hip arthroscopy? Arthroscopy 30(1):99–110. https://doi.org/10.1016/j.arthro.2013.10.005. PMID: 24384276

Zaltz I, Leunig M (2012) Parafoveal chondral defects associated with femoroacetabular impingement. Clin Orthop Relat Res 470:3383–3389. https://doi.org/10.1007/s11999-012-2453-x

Zoga AC, Hegazi TM, Roedl JB (2016) Algorithm for imaging the hip in adolescents and young adults. Radiol Clin N Am 54:913–930. https://doi.org/10.1016/j.rcl.2016.05.016

Zuckerman SL, Wegner AM, Roos KG, Djoko A, Dompier TP, Kerr ZY (2018) Injuries sustained in National Collegiate Athletic Association men's and women's basketball, 2009/2010–2014/2015. Br J Sports Med 52(4):261–268. https://doi.org/10.1136/bjsports-2016-096005. Epub 2016 Jun 30. PMID: 27364907